# Spectrum Sensing of Multiple Channels Using Multiple Sensors

by

Che Kang Liang

A thesis submitted to the
Department of Electrical and Computer Engineering
in conformity with the requirements for
the degree of Master of Applied Science

Queen's University
Kingston, Ontario, Canada
November 2011

# Abstract

Cognitive radio (CR) is a class of wireless communication technologies that have the ability to learn from the surrounding radio environment and the intelligence to adapt communication resources to enhance quality of service. The problem of acquiring information from a CRs radio environment is called spectrum sensing, which can take on many forms. In particular, this thesis concerns the determination of whether a spectrum band (or channel) is in a busy or idle state. The binary nature of a channels availability means that spectrum sensing can be cast as a hypothesis testing problem. While an abundant literature exists on spectrum sensing as a signal detection problem, this thesis treats spectrum sensing differently, and features the following elements: 1) the system is equipped with an arbitrary number of sensors; 2) sensing is performed over multiple channels; 3) each channels availability is modelled by random periods of busy and idle times corresponding to packet transmission; and 4) the optimization criteria minimizes detection delay subject to a reliability constraint.

A related spectrum sensing problem formulation based on the use of a single sensor has been proposed in the recent literature. The previous research employs an optimization framework based on modeling channel uses as an on-off process via partially observable Markov decision processes (POMDP). This thesis generalizes previous results from single-sensor to multiple-sensor spectrum sensing, i.e., detecting

idle periods with multiple sensors. In addition, an alternative reduced-complexity algorithm is proposed. For both proposed detectors, the performances are evaluated based on Monte Carlo simulation with calculated confidence intervals, and the results show that 1) adding sensors generally improves the system performance by reducing detection delay (improved agility); 2) the application of previously existing quickest detection methods result in error floors complicating test design. Finally, performance assessment using a channel model derived experimentally from the wireless local area network (WLAN) traffic is conducted and compared to that obtained using a geometrically-distributed channel traffic model.

# Acknowledgments

I would like to thank God for giving me the courage to step out of my comfort zones and the tenacity to endure times of difficult challenges and great uncertainties. I would also like to thank my father and my grandmother for always trusting and supporting me with my decisions, even those decisions that you do not fully agree at a time. And in addition, I need to express my utmost gratefulness for my fiancee, whom I got engaged during the writing of this thesis. Over the two years that we have lived away from each other, you never once complained for being apart and have stayed so strong throughout this process. By being strong you kept me strong. By believing you gave me faith in us. I could not have made it this far without your love and support.

Finally, I want to express my sincerest thanks to my supervisor Dr. Steven Blostein. Your encouragement always lifts my spirit and your criticism always enlightens me. Working with you has been a humbling and rewarding experience, and I would not have it any other way. Thank you, I am grateful for everything you have done for me.

# Acronym

| | |
|---|---|
| CR | Cognitive Radio |
| MAR | Minimum Asymptotic Risk |
| MMSSD | Multiband Multi-sensing Spectrum Sensing Detector |
| POMDP | Partially Observable Markov Decision Processes |
| RC-MMSSD | Reduced Complexity Multiband Multi-sensing Spectrum Sensing Detector |
| SNR | Signal-to-Noise Ratio |
| SPRT | Sequential Probability Ratio Test |
| UDP | User Datagram Protocol |
| WLAN | Wireless Local Area Network |

# Table of Contents

**Abstract** i

**Acknowledgments** iii

**Acronyms** iv

**Table of Contents** v

**List of Tables** viii

**List of Figures** ix

**1 Introduction** . . . . . 1

1.1 Motivation . . . . . 1

1.2 Contributions . . . . . 7

1.3 Organization of Thesis . . . . . 8

**2 Background** . . . . . 11

2.1 General Description of Spectrum Sensing . . . . . 11

2.2 Classical Hypothesis Testing . . . . . 12

2.2.1 Energy Detection . . . . . 14

2.2.2 Sequential Probability Ratio Test . . . . . 15

2.3 Quickest Detection . . . . . 17
2.3.1 Page's CUSUM . . . . . 19
2.3.2 Shiryaev's Problem . . . . . 21
2.3.3 Minimum Asymptotic Risk Detection . . . . . 24

**3 System Models and Problem Formulation . . . . . 27**
3.1 System Models . . . . . 27
3.1.1 Channel Usage Models . . . . . 28
3.1.2 Signal Model for Observations . . . . . 29
3.2 Problem Formulation . . . . . 30
3.2.1 General Multiband Multi-sensor Detection . . . . . 30
3.2.2 Partially Observable Markov Decision Processes . . . . . 32
3.2.2.1 State Space . . . . . 33
3.2.2.2 Action Space . . . . . 33
3.2.2.3 State Transition . . . . . 34
3.2.2.4 Observation Model . . . . . 35
3.2.2.5 Cost Model . . . . . 36
3.2.2.6 Sufficient Statistic . . . . . 36

**4 New Detection Methods for Multi-Channel Spectrum Sensing . . 39**
4.1 Optimal Decision Test for the Problem of
POMDP . . . . . 40
4.2 Multiband Multi-Sensor Spectrum Sensing
Detector . . . . . 45

4.3 Reduced-Complexity Multiband Multi-Sensor Spectrum Sensing Detectors . . . 49
4.4 Appendix: Proof of Lemma 1 . . . 54

**5 Simulation Results and Discussions . . . 69**
5.1 Performance Impacts of Extra Sensors . . . 71
5.2 MMSSD versus RC-MMSSD . . . 75
5.3 MMSSD versus Quickest Detection Methods . . . 78
5.3.1 MMSSD versus Page's CUSUM . . . 81
5.3.2 RC-MMSSD versus Page's CUSUM when $L >> M$ . . . 85
5.3.3 MMSSD versus Shiryaev's Bayesian Detector . . . 88
5.3.4 MMSSD versus Minimum Asymptotic Risk Detector . . . 90
5.4 Performance of MMSSD in WLAN Traffic . . . 91

**6 Summary and Conclusions . . . 101**
6.1 Summary . . . 101
6.2 Conclusions . . . 103
6.3 Future Work . . . 106

**Bibliography . . . 107**

# List of Tables


2.1 The algorithm of CUSUM Detection . . . . . 21

2.2 The algorithm of Shiryaev's Bayesian Detector . . . . . 24

2.3 The algorithm of the MAR detection . . . . . 26

4.1 The operation of a MMSSD is described in an algorithmic form. . . . 48

4.2 The operation of a RC-MMSSD is described in an algorithmic form where $\Omega$ denotes the pool of unobserved channels at the current time $t$. 52

5.1 The values of parameters for the WLAN traffic model. . . . . 95

5.2 The values of the parameters in the exponential ON-OFF model, $m_I$ and $\lambda_o$, are chosen to minimize the KS distance between the nominal distribution and the mixture distribution of the WLAN traffic model. 97

# List of Figures

3.1 The transition dynamics for the $l^{th}$ channel. The same would apply to all other channels. When the action taken at time $t$ belongs to set $\mathcal{C}$, the channel will switch between the busy and idle states; otherwise, the process reaches an absorption state. . . . . 35

5.1 The false alarm rates of MMSSD with different numbers of sensors $M$. The 95% confidence interval is less than $\pm 0.01$ ($m_B = 300$, SNR=0 dB, $\eta_d = 0.9, L = 4, W = 10^5$). . . . . 73

5.2 The expected detection delays of MMSSD with different numbers of sensors $M$. The 95% confidence interval does not exceed $\pm 1$ ($m_B = 300$, SNR=0 dB, $\eta_d = 0.9, L = 4, W = 10^5$). . . . . 74

5.3 The false alarm rate of RC-MMSSD for different numbers of sensors, $M$. The 95% confidence interval is less than $\pm 0.01$ ($m_B = 300$, SNR=0 dB, $\eta_d = 0.9, L = 100, W = 10^5$). . . . . 75

5.4 The expected detection delay of RC-MMSSD for different numbers of sensors $M$. The 95% confidence interval does not exceed $\pm 1$ ($m_B = 300$, SNR=0 dB, $\eta_d = 0.9, L = 100, W = 10^5$). . . . . 76

5.5 The false alarm rates of MMSSD and RC-MMSSD with respect to the number of available channels, for both SNR=0 dB and SNR=10 dB. Note the violation of the prescribed false alarm constraint $\alpha = 0.1$ when $L < 30$. The 95% confidence interval is less than $\pm 0.01$ ($\lambda_0 = 0.25, m_B = 300, \eta_d = 0.9, M = 4, W = 10^5$). . . . . 77

5.6 The expected detection delays of MMSSD and RC-MMSSD with respect to the number of available channels, for both SNR=0 dB and SNR=10 dB. The 95% confidence interval does not exceed $\pm 1$ ($\lambda_0 = 0.25, m_B = 300, \eta_d = 0.9, M = 4, W = 10^5$). . . . . 78

5.7 The false alarm rates reach an error floor in spite of increasing the detector threshold. The dashed line, i.e., where the ratio of expected detection delay to average idle time, $m_I$, in the top plot crosses 1, indicates where expected detection delay begins to exceed the average idle time, and where the false alarm rates begin to flatten in the bottom plot. . . . . 81

5.8 A comparison of the expected detection delays between full-sensing CUSUM detection and MMSSD detection that uses 3 and 5 sensors. (SNR=10dB, $m_B = 620, L = 5, W = 10^5$). The 95% confidence interval does not exceed $\pm 1$. . . . . 82

5.9 A comparison of the false alarm rate between a full-sensing CUSUM detection and MMSSD detection that uses 3 and 5 sensors. The error bars are the 95% confidence intervals for each points. (SNR=10dB, $m_B = 620, L = 5, W = 10^5$). . . . . 83

5.10 The probability mass function (PMF) of the duration of an idle period becomes flattened as the value of $p_I$ tends to zero. . . . . 84

5.11 The expected detection delays of a full-sensing CUSUM detection and full-sensing MMSSD detection, and is plotted with respect to different SNR's. $(m_I = 300, m_B = 30, \lambda_0 = 0.9, L = 5)$. The 95% confidence interval does not exceed $\pm 1$. . . . . 86

5.12 A comparison of the false alarm rate between a full-sensing CUSUM detection and full-sensing detection. The error bars are the 95% confidence intervals for each point. False alarm rates of the MMSSD's are designed to be slightly lower than those of CUSUM. $(m_I = 300, m_B = 30, \lambda_0 = 0.9, L = 5)$. . . . . 87

5.13 A comparison of the expected detection delay of an RC-MMSSD system that uses 3 sensors and CUSUM with 3 sensors and 30 sensors. (SNR=10dB, $m_B = 620, W = 10^5$). The 95% confidence interval does not exceed $\pm 1$. . . . . 88

5.14 A comparison of the false alarm of RC-MMSSD system that uses 3 sensors to CUSUM with 3 sensors and 30 sensors. (SNR=10dB, $m_B = 620, W = 10^5$). From the figure, the false alarm rates are similar with a statistical confidence level of 95%. . . . . 89

5.15 The expected detection delay of Shiryaev's Bayesian detection and MMSSD with M=3 and M=5. (SNR=10dB, $m_B = 620, L = 5, W = 10^5$). The 95% confidence interval does not exceed $\pm 1$ sample. . . . 90

5.16 The false alarm rates of Shiryaev's Bayesian detection and MMSSD with M=3 and M=5 are designed to be 0.01±0.01 in order to establish a baseline for comparison. (SNR=10dB, $m_B = 620, L = 5, W = 10^5$). 91

5.17 The false alarm rates of full-sensing MAR detection and MMSSD are designed to be 0.01±0.01 in order to establish a baseline for comparison. (SNR=10dB, $m_B = 620, L = 5, W = 10^5$). . . . . 92

5.18 The expected detection delay of full-sensing MAR detection vs. full-sensing MMSSD. (SNR=10dB, $m_B = 620, L = 5, W = 10^5$). The 95% confidence interval does not exceed ±1. . . . . 93

5.19 The states and the dynamics in the WLAN traffic models. . . . . 94

5.20 The KS distance between a WLAN model with the traffic of 75 packets per second and an exponential model parameterized by the variable $m_I$. When $m_I = 0.0022$, the KS distance is minimized. . . . . 96

5.21 The expected detection delay of MMSSD in a WLAN-based traffic model is compared to the nominal traffic model (SNR=10dB, $m_B = 620, L = 3, W = 10^5$). The 95% confidence interval does not exceed ±1. 98

5.22 The false alarm rate of MMSSD in a WLAN-based traffic model is compared to the nominal traffic model. The 95 percent confidence intervals are less than ± 1e-3 and not plotted to maintain legibility. (SNR=10dB, $m_B = 620, L = 3, W = 10^5$). . . . . 99

# Chapter 1

# Introduction

## 1.1 Motivation

Cogntive Radio (CR) has received much research attention in recent years for its potential to address the problem of spectrum scarcity. As the demands for bandwidth from smartphones significantly outgrow the supply of spectrum, the cost to transmit information wirelessly is increasing rapidly. Furthermore, the surveys [4, 14, 15] have shown that many commercial wireless networks around United States have experienced an under-utilization of their licensed spectrum bands. As a result, the need to improve the efficiency in bandwidth consumption has been highlighted as the main motivation for the development of CR.

CR is first proposed in [16] to address the issue of spectrum under-utilization. In general, CR describes a class of wireless technology that enhances communication performance by adapting its mode of communication to the surrounding radio environment. Spectrum sensing is one of the main methods for a CR to acquire information related to the radio environment and therefore plays an important role in

the design of CR.

Spectrum sensing concerns the problem of determining whether a spectrum band is available for CRs to conduct wireless communication. The objective of spectrum sensing may vary depending on what type of spectrum-related information is to be acquired. For example, some CR systems need to determine the presence of a wireless device in a spectrum band while other CR systems need to identify the type of wireless device it is. This leads to different types of spectrum sensing problems. In this thesis, the particular spectrum sensing problem of interest is to identify the availability states of spectrum bands.

For the rest of the thesis, a *spectrum band* will also be referred to as a *channel*. A channel can be in one of two availability states, i.e., it is in either a busy or an idle state. Given this, spectrum sensing is to provide the ability to determine the availability of a channel, so a CR can either identify an unused spectrum band to access, or determine when it needs to vacant the spectrum band for primary devices. In a hierarchical spectrum access scheme, primary devices are devices that have prioritized spectrum access over the CR devices. Typically, the "primary" networks are operated by licensed users, i.e., those who hold the licenses to operate in certain channels, while the "secondary" CR networks contain the unlicensed devices, who seek to access the same channels opportunistically. Therefore, CR is only permitted to access these spectrum bands under the pretence that it does not interfere with the transmission of the primary devices.

Given that the goal is to discern the availability state of a channel by observing it, the problem of spectrum sensing is naturally cast into a detection problem. Research

that applies detection theories to spectrum sensing problems is in abundance. Spectrum sensing methods based on classical hypothesis testing are studied in the context of energy detection [9,22], matched filter detection [22], and feature detection [1,2,17]. In the framework of classical hypothesis test described in [1, 2, 9, 17, 22], the primary criteria for the detector design is reliability, which is measured via the false alarm rate and the missed detection rate of the detector. However, the criteria does not concern agility, i.e., how responsive a detector is. Agility of a detector is measured by the expected amount of time that a detector needs to produce a decision. The methods proposed in [1, 2, 9, 17, 22] process a fixed block of observations and hence do not optimize agility of the system. In the context of CR, good system agility and reliability are both desirable properties for a spectrum sensing detector, because the time that is spent sensing a channel is both an overhead that reduces CR's capacity, and also a cause of interference to primary devices.

Sequential detection is an alternative scheme that optimizes a detector's agility. In [24], the spectrum sensing problem is addressed using sequential detection. By employing the sequential probability ratio test (SPRT), agility of the spectrum sensing system is optimized by minimizing the number of observations needed to complete the detection. With SPRT, decisions are produced after a sufficient number of observations is obtained. So the time to perform SPRT is usually less than that of a fixed-sample-size detector given that the same reliability is achieved. However, the problem formulation of SPRT assumes that the channel remains in a state over the duration of the detection process. If the number of observations is large, a channel may change its availability state over the time horizon of the detection, violating this assumption. To better represent the dynamics of changes in the channel's availability,

a different kind of sequential detection framework, i.e., *quickest detection*, is proposed.

Quickest detection is a sequential detection scheme that aims to detect a change in a random process. The application of quickest detection to spectrum sensing has been demonstrated in [10, 11, 28], where it is assumed that a channel experiences a change in its availability state and quickest detectors seek to detect that change as quickly as possible. The quickest detection problem formulation does not assume that the channel remains in one state, thus it is a more flexible model to represent the channel's availability state.

In some spectrum sensing scenarios, the traffic patterns in a channel can be characterized using stochastic models. Since the traffic patterns provide information on when a change of availability state will occur in a channel, this information has the potential to be used by a quickest detector to improve its performance. However, this information is not taken into account in [10, 11, 28] where it is assumed that the change time is unknown and nonrandom. On the other hand, the quickest detection problem formulation in [21, 25] uses a Bayesian approach, in which the problem is specially formulated based on the assumption that the change time is random. This latter problem is known as *Shiryaev's Problem*, and incorporates extra information about the statistical dynamics of the channel's state and the traffic patterns in a channel, in contrast to other quickest detection methods in [10, 11, 28].

Applying quickest detection methods in [10–12, 21, 25, 28] to spectrum sensing has a number of drawbacks. The first issue is that quickest detection still does not adequately model the real-world dynamics of the changes of availability states in a channel. Quickest detection assumes that a channel only experiences a change once, which contradicts the nature of the channel usage pattern that consists of multiple

periods of busy and idle times. It is shown later in this thesis that by assuming that only a single change point exists in a channel, quickest detectors encounter a performance floor in terms of reliability. When multiple busy and idle periods exist, a different model is needed to represent the multiple change points.

The second issue that limits the application of quickest detection for spectrum sensing is that quickest detection only concerns detecting changes in a single channel. In practice, idle time periods may appear in one of multiple channels. This calls for a new problem formulation that considers a different detection problem formulated over multiple channels. The problem formulation and framework proposed in [29] based on partially observable Markov decision processes (POMDP) addresses both of these shortcomings of quickest detection. POMDP addresses the first drawback by modeling the dynamics of a channel's availability states as an on-off process, which inherently accepts that a channel can transition between busy and idle states multiple times at multiple change points. Furthermore, POMDP addresses the second drawback by providing a framework to model multiple channels for spectrum sensing system would like to sense.

Both POMDP and quickest detection problems in [21, 25, 29] assume the change times to be unknown and random with a known a priori distribution. While the authors of [21, 25] have proposed a Bayesian quickest detection framework for a random change time of any probability distribution, a quickest detection design procedure is only known in the literature for a geometrically distributed change time. In [29], the derivation of its proposed optimal detector structure for spectrum sensing is also based on the premise that the change times are geometrically distributed. The geometric distribution model for the change times has been widely adopted for its

analytical tractability rather than for its ability to accurately represent real-world traffic dynamics. Sophisticated models have been purposed that better characterize traffic conditions and change times than geometric distributions. In [20, 26], analytical frameworks are developed to derive a random model for a duration of idle state. In [7, 8], an empirical approach to fitting real-world WLAN traffic usage to a distribution is studied. Although these are better models for change times, incorporating these models into a quickest detection and POMDP framework is a task that is non-trivial and needs to be further explored through research. Hence, this thesis will focus on the use of existing frameworks based on the geometric change-time model for the development of its proposed detectors. Later in the thesis, the applicability of the geometric distribution model is assessed using a more realistic traffic model derived from real data traffic [7, 8].

In [29], a framework based on POMDP is presented to consider a spectrum sensing problem where a detector searches for an idle period across multiple channels that each transition back and forth between idle and busy states. However, the framework in [29] assumes that the detector uses only one sensor, and since a spectrum sensing system may be processing multiple co-located sensor inputs, it thus lacks the flexibility to apply POMDP to problems multi-sensor processing. Furthermore, it is often the case that the number of sensors in a system is fewer than the number of channels available. This motivates the development of a spectrum sensing method that uses the scarce sensing resources efficiently. This thesis aims to generalize the work in [29] to problems that involve multiple sensors. In addition, this thesis also assumes that the duration of either idle or busy periods are geometrically distributed. In contrast to [29], the number of sensors considered in this thesis is arbitrary and greater than

one. Based on this problem, this thesis proposes detector designs to minimize the time required to identify an idle period, subject to a reliability constraint.

## 1.2 Contributions

The contributions of this thesis are listed as the following:

1. A problem formulation for the spectrum sensing problem is presented based on partially observable Markov decision processes (POMDP). In particular, this thesis is concerned with detecting an idle period across multiple channels using an arbitrary number of co-located sensors. Based on the POMDP formulation, the criteria for the detector design is formulated.

2. The detector designs from [29] are generalized to accommodate more than one sensor. As a result, two new detector designs are proposed. In particular,

   (a) the optimal detector structure derived in [29] is shown to apply generally to the problem of multiple sensors,

   (b) a sub-optimal detector design, named the *multiband multi-sensor spectrum sensing detector* (MMSSD), is proposed as a multi-channel spectrum sensing scheme that uses an arbitrary number of sensors,

   (c) a second sub-optimal detector and implementable design, named the *reduced complexity multiband multi-sensor spectrum sensing detector* (RC-MMSSD), is proposed as a low complexity version of MMSSD to handle spectrum sensing in a large number of channels,

   (d) detector threshold design methods are developed,

(e) and the performance impact of increasing the number of sensors is evaluated through Monte Carlo simulation.

3. The performance of the proposed multi-sensor detector is benchmarked against quickest detection methods. Specifically,

   (a) a procedure is presented to fairly compare the proposed detector designs to quickest detection methods,

   (b) a limitation on the reliability performance of quickest detectors is demonstrated in the context of on-off processes,

   (c) the performance impact of incorporating an a priori distribution of change times is investigated via comparisons with Page's CUSUM [10, 11],

   (d) and the differences in performance among MMSSD, RC-MMSSD, and other quickest detectors are characterized. These include Shiryaev's Bayesian detector [21, 25] and minimum asymptotic risk (MAR) detector [12].

4. The applicability of the proposed detectors to a realistic spectrum sensing model is assessed. The reference model is based on a channel usage model derived experimentally from wireless local area network (WLAN) user-datagram-packet (UDP) traffic [8]. The adequacy of assuming that the change times are geometrically distributed is tested.

## 1.3 Organization of Thesis

The organization of the thesis is summarized below.

In *Chapter 2*, a brief survey of existing detection frameworks that have been studied in the context of spectrum sensing is given. This chapter provides the background to the problem considered in this thesis and highlights how these approaches differ from one another and what these differences mean for the problem of spectrum sensing. The algorithms for the quickest detectors that will be used for subsequent comparison are also provided.

In *Chapter 3*, the main problem considered in this thesis is described. This chapter presents the system models, describes a problem formulation based on partially observable Markov decision processes (POMDP), and constructs the design criteria for the proposed detector designs.

In *Chapter 4*, new detector designs are proposed based on the design criteria stated in the previous chapter. The procedure that generalizes the optimal detector structure from one sensor to an arbitrary number of sensors is described along with generalized optimality. In addition, the proof of an optimality result that motivates the procedure is also presented. Details on the new detector designs are given, such as the rules to choose the threshold values as well as the applicability conditions for the proposed detector designs.

In *Chapter 5*, the results based on Monte Carlo simulations are given and the performance in terms of expected detection delays and false alarm rates are compared. For the comparisons between the proposed detector designs and the quickest detectors, this chapter describes the methodologies used to ensure fairness. In addition to the simulation results, discussions of the results are provided along with insights gained.

In *Chapter 6*, a summary and conclusion are provided. The summary captures the highlights from each of the chapters while the conclusion summarizes and comments

on the contributions of the thesis. It also explores topics for possible future research.

# Chapter 2

# Background

This chapters surveys the various problem formulations and solutions in the existing literature on the problem of spectrum sensing. Two broad categories of spectrum sensing problem formulations are examined: classical hypothesis testing and those based on quickest detection. Each problem formulation gives rise to different detection methods. The procedures for each of the methods are are described and discussed. For the quickest detection methods, the descriptions of the algorithms are provided in tables.

## 2.1 General Description of Spectrum Sensing

Spectrum sensing is the problem of determining whether a spectrum band is occupied or not. Such capability offers wireless systems the ability to decide which spectrum band they can access without involving a central entity, such as a base station. Using the signals received over air, a wireless system seeks out and opportunistically accesses an unused spectrum band. Since these systems appear to possess awareness about

the surrounding environment, they are called "cognitive radios".

In essence, spectrum sensing is a detection problem, because the objective of a detection problem is often to detect the presence of a signal, which in this case is the signal belonging to an occupant of the spectrum band. By applying detection theory, a reliable spectrum sensing system can be designed for cognitive radio.

To construct a detection problem for spectrum sensing, the spectrum band is modelled as a random system whose outputs depend on whether the band is occupied, or vacant. These outputs pertain to the observations from the receivers on the cognitive radio and offer information about the availability of the spectrum band. A detector is to be designed to extract this information with observations as its input, and produces a result with a reasonable level of reliability and overhead.

Different detection methods have been applied to the problem. In the upcoming sections, some of these detection approaches are described in detail.

## 2.2 Classical Hypothesis Testing

There is an abundance of literature that studies spectrum sensing through the framework of classical hypothesis testing [1, 2, 9, 17, 22]. To illustrate the framework, the problem involving an energy detection solution [9, 22] is described in this section. Suppose that there is a channel that may be occupied by another device, and a spectrum sensing system is deployed to determine whether the channel is available. It is assumed that while the spectrum sensing system performs the detection, the channel is either occupied, or idle. Let $X_t, t = 1, 2, ..., n$, be independent and identically distributed (i.i.d.) observations from the channel. The following hypotheses are

constructed:

$$\begin{cases} \mathcal{H}_0 : X_t = w_t, \\ \mathcal{H}_1 : X_t = gs_t + w_t, \quad t = 1, 2, ..., n \end{cases} \tag{2.1}$$

where $w_t$ is additive white Gaussian noise with mean equal to zero and variance equal to $\sigma^2$, $s_t$ is the signal transmitted by the other device occupying the channel that is unknown to the detector, $g$ is the slow fading channel coefficient and $n$ is the number of the observations. It is assumed that the term $gs_t$ is a zero-mean Gaussian random variable with variance $P$, and that $P$ is known in the problem. For a non-coherent detection problem related to spectrum sensing, this model has been adopted in [10,22]. It is clear that $\mathcal{H}_1$ pertains to the state in which the channel is occupied, and $\mathcal{H}_0$ to an idle state.

The performance of a detector is measured by two metrics: the probability of correct detection of $\mathcal{H}_1$, defined as

$$P_{\text{detection}} \equiv Pr(\mathcal{H}_1|\mathcal{H}_1), \tag{2.2}$$

and the probability of false alarm, denoted as

$$P_{\text{false alarm}} \equiv Pr(\mathcal{H}_1|\mathcal{H}_0), \tag{2.3}$$

where $Pr(\{\cdot\})$ denotes "take the probability of". Based on these defined performance metrics, a detector is designed with the following Neyman-Pearson criterion [19]:

$$\begin{aligned} &\max Pr(\mathcal{H}_1|\mathcal{H}_1) \\ &\text{subject to } Pr(\mathcal{H}_1|\mathcal{H}_0) \leq \alpha \end{aligned} \tag{2.4}$$

The criterion (2.4) indicates that a detector is designed to maximized the probability of detection when $\mathcal{H}_1$ is true while the false alarm rate being subject to a constraint $\alpha \in (0, 1)$.

### 2.2.1 Energy Detection

A solution to the classical hypotheses testing problem is energy detection. This method assumes that the number of observations is fixed throughout the detection, i.e., $n$ is a constant. For this reason, energy detection is considered to be a fixed-length detection method. Let $\overline{\mathbf{x}} \equiv \{x_1, x_2, ..., x_n\}$ be realizations of the random observations $\overline{\mathbf{X}} \equiv \{X_1, X_2, ..., X_n\}$. The test for energy detection is derived from the likelihood ratio test, where a likelihood ratio is compared to a threshold to discern between $\mathcal{H}_1$ and $\mathcal{H}_0$. Since the random observations are independent, the likelihood ratio for $n$ observations is defined as

$$L(\overline{\mathbf{x}}) = \prod_{i=1}^{n} l(x_i) = \prod_{i=1}^{n} \frac{p(x_i|\mathcal{H}_1)}{p(x_i|\mathcal{H}_0)} \tag{2.5}$$

where $p(x_i|\mathcal{H}_1)$ and $p(x_i|\mathcal{H}_0)$ are the conditional probability density functions (pdf) of observations at time $t$ under the hypotheses $\mathcal{H}_1$ and $\mathcal{H}_0$, respectively. Given the system model in (2.1), the likelihood ratio test can be simplified to that of energy detection, which has the following structure:

$$T(\overline{\mathbf{x}}) \equiv \sum_{i=1}^{n} x_i^2 \underset{\mathcal{H}_1}{\overset{\mathcal{H}_0}{\lessgtr}} \eta \tag{2.6}$$

where the test statistic $T(\overline{\mathbf{x}})$ is compared to a constant threshold $\eta$ to decide between $\mathcal{H}_0$ and $\mathcal{H}_1$. According to the Neyman-Pearson Lemma, an energy detector with a constant threshold $\eta$, with which $P_{\text{false alarm}} = \alpha$, is a detector that maximizes $P_{\text{detection}}$ among all the detectors that process $n$ observations and have an equal $P_{\text{false alarm}}$. With $x_i$ being a zero-mean Gaussian variable, the test statistic $T(\overline{\mathbf{x}})$ has a chi-square distribution with $n$ degrees of freedom. Closed-form solutions for the performance metrics are available if $n$ is an even number. The probabilities of false alarm and of

detection as functions of the threshold $\eta$ are, respectively,

$$P_{\text{false alarm}} = Pr(T(\overline{\mathbf{x}}) > \eta | \mathcal{H}_0) = Q_{2n}\left(0, \frac{\sqrt{\eta}}{\sigma_0}\right), \tag{2.7}$$

and

$$P_{\text{detection}} = Pr(T(\overline{\mathbf{x}}) > \eta | \mathcal{H}_1) = Q_{2n}\left(0, \frac{\sqrt{\eta}}{\sigma_1}\right) \tag{2.8}$$

where $Q_{2n}(a, b)$ is the generalized Marcum Q function. The function is defined in [13], which also provides tabulated values. To find the threshold that satisfies $P_{\text{false alarm}}$, one would need to solve for $\eta$ in (2.7).

As can be seen in the detector structure in (2.6), the number of observations $n$ is a parameter required to be pre-designed, that does not change dynamically during the process of detection. In the next section, a different problem formulation is visited where the number of the observations is not fixed but is instead modelled as a random variable to achieve a certain performance criteria.

### 2.2.2 Sequential Probability Ratio Test

An alternative solution to classical hypothesis testing is the sequential probability ratio test method (SPRT) [24]. As its name suggests, SPRT performs detection every time a new observation sample becomes available. The detection stops as soon as a sufficient number of observations has been sampled. Therefore, since it depends on observations, the number of observations required to make a decision is a random variable, denoted by $N$. If observations are independent and identically distributed (i.i.d.), the SPRT is optimal [27], i.e. it minimizes the number of observations while achieving a certain level of performance in terms of both $P_{\text{detection}}$ and $P_{\text{false alarm}}$.

The observed samples are processed sequentially in the SPRT. At every discrete

time $t$, SPRT recursively computes the likelihood ratio based on the current observation and the likelihood ratio in the previous time t-1. Let $\overline{\mathbf{x}}_t \equiv \{x_1, x_2, ..., x_t\}$, and the likelihood ratio be computed recursively as

$$L(\overline{\mathbf{x}}_t) = \frac{p(x_t|\mathcal{H}_1)}{p(x_t|\mathcal{H}_0)} l(\overline{\mathbf{x}}_{t-1}), \quad t = 1, 2, 3, ... \tag{2.9}$$

where $p(x_t|\mathcal{H}_1)$ and $p(x_t|\mathcal{H}_0)$ are the conditional probability density functions (pdf) of observations at time $t$ under the hypotheses $\mathcal{H}_1$ and $\mathcal{H}_0$, respectively, and $l(\overline{\mathbf{x}}_1) = \frac{p(x_1|\mathcal{H}_1)}{p(x_1|\mathcal{H}_0)}$.

Following the computation of the likelihood ratio, SPRT applies a decision rule involving two thresholds $\eta_1$ and $\eta_0$ as below

$$\begin{aligned} l(\overline{\mathbf{x}}_t) \geq \eta_1 : &\quad \text{accept } \mathcal{H}_1 \\ l(\overline{\mathbf{x}}_t) \leq \eta_0 : &\quad \text{accept } \mathcal{H}_0 \\ \eta_0 < l(\overline{\mathbf{x}}_t) < \eta_1 : &\quad \text{take another sample.} \end{aligned} \tag{2.10}$$

The performance constraints of the detector, such as the constraint on the false alarm rate, $\alpha$, and on the missed detection rate, $\beta$, are considered to be the key parameters in the SPRT threshold design. Specifically, $\beta$ is defined as

$$\beta \geq P_{\text{missed detecton}} \tag{2.11}$$

where $P_{\text{missed detecton}} \equiv 1 - P_{\text{detection}}$ is the missed detection rate of a detector. The thresholds can be determined from the error probabilities according to the following bounds [27]

$$\eta_1 \leq \frac{1-\beta}{\alpha} \tag{2.12}$$

and,

$$\eta_0 \geq \frac{\beta}{1-\alpha}. \tag{2.13}$$

The inequalities in (2.12) and (2.13) become equalities if $l(\overline{\mathbf{x}}_t)$ is equal to the exact values of either $\eta_1$ and $\eta_2$ when the detection process stops. Since $l(\overline{\mathbf{x}}_t)$ is likely to cross either thresholds when the detection stops, $\alpha$ and $\beta$, serve as upper bounds to performance metrics $P_{\text{false alarm}}$ and $P_{\text{missed detection}}$, respectively.

## 2.3 Quickest Detection

Quickest detection is a significantly different spectrum sensing problem formulation compared to that of classical hypothesis testing. The major difference lies in the inherent assumption in each type of problem about the dynamics of the states of spectrum occupancy. Classical hypothesis testing is based on the assumption that each hypothesis pertains to one state. By detecting a state of a spectrum band, it is implied that the random process that models the spectrum band remains constant in that one state. In the quickest detection problem formulation, a change in the stochastic nature of the random process is assumed to occur, and the detection of such changes become the objective of the problem.

Suppose that a spectrum band occupancy is modelled as a random process and the problem is to identify the onset of an idle period, and that the process falls into one of these two hypotheses:

$$\begin{aligned} &\mathcal{H}_0 : X_t = Ps_t + w_t, t = 1, 2, ..., n \\ &\mathcal{H}_1 : \exists \tau \in 1, 2, ..., n \quad \text{such that,} \\ &\qquad X_t = \begin{cases} Ps_t + w_t, & t = 1, 2, ..., \tau - 1 \\ w_t, & t = \tau, \tau + 1, ..., n \end{cases} \end{aligned} \tag{2.14}$$

where $w_t, s_t$, and $P$ are defined identically to (2.1). Under the hypothesis $\mathcal{H}_0$, no change occurs over time duration from $t = 1$ to $n$, so a spectrum band remains in an

idle state. On the other hand, under the hypothesis $\mathcal{H}_1$, the random process switches abruptly from being in an idle state to a busy state at time $\tau$ and its stochastic nature changes accordingly. The time $\tau$ is referred to as the change time. Based on the model in (2.14), before the change time, an observation $X_t$ is a sample drawn from the distribution of a busy state $f_0$, which is a zero-mean normal distribution with variance $(P + \sigma^2)$, and after the change time, $X_t$ is drawn from the distribution of an idle state $f_1$, i.e., a zero-mean normal distribution with variance $\sigma^2$.

Suppose at the time $t_{\text{stop}}$, a detector raises an alarm that a spectrum band has become idle. If $t_{\text{stop}} \geq \tau$, i.e., the alarm follows the onset of the idle period, the detector has been correct in declaring the state of the spectrum band and $T_{\text{delay}} = t_{\text{stop}} - \tau$ is the detection delay from when the change occurs to when the alarm is able to detect the change. If $t_{\text{stop}} < \tau$, the detector has alarmed the change prematurely, which is considered to be a false alarm event.

To measure the performance of a quickest detector, some metrics must be established. The first performance measure is detection delay, which is an overhead of detection. Less detection delay means that a detector is more agile, i.e., it can promptly alarm the availability of an idle period. As $T_{\text{delay}}$ is a random variable because observations are random, the mean of $T_{\text{delay}}$ is the average detection delay, conditioned on that $\mathcal{H}_1$ is true and a value of $\tau$:

$$\mathbb{E}_{\mathcal{H}_1,\tau}[T_{\text{delay}} | t_{\text{stop}} \geq \tau] \tag{2.15}$$

where $\mathbb{E}(\cdot)$ is the conditional expectation operator over the distribution of the random observations $\overline{\mathbf{X}} \equiv \{X_1, X_2, ..., X_{t_{\text{stop}}}\}$. In one problem formulation, the change time $\tau$ is modelled as a random variable, while in another problem formulation, the change time is assumed to be unknown.

The second performance measure concerns reliability, or the level of false alarms, of a detector. Again, different quickest detection problem formulations include different ways of quantifying reliability. In the following sections, two problem formulations, which measure the average detection delay and the level of false alarm in different ways, are examined.

### 2.3.1 Page's CUSUM

In a problem formulation that leads to Page's CUSUM algorithm [10], the change time $\tau$ is assumed to be unknown so that the worst-case detection delay is used to quantify the detection delay,

$$\overline{T}_{\text{delay}} = \sup_{\tau \geq 1} \text{ess sup}\, \mathbb{E}_{\mathcal{H}_1,\tau}[T_{\text{delay}} | t_{\text{stop}} \geq \tau]. \tag{2.16}$$

where ess sup of a function $f$ is the essential supremum of the function, and $\mathbb{E}(\cdot)$ is a conditional expectation operator over the distribution of the random observations $\overline{\mathbf{x}} \equiv \{X_1, X_2, ...X_{t_{\text{stop}}}\}$.

Measuring reliability involves the use of a performance metric named the average false alarm run length. It is defined as the average length of time that elapses before a detector declares a false alarm, given that no change has occurred in a spectrum band. In particular, the average false alarm run length of a false alarm, or $T_{\text{ARL}}$, is

$$T_{\text{ARL}} = \mathbb{E}_{f_0}[T_{\text{stop}}], \tag{2.17}$$

where $T_{\text{stop}}$ is a random stopping time of a quickest detector and the expected value of $T_{\text{stop}}$ is conditioned on observations having marginal distributions that are equal to $f_0$, which is the distribution of $X_t$ in a busy state when $X_t = Ps_t + w_t$. The objective of a detector is to minimize the worst-case detection delay while maintaining the

average false alarm run length above a given threshold. Given $T_{\text{ARL}}^{\min}$ as the minimum threshold for the average false alarm run length, and $\Gamma$ as a set of all decision rules, the design criteria is

$$\begin{aligned} &\min_{\Gamma} \quad \overline{T}_{\text{delay}} \\ &\text{subject to } T_{\text{ARL}} \geq T_{\text{ARL}}^{\min}. \end{aligned} \tag{2.18}$$

As is evident above, the problem formulation is constructed as a minimax formulation, where the objective is to minimize the maximum possible detection delay that the random process may experience.

The problem formulation leads to Page's CUSUM algorithm. It is a sequential detection method that computes test statistics and performs a test at every time t. Let $l'(x_t)$ be the log-likelihood function of an observation at time $t$, and

$$l'(x_t) = \log l(x_t) = \log \frac{f_1(x_t)}{f_0(x_t)}, \tag{2.19}$$

where $f_0(x)$ and $f_1(x)$ are the probability density functions of an observation before and after the change time $\tau$. The test statistic of Page's CUSUM, denoted as $Q_t$, is updated at each time $t$ according to the following equation:

$$Q_t = \max\{0, Q_{t-1} + l'(x_t)\}, \tag{2.20}$$

where the initial value of the test statistic at $t = 0$ is $Q_0 = 0$. At time $t$, CUSUM performs a decision test according to the following detector structure after the likelihood ratio is computed:

$$\begin{aligned} Q_t \geq h: &\quad \text{stops and declare the channel to be idle} \\ Q_t < h: &\quad \text{take another sample} \end{aligned} \tag{2.21}$$

Table 2.1: The algorithm of CUSUM Detection

**Algorithm for Page's CUSUM**

$Q_0 \leftarrow 0$
$t \leftarrow 1$
**repeat**
  {Get observations $x_t$}
  {Compute $l'(x_t)$}
  $Q_t \leftarrow Q_{t-1} + l'(x_t)$
  **if** $Q_t < 0$ **then**
    $Q_t \leftarrow 0$
  **end if**
**until** $Q_t \geq h$
{Stop and declare the channel to be idle.}

where $h$ is the threshold. For clarity, the decision algorithm is provided in Table 2.1. In [18], CUSUM is shown to be the optimal detection method that minimizes the worst-case detection delay among all the detectors that have the same or longer average false alarm run length, for any value of average false alarm length.

### 2.3.2 Shiryaev's Problem

In [21, 25], a different approach to quickest detection, called Shiryaev's Problem, is considered. Shiryaev's Problem has a Bayesian framework since it treats the change point $\tau$ as a random variable, with known a priori distribution.

To formulate the problem, the following performance metrics are first defined. Let $\hat{T}_{\text{delay}}$ be the average detection delay of the detector, and

$$\hat{T}_{\text{delay}} = \mathbb{E}[T_{\text{delay}} | t_{\text{stop}} \geq \tau], \tag{2.22}$$

where the expectation $\mathbb{E}[\cdot]$ is computed over the joint probability density involving

the random variables consisting of the change time $\tau$ and the sequence of random observations $\overline{\mathbf{X}} \equiv \{X_1, X_2, X_3, ...\}$. To measure the false alarm performance, Shiryaev's Problem specifies the performance in terms of a false alarm rate, which is different from CUSUM. Let $P_{\text{fa}}$ denote the false alarm rate, where

$$P_{\text{FA}} = Pr(t_{\text{stop}} < \tau). \tag{2.23}$$

Since both high average detection delay and high false alarm rate are undesirable, a risk function that treats both of these measures as costs is defined, and the objective for the detector is to result in a stopping time $t_{\text{stop}} \in \mathcal{T}$ that minimizes such cost involving detection delay and false alarm rate:

$$\inf_{t_{\text{stop}} \in \mathcal{T}} \quad [P_{\text{FA}} + c\hat{T}_{\text{delay}}], \tag{2.24}$$

where the variable $c \in \{c \geq 0 | P_{\text{FA}} < \alpha\}$ is a trade-off constant between the false alarm rate and the average detection delay, and its value must be chosen such that the false alarm constraint $\alpha$ is satisfied. Before a solution to (2.24) may be proposed, an a priori distribution needs to be defined for the change time $\tau$. It is assumed in [21] the change time distribution is geometric, and in discrete time, its probability mass function (pmf) is

$$Pr(\tau = k) = \begin{cases} \pi & k = 0 \\ (1-\pi)\rho(1-\rho)^{k-1} & k = 1, 2, 3, ... \end{cases} \tag{2.25}$$

where the parameter $\rho = Pr(\tau = k | \tau \geq k)$. The same assumption about the change time is adopted for the new methods developed in this thesis. The assumption has also been adopted in [29] concerning spectrum sensing and a justification based on analytical tractability is described in Section 3.2.2. Later on, the validity of this assumption is examined through simulations.

An optimal solution for the problem formulation (2.24) with the geometric change time distribution in (2.25) is cited in [21]. In this case, the optimal stopping time, denoted as $T^*_{\text{stop}}$, has the following structure:

$$T^*_{\text{stop}} = \inf\{t \geq 0 | \pi_t \geq \pi^*\} \tag{2.26}$$

where $\pi^* \in [0, 1]$ is an appropriately chosen threshold, and $\pi_t$ is the a posteriori probability of a spectrum band being idle, which at each time t is updated. The detection algorithm is described in Table 2.2. At discrete time $t$, the test statistic in (2.26) is updated via

$$\pi_t = \frac{f_1(x_t)[\pi_{t-1} + \rho(1 - \pi_{t-1})]}{f_1(x_t)[\pi_{t-1} + \rho(1 - \pi_{t-1})] + f_0(x_t)(1 - \rho)(1 - \pi_{t-1})}, \quad t = 1, 2, 3, ... \tag{2.27}$$

where $f_0(x)$ and $f_1(x)$ are the probability densities of an observation before and after the change time $\tau$, respectively, and $\pi_0 = \pi$. Note that the test statistic $\pi_t$ is the probability of a spectrum band being idle at time $t$, or

$$\pi_t = \Pr(\text{“spectrum is idle at time t”} | x_1, x_2, ..., x_t). \tag{2.28}$$

No closed-form expression exists, however, for determining $\pi^*$ to satisfy a given probability of false alarm. It can be obtained iteratively but nested integrations are involved. A way to design the threshold for (2.26) is to design the detector to exceed the false alarm constraint. Following results in [25], a threshold, $\pi^*$, to satisfy $P_{FA} \leq \alpha$ is chosen as

$$\pi' = 1 - \alpha. \tag{2.29}$$

This follows directly from (2.26), (2.28) and the definition of $P_{\text{FA}}$. As seen in the

Table 2.2: The algorithm of Shiryaev's Bayesian Detector

**Algorithm for Shiryaev's Bayesian Detector**

$\pi_0 \leftarrow \pi$
$t \leftarrow 1$
**repeat**
  {Get observations $x_t$}
  {Compute $\pi_t(x_t)$}
  $t \leftarrow t + 1$
**until** $\pi_t \geq \pi'$
{Stop and declare the channel to be idle.}

proposed stopping rule (2.26), the detector stops when

$$\begin{aligned}
&\inf\{t \geq 0 | \pi_t \geq \pi^*\} \\
&\equiv \inf\{t \geq 0 | \Pr\{\text{spectrum idle at time } t\} \geq 1 - \alpha\} \\
&\equiv \inf\{t \geq 0 | \, \mathbb{E}\left[\mathrm{I}_{\{\text{spectrum idle at time } t\}}(X_1, X_2, ..., X_t)\right] \geq 1 - \alpha\} \qquad (2.30)
\end{aligned}$$

where $\mathrm{I}_{\{\text{spectrum idle at time } t\}}(X_1, X_2, ..., X_t)$ is the indicator function with value 1 if spectrum is idle and 0 otherwise. The rule is equivalent to

$$\inf\{t \geq 0 | 1 - \mathbb{E}\left[\mathrm{I}_{\{\text{spectrum idle at time } t\}}(X_1, X_2, ..., X_t)\right] \leq \alpha\}, \qquad (2.31)$$

which, by definition, is

$$\inf\{t \geq 0 | P_{\mathrm{FA}} \leq \alpha\}. \qquad (2.32)$$

### 2.3.3 Minimum Asymptotic Risk Detection

It can be seen that the previous quickest detectors have different measures for their reliability performances. While Page's CUSUM aims to meet a minimum $T_{\mathrm{ARL}}^{\min}$,

Shiryaev's Problem constructs a risk function with the appropriate tradeoff constant $c$ such that the constraint on the false alarm rate $\alpha$ is satisfied. The minimum asymptotic risk (MAR) detection is another quickest detection framework developed in [12]. The problem formulation of MAR is based on a modified version of Shiryaev's Problem that incorporates both of these measures of reliability.

In [12], the problem formulation for MAR detection is called the *modified Shiryaev's criterion*, which is defined as such.

$$\begin{aligned} \min \quad & \mathbb{E}_{\mathcal{H}_1}[T_{\text{delay}} | t_{\text{stop}} \geq \tau] \\ \text{subject to } & T_{\text{ARL}} \geq T_{\text{ARL}}^{\min}, \\ \text{and } & P_{FA} < \alpha. \end{aligned} \tag{2.33}$$

where $T_{\text{ARL}}$ and $P_{FA}$ are defined in (2.17) and (2.23), respectively, and $\mathbb{E}_{\mathcal{H}_1}[T_{\text{delay}} | t_{\text{stop}} \geq \tau, \overline{\mathbf{x}}]$ is the expected detection delay, as defined in (2.15). The modified Shiryaev's criterion assumes that the change time $\tau$ is a fixed, unknown, and non-random entity.

Based on the modified Shiryaev's criterion, the minimum asymptotic risk detector is proposed. Let $Q'_t$ be non-logarithmic version of the Page's CUSUM statistic (2.20) at time $t$, where

$$Q'_t = \max\{1, Q'_{t-1}\} l(x_t), \tag{2.34}$$

In the MAR decision rule, the following test statistic is computed at time $t$:

$$\hat{r}(x_t) = \frac{Q'_t \epsilon \psi - (1-\epsilon)}{Q'_t \epsilon + 1 - \epsilon} t, \quad t = 1, 2, 3, ... \tag{2.35}$$

where $\epsilon$ and $\psi$ are MAR design parameters, and $Q_0 = 1$. The design methods for the design parameters $\epsilon$ and $\psi$ are not available as the closed-form expressions. However,

Table 2.3: The algorithm of the MAR detection

**Algorithm for the MAR Detection**

$Q'_0 \leftarrow 1$
$t \leftarrow 1$
**repeat**
  {Get observations $x_t$}
  {Compute $l'(x_t)$}
  $Q'_t \leftarrow Q'_{t-1} + l(x_t)$
  **if** $Q'_t < 1$ **then**
    $Q'_t \leftarrow 1$
  **end if**
  {Compute $\hat{r}(x_t)$}
**until** $\hat{r}(x_t) > \hat{r}(x_{t-1})$
{Stop and declare the channel to be idle.}

the performances of the MAR detector have been shown to be insensitive to the fact whether $\epsilon$ and $\psi$ are different or not [12]. Thus, when designing for MAR, the parameters $\epsilon$ and $\psi$ can be set to be the same value, and only one parameter needs to be designed. The detection rule for MAR to stop and declare a change is when

$$\hat{r}(x_t) > \hat{r}(x_{t-1}). \tag{2.36}$$

Table 2.3 provides a description of the algorithm used for the MAR detection.

An important result in [12] shows that the test statistic $\hat{r}(x_t)$ converges to a non-causal Bayesian risk function composed of expected delay time, false alarm rate, and average run length, under the asymptotic condition that either $l(x_t) \to 1$ or $\alpha \to 0$ is true. Therefore, under the modified Shiryaev's criterion (2.33), the MAR detection is asymptotically optimal.

# Chapter 3

# System Models and Problem Formulation

In the previous chapter, various problem formulations and detection methods are surveyed. It has been seen that the problem of spectrum sensing can be cast in different ways. This chapter describes a system model and problem formulation that incorporates a greater degree of channel dynamics into the system. These are developed as the basis for the new spectrum sensing methods that form the main contribution of this thesis.

## 3.1 System Models

In this section, the system model to describe the dynamics of a channel's state is proposed. Also, a signal model for an observation in both idle and non-idle periods is described.

### 3.1.1 Channel Usage Models

Suppose that there are $L$ channels where each channel undergoes periods of idle and busy states. In an idle state, the primary device of the channel is not active. In a busy state, the primary device occupies the channel and access from a cognitive radio device is not permitted. Assuming that the system is modelled in discrete-time, the periods of busy and idle states in a channel are represented by a discrete-time ON-OFF process, where the ON and OFF phases represent the busy and idle states, respectively. Stochastic models are given for when a primary device emerges and when it exits: it is assumed that a primary device emerges in and exits from a channel according to an exponential ON-OFF process, in which the durations of busy and idle periods are assumed to be random and geometrically distributed. Let $T_{\text{busy}}$ and $T_{\text{idle}}$ be the random durations of a busy period and an idle period in $l^{\text{th}}$, respectively, and their respective probability mass functions (pmf) are

$$Pr(T_{\text{busy}} = k) = (1 - p_B)^{k-1}(p_B), \quad k = 1, 2, 3, ... \tag{3.1}$$

$$Pr(T_{\text{idle}} = k) = (1 - p_I)^{k-1}(p_I), \quad k = 1, 2, 3, ... \tag{3.2}$$

$p_B$ and $p_I$ are probabilities that a respective busy or idle period, has a duration equal to $k$ given that the duration is greater than $k - 1$. In addition to $p_I$ and $p_B$, let $\lambda_o$ be the fraction of idle periods to the total time period, which is a function of average durations of busy and idle periods. To illustrate this relationship, let $m_B$ and $m_I$ be the average durations of a busy and an idle period, respectively. According to the Poisson arrival process,

$$m_B = 1/p_B, \tag{3.3}$$

$$\text{and } m_I = 1/p_I. \tag{3.4}$$

The fraction of idle periods to the total time period, or just fraction of idle time for short, is by definition

$$\lambda_o = \frac{m_I}{m_I + m_B}. \tag{3.5}$$

Across $L$ channels, it is assumed that the ON-OFF process used to model the channel usage is the same, i.e., the channel usage dynamics of each channel are described by (3.1)-(3.5) using identical values for the parameters $m_I, m_B, p_I$, and $p_B$, and that channel usage behaviours in each channel are statistically independent from one another.

### 3.1.2 Signal Model for Observations

Suppose a spectrum sensing system that is equipped with $M$ co-located sensors simultaneously observes different channels. As a result, at a given time $t$, the $M$ observations that correspond to the channels being observed form a $M$-set of $L$ possible channel observations. For example, let $X_l(t)$ be a random variable denoting the observation at time $t$, of channel $l$, for $1 \leq l \leq L$. For example, for the case of $M = 4$ and $L = 10$, let $\{1, 3, 6, 8\}$ denote one of the 4-sets of channel indices being observed. Then the corresponding observations are $\{X_1(t), X_3(t), X_6(t), X_8(t)\}$.

The signal model describes the probability distributions underlying these random observations. The probability distribution behind a random observation $X_l(t)$ depends on the state of the channel $l$, i.e., whether the channel is in a busy or in an idle state. The signal model is directly formulated as an energy detection problem because little knowledge of signalling is assumed. As a consequence of this formulation, when the channel being observed is in an idle state, the observation $X_l(t)$ is drawn from a zero-mean Gaussian distribution that has a variance of $\sigma^2$, and when the channel is in

a busy state, the observation $X_l(t)$ is drawn from a zero-mean Gaussian distribution that has a variance of $(\sigma^2 + P)$. The signal-to-noise ratio (SNR) in decibel units (dB) is defined as $10 \log_{10}(P/\sigma^2)$.

## 3.2 Problem Formulation

### 3.2.1 General Multiband Multi-sensor Detection

Consider a spectrum sensing system equipped with $M$ sensors, is to simultaneously detect an idle period from $L$ channels. In each observed time instant, the spectrum sensing system observes $M$ observations, processes the observations, and generates an action that is either 1) *stop and declare*: indicating that an idle period has been discovered and terminate the detection process, or 2) *continue and observe*: continue the detection process for a longer time in a set of $M$ channels that may be the same or different from the channels that were observed at the current time $t$. In contrast to classical detection methods, which sample observations over multiple time instants, the described sequential detection method performs processing and produces an action in each observation period. In addition, the process stops as soon as a satisfactory level of reliability is reached.

The performance measures for the sequential detection method are the false alarm rate and the expected detection delay time. The false alarm rate, denoted as $P_{\text{FA}}$, is the probability of declaring a channel idle at time $t$ when the channel state is busy. This type of false alarm leads to cognitive radios causing interference to primary devices and therefore should be kept to a low level. To define the expected detection delay time, a random variable must be defined. Let $T_{\text{declare}}$ be the random elapsed

time from when the detection process begins to when the detection process declares a discovery. The expected detection delay time is therefore $\mathbb{E}[T_{\text{declare}}]$, where $\mathbb{E}[\cdot]$ is the expectation operator over the probability space of the random observations as well as the random change time, as defined in Sections 3.1.1 and 3.1.2.

Given a false alarm constraint $\alpha$, the design criterion for the proposed sequential detector is:

$$\begin{aligned} &\min \mathbb{E}\left[T_{declare}\right] \\ &\text{subject to } \mathrm{P}_{FA} \leq \alpha. \end{aligned} \tag{3.6}$$

Compared to other quickest detection formulations, the problem formulation (3.6) is similar in some ways but different in others. First of all, the formulation (3.6) considers $L$ channels and $M$ observations in each time instant while the previous problem formulations consider just one single channel. Secondly, the formulation (3.6) supposes that each channel experiences periods of usages, and models these periods as an ON-OFF process. Thirdly, similar to Shiryaev's Problem, the formulation (3.6) models these periods as having durations that can be characterized by a random distribution, which leads to models that can characterize the onset of change times. As the change times have been assigned probability densities, the formulation (3.6) differs from Page's CUSUM, which is a minimax approach as the CUSUM criterion seeks to minimize the worst-case delay of the detector, in that it minimizes the expected detection delay that factors in the distributions of change times. Finally, a significant difference compared to some of the previous quickest detectors is that the formulation (3.6) only considers the constraint on false alarm rate, while leaving out the average run length to a false alarm.

### 3.2.2 Partially Observable Markov Decision Processes

The random model to represent the durations of busy and idle states is the geometric distribution, which is the result of assuming that the primary device enters into and exits from a channel according to the exponential ON-OFF process. An exponential ON-OFF process is defined a random process made up of a sequence of events of either primary device entering or exiting from the channel, and the time elapsed between each successive event is exponentially distributed. Since the discrete time analogue of the exponential distribution is the geometric distribution and the process in question is discrete time, it is adopted as the channel usage model.

A property of the geometric distribution is that the random process is invariant to time-shifts, that is, given that a channel is in one state at time $t$, the probability that the channel will switch state in a future time instant $(t + \delta t)$, for $\delta t = 1, 2, 3, ...$, is a function of $\delta t$ and is invariant to the value of $t$. Because the dynamics of state transitions in the future only depend on the current state of the channel, they can be accurately modelled as a Markov process.

Based on [29], the use of a partially observable Markov decision process (POMDP) to formulate a problem to solve (3.6) is introduced. The POMDP is a decision theoretic framework that relies on the property of the time-shift invariance in the channel usage model. Compared to classical quickest detection methods such as Shiryaev's Problem [21] and Pages's CUSUM [10], a fundamental difference is that the channel is seen as an ON-OFF process in the POMDP formulation, whereas in [10, 25] the channel is assumed to start at one state, switch to the other state and remain in the other state; in other words, only one change would occur over the entire time horizon. It can be clearly observed that an ON-OFF process is a

more realistic model for the channel process occupancy than the model assumed in the classical quickest detection methods. Furthermore, by assuming a single change point, the classical quickest detectors do not take into account the particular false alarm situation where the detector declares a channel to be idle after that channel has exited the idle state.

The problem of detecting an idle period among $L$ channels, employing only one sensor ($M = 1$) has been studied in [29]. Our contribution extends the framework laid out in [29] to include an arbitrary number of sensors. In the following is a formulation that generalizes POMDP in [29] to the case of multiple sensors.

#### 3.2.2.1 State Space

The channels underlying the system each have an independent state. These states are defined as $\{Z_1(t), ..., Z_L(t)\}$, where $Z_l(t) \in \{0, 1, \Delta\}$, for $1 \leq l \leq L$ and $t = 1, 2, 3, ...$, is state of the $\mathrm{l}^{\mathrm{th}}$ channel at time $t$. The first two values of $Z_l(t)$, i.e., State 0 and State 1, respectively represent busy and idle states. In addition to State 0 and State 1, there is the absorption state, denoted by $\Delta$, that defines the end of the detection process. When the absorption state $\Delta$ is reached, the states for all channels become equal to the state $\Delta$.

#### 3.2.2.2 Action Space

Let $a_t$ be the action taken at time $t$. The action space consists of all the possible actions for $a_t$, and is separated into two sets. The first set, denoted as $\mathcal{C}$, contains $\binom{L}{M}$ distinct actions to observe $M$ out of $L$ channels. To define an element in the set $\mathcal{C}$, it is necessary to first define a separate set of actions: let $\{C_1, C_2, C_3, ..., C_L\}$ be a set

containing all the actions that corresponds to observing each of the $L$ channels, where an element in this set, which is denoted by $C_l$, for $1 \leq l \leq L$, indicates the action of observing channel $l$. As the number of sensors is less than or equal to the number of channels, only the subsets that are the $M$-sets of the set $\{C_1, C_2, C_3, ..., C_L\}$, i.e., observing $M$ channels, constitute a valid action for $a_t$ and thus collectively form the set $\mathcal{C}$. Let each $M$-set in $\mathcal{C}$ be denoted by an index $j$, so that a particular $M$-set can be referred to as $\overline{C}_j$, where $1 \leq j \leq \binom{L}{M}$. For example, suppose an $M$-set in $\mathcal{C}$ that contains channel indices 2, 4, 5 is denoted as $\overline{C}_6$, then the $M$-set that corresponds to $\overline{C}_6$ would be expressed as $\{C_2, C_4, C_5\}$, which indicate that this particular action is to continue to observe channels 2, 4, and 5.

The second set, denoted as $\mathcal{D}$, is related to actions of declaring a channel idle. Within $\mathcal{D}$, each action is denoted as $D_i$ and represents declaring the $l^{th}$ channel idle, $1 \leq l \leq L$.

#### 3.2.2.3 State Transition

As described earlier, the assumption that the duration of each state is geometrically distributed is consistent with the use of a state transition model to represent the dynamics of change in channel states. Given the channel state for a channel at time $t$, or $Z_l(t)$, the dynamics of the state change are functions of the action space as well as parameters $p_B$ and $p_I$. These are illustrated in the state transition diagram Fig. 3.1. As all channels are assumed to have independent and identically distributed transition dynamics, Fig. 3.1 applies across $L$ channels.

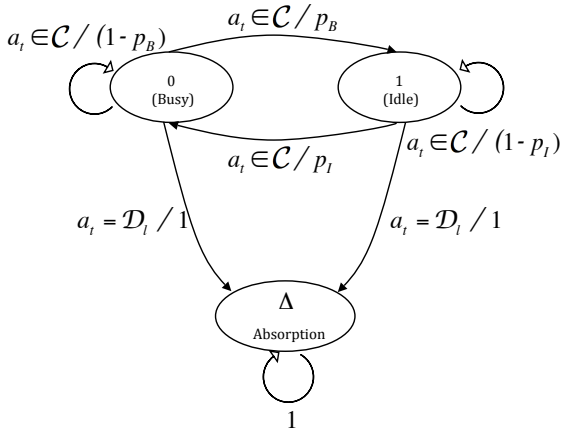


Figure 3.1: The transition dynamics for the $l^{th}$ channel. The same would apply to all other channels. When the action taken at time $t$ belongs to set $\mathcal{C}$, the channel will switch between the busy and idle states; otherwise, the process reaches an absorption state.

#### 3.2.2.4 Observation Model

When the number of sensors is less than or equal to the number of available channels, i.e., $M \leq L$, the detector observes the channels according $a_{t_1}$, i.e., the action that the detector has taken in the previous time slot. If $a_{t-1} = \overline{C}_j$, $M$ observations are sampled from the channels in the $j^{\text{th}}$ $M$-set. Note that the decision on what channels to observe is conveyed in the action taken at time $t-1$, and only the observed channels generate observations. Since there are as many observations as there are sensors, observations is size $M$. It is assumed that no two sensors can observe the same channel at time $t$.

Suppose $l$ is an index for an observed channel at time $t$. The random observation from this channel is denoted as $X_l(t)$. The pdf that a sample of $X_l(t)$ is drawn from

depends on the state of the selected channel at time $t$, i.e., $Z_l(t)$. When $Z_l(t) = 0$, the channel is in a busy state and the observation $X_l(t)$ is drawn from a probability density function (pdf) pertaining to State 0, denoted as $f_0$. When $Z_l(t) = 1$, $X_l(t)$ is otherwise drawn from another pdf pertaining to State 1, denoted as $f_1$. According to the signal model presented in Section 3.1.2, the pdf $f_0$ is a zero-mean Gaussian distribution with variance of $P + \sigma^2$ and the pdf $f_1$ is a zero-mean Gaussian distribution with variance of $\sigma^2$. When the process reaches the absorption state, the process terminates and stops generating observations.

#### 3.2.2.5 Cost Model

The cost model defines the cost incurred by each action taken. Let $R_{a_t}(t)$ be the cost incurred at time $t$ under the action $a_t$. If the action is to continue, i.e., $a_t \in \mathcal{C}$, unit cost is incurred, or $R_{a_t}(t) = 1$. On the other hand, if the action is to stop and declare the i$^{th}$ channel idle when the channel is in fact busy, a cost of $\gamma$ is incurred to reflect the cost of the false alarm, i.e., $R_{a_t}(t) = \gamma > 0$.

#### 3.2.2.6 Sufficient Statistic

As implied by the name of the framework, the state of each channel is partially observable. As time progresses, the system gathers the available information from the system and builds knowledge about the states of all the channels. This knowledge is said to constitute the sufficient statistics, or the belief vector, of the channel states. As each channel individually has a state, a belief vector of size $L$ is maintained and updated. The belief vector is denoted as $\mathbf{\Lambda}(t) \equiv [\lambda_1(t), ..., \lambda_L(t)]$, where $\lambda_l(t), 1 \leq l \leq L$, is the a posteriori probability that the $l^{th}$ channel is in an idle state at time $t$ given

all the past observations made in this channel, i.e.,

$$\lambda_l(t) \equiv Pr(Z_l(t) = 1| \text{ past observations in the channel } l \text{ }). \tag{3.7}$$

The past observations form a sequence of observations that are not necessarily contiguous in time because the detector may dynamically switch channels in or out of a channel of its observed list while performing spectrum sensing.

Based on the state transition and observation models, an update function is proposed to update the sufficient statistic (or the belief value) with the latest observations at every time $t$, for a system that has $M \geq 1$ sensors:

Given that the action at time $t-1$ belongs to set $\mathcal{C}$, i.e., $a_{t-1} = \overline{C}_j$,

$$\lambda_l(t) = \begin{cases} \widehat{\mathcal{T}}(\lambda_l(t-1), x) & C_l \in \overline{C}_j \text{ , and } X_l(t) = x, \\ \widetilde{\mathcal{T}}(\lambda_l(t-1)) & C_l \notin \overline{C}_j \end{cases} \tag{3.8}$$

That is, if one of $M$ sensors is assigned channel $l$ at time $t$, the update function $\widehat{\mathcal{T}}(\lambda_l(t-1), x)$ is applied to update the belief value; otherwise, $\widetilde{\mathcal{T}}(\lambda_l(t-1))$ is used instead.

The update equations for $\lambda_l(t)$ evolve recursively. When the channel is observed by a sensor at time $t$, the update function that utilizes the observation $x$ is [29]

$$\widehat{\mathcal{T}}(\lambda, x) = \frac{(\lambda\overline{p}_I + \overline{\lambda}p_B)f_1(x)}{(\lambda\overline{p}_I + \overline{\lambda}p_B)f_1(x) + (\lambda p_I + \overline{\lambda}\,\overline{p}_B)f_0(x)} \tag{3.9}$$

where the operator $\overline{(\cdot)}$ is defined as $1 - (\cdot)$, and $p_I$ and $p_B$ are provided a priori by the channel usage model. Note that in the special case of $p_I = 0$ and $\overline{p}_I = 1$ (i.e., $\lambda_o = 1$), the above equation reduces to the test statistic (2.27) used in the test of Shiryaev's Bayesian detector. This indicates that the problem formulation based on POMDP is in fact a generalized form of Shiryaev's Problem.

When the $l^{th}$ channel is not observed at time $t$, the update function on the transition dynamic evolves solely based on the a priori information and is given as in [29]:

$$\widetilde{\mathcal{T}}(\lambda) = \lambda\overline{p}_I + \overline{\lambda}p_B. \tag{3.10}$$

In the context of the POMDP formulation, a detector is expressed as a function that maps the belief vector to an action on a per time slot basis. Such a function, denoted as $\Theta(\mathbf{\Lambda}(t)) = a_t$, is called a policy. The optimal policy is one that satisfies the following criterion, which is based the problem (3.6) being re-cast in the POMDP formulation. For given $M$ and $L$,

$$\Theta^* = \arg\min_{\Theta} \mathbb{E}\left[\sum_{t=0}^{\infty} R_{\Theta(\mathbf{\Lambda}(t))}|\mathbf{\Lambda}(0)\right] \tag{3.11}$$

where $R_{\Theta(\mathbf{\Lambda}(t))} = R_{a_t}(t)|_{a_t=\Theta(\mathbf{\Lambda}(t))}$ and $\mathbf{\Lambda}(0) = [\lambda_0, \lambda_0, ..., \lambda_0]$ is the a priori belief vector value. To satisfy the constraint on the false alarm rate in (3.6), the value of the trade-off constant $\gamma$ defined in the cost model needs to be properly chosen. However, it is not necessary to define $\gamma$ in terms of $\alpha$. As shown in Section 4.2, an alternative method is used ensure the policy $\Theta(\mathbf{\Lambda}(t))$ meets the false alarm requirements. In next chapter, the solution to the problem formulation posed by the POMDP is proposed.

# Chapter 4

# New Detection Methods for Multi-Channel Spectrum Sensing

In the last chapter, physical spectrum bands are considered as homogeneous channels in which a cognitive radio user tries to discover an idle period that it can opportunistically access. System models that describe random characteristics of channel usages and of the nature of the received signals have been developed to set up a problem formulation utilizing partially observable Markov decision processes (POMDP).

In this chapter, novel detection methods for a multiband and multi-sensors scenario are proposed based on the POMDP framework. An optimal, but un-implementable decision test is first derived. Using the insights gained from the optimal detection test, two practical detection methods are developed.

## 4.1 Optimal Decision Test for the Problem of POMDP

The problem of detecting an idle period with multiple channels using multiple sensor is posed in the context of POMDP. The criteria in Eq. (3.11) summarizes the problem. The development of an optimal detector for this problem is shown in detail in [29] for the special case of $M = 1$. Based on the procedure in [29], this section demonstrates that the generalization to $M \geq 1$ follows a similar procedure, under certain assumptions.

To develop a detector structure that solves (3.11), a value function must be defined to represent the optimal expected cost. The value function expresses the minimum expected cost that one can obtain from the present time $t$ into the infinite future, over all possible sequences of actions.

The value function is a function of sufficient statistics, which are also known as the belief values. Section 3.2.2.6 defines sufficient statistics as $\mathbf{\Lambda}(t) \equiv [\lambda_1(t), ..., \lambda_L(t)]$. By definition, sufficient statistics capture all the a posteriori information about the state of the process up to time $t$. Since the POMDP is invariant to time shift, the absolute time indices of the sufficient statistics $\mathbf{\Lambda}(t) \equiv [\lambda_1(t), ..., \lambda_L(t)]$ do not offer any information about the state of the process. For example, if a process has the sufficient statistics at times $t$ and $t + k$, for $k \in \mathbb{Z}$, and that $\mathbf{\Lambda}(t) = \mathbf{\Lambda}(t + k)$, then it can be said the process at the times $t$ and $t+k$ shares the identical random properties and dynamics. Therefore, for the remainder of the chapter, the sufficient statistics would be usually referred to as $\mathbf{\Lambda} \equiv [\lambda_1, ..., \lambda_L]$. It is assumed that when the time indices are omitted, the sufficient statistics concern the current time $t$.

Suppose that there are $M$ sensors and $L$ available channels, where $M \leq L$. The value function is defined as

$$\begin{aligned} V(\lambda_1, ..., \lambda_L) = \min\{&V_{\overline{C}_1}(\lambda_1, ..., \lambda_L), V_{\overline{C}_2}(\lambda_1, ..., \lambda_L), ..., \\ &V_{\overline{C}_{|\mathcal{C}|}}(\lambda_1, ..., \lambda_L), V_{D_1}(\lambda_1, ..., \lambda_L), V_{D_2}(\lambda_1, ..., \lambda_L), ..., \\ &V_{D_L}(\lambda_1, \lambda_2, \lambda_3)\}, \end{aligned} \tag{4.1}$$

where $V_{\overline{C}_j}(\lambda_1, ..., \lambda_L)$, $1 \leq j \leq |\mathcal{C}|$, denotes the conditional value function for the action $\overline{C}_j$. The size of $\mathcal{C}$ is $|\mathcal{C}|$ and has a value of $\binom{L}{M}$. $V_{D_l}$, $1 \leq l \leq L$, are the value functions of declaring the $l^{th}$ channel as idle. Conditional value functions are defined as the minimum expected cost that one can obtain from the current time into the infinite future if an action, such as $\overline{C}_j$ or $D_l$, is taken at the current time $t$.

It is evident that the value function in (4.1) is equal to the conditional value function for the action that yields the lowest value. Specifically, the conditional value functions for the actions $D_l$ are defined as follows:

$$V_{D_l}(\lambda_1, \lambda_2, ..., \lambda_L) = (1 - \lambda_l)\gamma \tag{4.2}$$

where $\{\lambda'_1, ..., \lambda'_L\}$ are the sufficient statistics for time $t + 1$ and $\gamma$ is a constant that trade off the relative importance between the false alarm rate and the average detection delay, for $\gamma \geq 1$, and $X_l$ is the random variable of an observation from the $l^{\text{th}}$ channel at time $t + 1$.

The conditional value functions for the actions $\overline{C}_j$ are difficult to define in a general way due to a lack of a clear notation for enumerating all the members $\overline{C}_j$ in the set $\mathcal{C}$. Hence, for illustrative purposes, a conditional value function for a particular action $\overline{C}_j$ is shown. Note that the following structure applies to all the other members in the set $\mathcal{C}$ straightforwardly: suppose there exists an action $\overline{C}_1 \in \mathcal{C}$ that pertains to

observing the channels $\{1, 2, ..., M\}$. The conditional value function for this action $\overline{C}_1$ is then defined as such:

$$V_{\overline{C}_1}(\lambda_1, ..., \lambda_L) = 1 + \int\int_{x_1, x_2, ...x_M} ... \int P(x_1, x_2, ..., x_M; \lambda_1, \lambda_2 ..., \lambda_M) V(\lambda_1^{'}, \lambda_2^{'}, ..., \lambda_L^{'}) dx_1 dx_2 ... dx_M, \tag{4.3}$$

where $P(x_1, x_2, ..., x_M; \lambda_1, \lambda_2, ..., \lambda_M)$ is the joint pdf of the observations from channels $1, 2, 3, ...,$ and $M$, which are channels that are included in the $M$-set $\overline{C}_1$.

The sufficient statistic for the $l^{\text{th}}$ channel, i.e. $\lambda_l'$, is a function of random observations at time $t+1$, the parameters from the channel usage model, and the sufficient statistic for the current time $\lambda_l$. For $1 \leq l \leq L$, the value of $\lambda_l'$ is computed via

$$\lambda_l^{'} = \begin{cases} \widehat{\mathcal{T}}(\lambda_l, x_l) & C_l \in \overline{C}_j \\ \widetilde{\mathcal{T}}(\lambda_l) & C_l \notin \overline{C}_j \end{cases}, \tag{4.4}$$

where the functions $\widehat{\mathcal{T}}(\cdot)$ and $\widetilde{\mathcal{T}}(\cdot)$ are defined in (3.9) and (3.10), respectively, and $\lambda_l$ is the sufficient statistic at time $t$. Since the sufficient statistic at $t+1$ ($\lambda_l'$) is a function of itself at time $t$ ($\lambda_l$), the update function above is recursive. If channel $l$ is sensed as a result of choosing the action $\overline{C}_j$, the update function $\widehat{\mathcal{T}}(\lambda_l(t-1), x)$ is to update $\lambda_l'$; if not, $\lambda_l' = \widetilde{\mathcal{T}}(\lambda_l(t-1))$ is used instead.

The expression in (4.3) reveals how the conditional value function is structured. The first term is the unit cost of choosing action $\overline{C}_j$ as opposed to $D_l$ at the current time $t$. The second term accounts for the expected minimum cost from time $t+1$ onward. It has a nested structure that embeds the value function $V(\lambda_1^{'}, ..., \lambda_L^{'})$. This implies that to find the expected cost for any time instant in the future and onward, the expected value of the sufficient statistics taken over the densities of random observations are all one needs to calculate.

Similar to the case of $M = 1$ case developed in [29], the conditional value functions for any value of $M$ given $L$ have some important properties, summarized by Lemma 1.

*Lemma 1:*

1.1: When $p_B + p_I \leq 1$ and $P(x_v, x_w; \lambda_v, \lambda_w) = P(x_v; \lambda_v)P(x_w; \lambda_w)$, for $(1 \leq v \leq L, 1 \leq w \leq L; v \neq w)$, the value functions $V_{\overline{C}_j}(\lambda_1, ...\lambda_L)$ are concave and monotonically decreasing with $\lambda_j$, for $1 \leq j \leq L$.

1.2: $V_{\overline{C}_j}(\lambda_1, ..., \lambda_L)$ are symmetric with respect to the planes $\{\lambda_i = \lambda_j; 1 \leq i \leq L, 1 \leq j \leq L, i \neq j\}$.

1.3: $V_{D_i}(\lambda_1, ...\lambda_L)$ is linearly decreasing with $\lambda_i$, for $1 \leq i \leq L$.

*Proof:* See Section 4.4.

Lemma 1.2 can be illustrated with an example. Suppose that $M = 2$ and $L = 3$, two actions $\overline{C}_1 = (C_1, C_2)$ and $\overline{C}_2 = (C_1, C_3)$ are considered, and variables $v$ and $w$ are any constants whose values are between [0,1]. The following symmetry exists between between their conditional value functions

$$V_{(C_1,C_2)}(\lambda_1, \lambda_2, \lambda_3)|_{\lambda_2=v,\lambda_3=w} = V_{(C_1,C_3)}(\lambda_1, \lambda_2, \lambda_3)|_{\lambda_2=w,\lambda_3=v}. \tag{4.5}$$

where the conditional value functions for the actions $(C_1, C_2)$ and $(C_1, C_3)$ are equal because the sufficient statistics are symmetric around the $\lambda_2 = \lambda_3$ plane.

The validity of Lemma 1 is conditioned on an important assumption: observations are random and statistically independent from each other. As a result of this assumption,

$$P(x_i, x_j; \lambda_i, \lambda_j) = P(x_i; \lambda_i)P(x_j; \lambda_j), \quad \forall i, j; i \neq j \tag{4.6}$$

Condition (4.6) is sastified if channels are mutually independent so that the joint pdf of observations from different channels is separable into products of marginal pdf's of

individual observations.

Lemma 1 leads to Theorem 2 in [29]:

*Theorem 2* [29]: The optimal structure $\Theta^*(\mathbf{\Lambda}(t))$ under the belief vector $\mathbf{\Lambda}(t)$ is the following:

$$\Theta^*(\mathbf{\Lambda}(t)) = \begin{cases} D_i, & \text{if } i = \underset{1\leq j\leq L}{\arg\max}(\mathbf{\Lambda}(t)) \\ & \text{and } \lambda_i \geq \eta_d(\mathbf{\Lambda}^-(t)) \\ \mathcal{C}, & \text{otherwise} \end{cases} \tag{4.7}$$

where $\mathcal{C}$ is the set of actions of continuing to observe channels, as defined in Section 3.2.2, $\mathbf{\Lambda}^-(t)$ denotes the set of sufficient statistics for the $L-M$ unobserved channels at time $t$, and $\eta_d(\mathbf{\Lambda}^-(t))$ is the function that maps $\mathbf{\Lambda}^-(t)$ to a stopping threshold value in $[0, 1]$.

The detector structure (4.7) suggests that there are unique boundaries that partition the $L$-dimensional space of the sufficient statistics into decision regions in which an optimal action exists and that optimal action can be either $\overline{C}_j$ (to continue) or $D_l$ (to stop). The function $\eta_d(\mathbf{\Lambda}^-(t))$ defines the boundaries that separate these regions. However, the detector structure (4.7) does not specify the rule that chooses which channels to sense.

Realizing a practical detector from (4.7) entails determining these decision regions in the space spanned by the sufficient statistics. It involves the computing value function in (4.1)-(4.2) iteratively. The nested integrations over a infinitely large domain make the computation numerically intractable. Due of complexity, the optimal policy (4.7) cannot be implemented. Therefore, the next sections propose two implementable detectors as a suboptimal low-complexity versions of the policy (4.7).

## 4.2 Multiband Multi-Sensor Spectrum Sensing Detector

Although it is not realistic to implement the optimal decision test (4.7), the structure of the test serves as a guide to the design of a practical detector. The proposed detector have the followings properties: (1) performs discovery of an idle period over multiple channels (multiband), (2) simultaneously senses multiple channels (multi-sensing), and (3) tracks the belief vector for all the channels. Due to these properties, the detector described here is named the *Multiband Multi-Sensor Spectrum Sensing Detector* (MMSSD).

Given a general number of sensors $M \geq 1$ and number of channels being detected $L$, the MMSSD has the following structure:

$$\Theta_{\text{MMSSD}}(\mathbf{\Lambda}(t)) = \begin{cases} D_i, & \text{if } i = \underset{1 \leq j \leq L}{\arg\max}(\mathbf{\Lambda}(t)) \\ & \text{and } \lambda_i \geq \eta_d(\mathbf{\Lambda}^-(t)) \\ \overline{C}_{j^*}, & \text{Otherwise} \end{cases} \tag{4.8}$$

where $\overline{C}_{j^*} \in \mathcal{C}$ is the action to continue to observe all the channels that have the $M$ largest belief values. $\mathbf{\Lambda}(t) = \{\lambda_1(t), ..., \lambda_L(t)\}$ is the belief vector that consists of belief values, computed using (4.4) at each time $t = 1, 2, ...$, and $\mathbf{\Lambda}^-(t)$ denotes a subset of belief values for the $L - M$ unobserved channels at time $t$. Using a M=2 and L=3 system as an example, if at time $t$, channels 2 and 3 have the highest belief values among $\mathbf{\Lambda}(t)$, i.e., $\lambda_2(t) > \lambda_1(t)$ and $\lambda_3(t) > \lambda_1(t)$, then $\overline{C}_{j^*} = \{C_2, C_3\}$.

The decision test of MMSSD (4.8) specifies a rule that directs a detector to choose which channels to sense; the detector senses the channels with the largest belief values.

Given the definition of the belief value, that is,

$$\lambda_l(t) \equiv Pr(Z_l(t) = 1| \text{ past observations in the channel } l \text{ }), \tag{4.9}$$

the best choice for what channels to sense are naturally those channels that have the highest likelihoods of being in the idle state. This is where the decision test of MMSSD (4.8) differs from the optimal decision test in (4.7), which does not offer a rule regarding to choosing which channels to sense.

As mentioned in the previous section, the threshold design for (4.8) is a challenging task because the function $\eta_d(\mathbf{\Lambda}^-(t))$, which defines the boundary between the decision regions to continue the detection and the regions to stop and declare a channel as idle, changes with time $t$ and is difficult to compute. To simplify the threshold design, an alternative threshold design method is proposed here for (4.8), where a predetermined constant threshold is assumed, denoted as $\eta_d$, rather than as a function. This threshold design method, however, results in a sub-optimal performance but offers the designer a viable method to design a detector that satisfies the constraint on the false alarm rate, or $P_{FA} \leq \alpha$, and a way to sidestep the difficult problem of optimal threshold design.

To develop the alternative threshold design rule, a few new variables must be first defined. Let $T_{\text{stop}}(\eta_d)$ be the random detection delay of the MMSSD employing the threshold $\eta_d$, i.e.,

$$T_{\text{stop}}(\eta_d) \equiv \inf\{n \geq 1 : \lambda_{\max}(n) \geq \eta_d\} \tag{4.10}$$

where $\lambda_{\max}(n) \equiv \max\{\lambda_1(n), ..., \lambda_L(n)\}$. As in the formulation of Shiryaev's Problem [25], $1 - \lambda_{\max}(T_{\text{stop}})$ is by definition the a posteriori probability that a false alarm would occur. A false alarm occurs when the channel declared to be idle is in a busy state. This probability is also a function of random-variable observations. Therefore,

an expected value of $1 - \lambda_{\max}(T_{\text{stop}})$ over all possible random observation sequences, represents the false alarm rate of the MMSSD detector, i.e.,

$$P_{FA} = \mathbb{E}_{\lambda_o}[1 - \lambda_{\max}(T_{\text{stop}})] \tag{4.11}$$

where the expectation operator $\mathbb{E}_{\lambda_o}[\cdot]$ is the expected value over all the possible random observation sequences conditioned on initial belief value of the sufficient statistics equal to $\lambda_o$. From (4.10) and (4.11) , an upper bound on $P_{FA}$ can be derived as follows:

$$\begin{aligned} &\lambda_{\max}(T_{stop}) \geq \eta_d \\ &1 - \mathbb{E}_{\lambda_o}[\lambda_{\max}(T_{stop})] \leq 1 - \eta_d \\ &P_{FA} \leq 1 - \eta_d. \end{aligned} \tag{4.12}$$

The first inequality is true by definition: At time $t = T_{\text{stop}}$, $\lambda_{\max}(T_{\text{stop}})$ is greater than the stopping threshold $\eta_d$. The final inequality in (4.12) shows that the threshold, $\eta_d$, that satisfies a given false alarm constraint, $\alpha$, is $\eta_d = 1 - \alpha$. This threshold design is suboptimal because it may cause the detector be too conservative in maintaining the false alarm rate. That is, the test statistic $\lambda_{\max}(T_{stop})$ is likely to overshoot the threshold $\eta_d$ in the detection process and result in an actual false alarm rate that is lower than the false alarm constraint. In other words, given a nominal false alarm rate $\alpha \in [0, 1]$, the threshold $\eta_d = 1 - \alpha$ provides a loose upper bound to the actual false alarm rate, $P_{\text{FA}}$. However, the upper bound on $P_{FA}$ becomes tighter as $\alpha$ tends to zero since

$$0 \leq P_{FA} \leq 1 - \eta_d = \alpha. \tag{4.13}$$

A description of the detection algorithm for MMSSD is provided in Table 4.1.

Table 4.1: The operation of a MMSSD is described in an algorithmic form.

**Algorithm for MMSSD**

**for** $l = 1$ to $L$ **do**
  $\lambda_l \leftarrow \lambda_0$
**end for**
$t \leftarrow t + 1$
**loop**
  **for** $l = 1$ to $L$ **do**
    **if** {Channel l is observed at time $t$} **then**
      {Fetch $x_l$}
      $\lambda_l \leftarrow \widehat{\mathcal{T}}(\lambda_{l-1}, x_l)$
    **else**
      $\lambda_l \leftarrow \widetilde{\mathcal{T}}(\lambda_{l-1})$
    **end if**
  **end for**
  $\lambda_{\max} \leftarrow \max\{\lambda_1, ..., \lambda_L\}$
  $l_{\max} \leftarrow \arg\max\{\lambda_1, ..., \lambda_L\}$
  **if** $\lambda_{\max} \geq \eta_d$ **then**
    {Declare channel $l_{\max}$ as idle}
    {Terminate detection}
  **else**
    {Rank the top $M$ channels based on $\{\lambda_1, ..., \lambda_L\}$}
    {These $M$ channels are sensed in the next time instant.}
    $t \leftarrow t + 1$
  **end if**
**end loop**

## 4.3 Reduced-Complexity Multiband Multi-Sensor Spectrum Sensing Detectors

The MMSSD carries a high complexity cost when the number of channels available for sensing, $L$, is large, because of the cost of memory to store the belief vector that is of length $L$ and of the computation to rank all belief values to find the top $M$ belief values at every time $t$. For example, identifying the top $M$ belief values among $L$ total belief values using a selection sorting algorithm is shown to have an expected running time of $\mathcal{O}(L + M \log M)$ [3], where the $\mathcal{O}(n)$ is the big-O notation used to indicate complexity. This section proposes a reduced complexity version of MMSSD, which has a complexity independent of the number of channels $L$. Also, under a specific condition, the reduced complexity version has performance that approaches that of MMSSD.

In [29], a detector is proposed under the so-called *infinite regime*, where it assumes an asymptotic condition $L \to \infty$ and $M = 1$. This thesis generalizes this work to arbitrary $M$ and shows that in the case of $L >> M$, it leads a reduced complexity version of MMSSD.

Consider the case where MMSSD is detecting for an idle period among $L$ channels, and $L$ is infinitely larger than $M$, i.e., $(L - M) \to \infty$. Let $j$ be the index of a channel at time $t$, where $1 \leq j \leq L - M$. Let $T^j_{\text{unobs}}$ be the random elapsed time during which the $j^{th}$ channel is not observed, and finally, let $r_j(t)$ be the overall ranking of the j$^{th}$ channel at time $t$, among observed and unobserved channels. A lower value of $r_j(t)$ means having a higher relative belief value, e.g., $r_j(t) = 2$ means that the $j^{\text{th}}$ unobserved channel has second highest belief value. Since MMSSD chooses to sense

channels with the $M$ highest rankings, the $j^{\text{th}}$ channel remains in the unobserved pool as long as its ranking satisfied $r_j(t) > M$. Then

$$T^j_{\text{unobs}} \equiv \sum_{t=1}^{\infty} \{1\}_{(r_j(t)>M)} \tag{4.14}$$

where $\{1\}_{(r_j(t)>M)}$ is an indicator function for the event $r_j(t) > M$. As $L - M$ approaches infinity, $\text{Prob}\,(r_j(t) > M) \to 1$ because the probability that the belief value for the j$^{th}$ channel is ranked in the top $M$ elements becomes vanishingly small. As a result, $T^j_{\text{unobs}}$ approaches infinity. This offers the insight that as the pool of unobserved channels grows large, the time that a channel dwells within the unobserved pool lengthens.

While a channel is in the unobserved pool, no observation of it is generated and the belief value is updated recursively with the a priori update function (3.10) at every time $t$. Given a belief value $\lambda_l(t)$ and that the $l^{\text{th}}$ channel is not observed for the next $N$ time instants, at the end of $N^{\text{th}}$ interval, the resulting belief value $\lambda_l(t+N)$ is

$$\begin{aligned}
\lambda_l(t+N) \equiv \widetilde{\mathcal{T}}^N(\lambda_l(t)) &= \widetilde{\mathcal{T}}(\widetilde{\mathcal{T}}^{N-1}(\lambda_l(t))) \\
&= \widetilde{\mathcal{T}}\left(\ldots \widetilde{\mathcal{T}}\left(\widetilde{\mathcal{T}}(\lambda_l(t))\right)\right) \\
&= p_B(1 + (1 - p_I - p_B) + (1 - p_I - p_B)^2 \\
&\qquad + \ldots + (1 - p_I - p_B)^N \lambda_l(t)),
\end{aligned} \tag{4.15}$$

where the third equality follows as a result of expanding $N$ layers of recursions. It is seen here that if $T^j_{\text{unobs}}$ is large, $\lambda_l(t + T^j_{\text{unobs}})$ depends less on the value of $\lambda_l(t)$ because the coefficient $(1 - p_I - p_B)^N$ becomes quite small. In the asymptotic case, with $T^j_{\text{unobs}} \to \infty$, the convergence below is observed:

$$\lim_{N\to\infty} \widetilde{\mathcal{T}}^N(\lambda) = \frac{m_I}{m_B + m_I} = \lambda_o, \tag{4.16}$$

where the condition for convergence is $p_I + p_B \geq 0$, which is met by the definitions of $p_I$ and $p_B$.

This result (4.16) indicates that if $(L-M) \to \infty$, the set of unobserved channels is infinitely large, and the channel in the unobserved will likely to spend a very long time in the unobserved pool. While it is in the unobserved pool, its belief value converges to $\lambda_o$. The belief values for all the channels in the unobserved pool then become the same. Consequently, it is no longer necessary for the detector store the belief values for all the unobserved channels when it knows a priori that an unobserved channel has the belief value is likely to be very close to $\lambda_o$.

In practice, for a finite sized unobserved pool, the above holds as an approximation, as long as $L$ is sufficiently larger than $M$. One can then assume that a channel's belief value converges to $\lambda_o$ while the channel is unobserved, because it is evident in (4.15) that the convergence to $\lambda_o$ is rapid as $N$ increases.

Assuming that all unobserved channels have the same belief value equal to $\lambda_o$, the process of deciding what channels to observe can be simplified. Instead of ranking against belief values of all channels, the determination of whether to continue to observe a channel reduces to a comparison to a threshold $\lambda_0$. If the belief value of the current channel is higher than $\lambda_o$, the channel is ranked higher than all channels in the unobserved pool, the detector continues to observe this channel; otherwise, the channel is ranked lower than all channels in the unobserved pool, and the detector should switch out of the current channel and sense another channel instead. For this reason, the threshold used for the comparison is called the *"switching threshold"*. Based on this idea, this thesis proposes a variant of MMSSD with reduced complexity (RC-MMSSD).

Table 4.2: The operation of a RC-MMSSD is described in an algorithmic form where $\Omega$ denotes the pool of unobserved channels at the current time $t$.

**Algorithm for RC-MMSSD**

**for** $m = 1$ to $M$ **do**
  **if** $\lambda_m \geq \eta_d$ **then**
    {Declare channel $k_m$ as idle}
  **else if** $\lambda_m < \lambda_o$ **then**
    {Switch out of channel $k_m$}
    $k_m \leftarrow$ index of a new channel selected from $\Omega$
    $\lambda_m(t) \leftarrow \lambda_o$ {Resetting $\lambda_m(t)$}
    Put the index of the replaced channel back into $\Omega$
  **else**
    {Continue to observe channel $k_m$}
  **end if**
**end for**

Due to the dynamics stated above, another interpretation of this result is as such: at the asymptotic condition $L-M \to \infty$, RC-MMSSD effectively chooses the same set of channels to observe as what MMSSD would have chosen by ranking, and therefore, MMSSD and RC-MMSSD share the same performance.

For RC-MMSSD, the belief vector is defined differently compared to MMSSD. The detector re-defines a belief vector of size $M$, $[\lambda_1(t), ..., \lambda_M(t)]$, where $\lambda_m(t)$, for $1 \leq m \leq M$, is the belief value for the channel being sensed by the $m^{\text{th}}$ sensor. It also defines a vector $\{k_1, k_2, ..., k_M\}$ in which each element $k_m$, for $1 \leq m \leq M$, acts as a pointer to the channel being sensed by the $m^{\text{th}}$ sensor. For example, the variable assignment $k_3 = 5$ indicates that the $3^{\text{rd}}$ sensor is sensing channel 5. With every iteration, the detector updates each belief value using observations from its corresponding observed channels via (3.9). Once the updated belief vector is obtained, the detector decides on the action based on the policy as described in Table 4.2.

The decision test to decide when to declare a channel idle has not changed in the RC-MMSSD, i.e., the threshold $\eta_d$ is used and designed in RC-MMSSD in exactly the same way for MMSSD. By setting $\eta_d = 1 - \alpha$, the detector satisfies the false alarm rate constraints $\alpha$.

One should be cautious about applying RC-MMSSD to scenarios where $L - M$ is small, as they may encounter problems in designing the threshold to meet a certain false alarm rate constraint. Consider a scenario where there is a small unobserved pool where $L - M = 1$, and RC-MMSSD is used. Suppose that events unfold in the following sequence: the $m^{\text{th}}$ channel has been swapped out due to $\lambda_m(t) < \lambda_o$; after a small $T^m_{\text{unobs}}$ has lapsed, the m$^{th}$ channel is called upon to be sensed again with its belief value assumed to be $\lambda_o$, and the $m^{th}$ channel is declared idle by RC-MMSSD.

Let $\delta\lambda(t)$ denote the error at time $t$ between the assumed belief value, $\lambda_o$, and the true belief value, $\lambda_m(t)$,

$$\delta\lambda(t) = \lambda_o - \lambda_m(t). \tag{4.17}$$

If the true belief value converges to $\lambda_0$, the value of $\delta\lambda(t+T^m_{\text{unobs}})$ is then zero. However, based on (4.15), a small $T^m_{\text{unobs}}$ implies that $\delta\lambda(t + T^m_{\text{unobs}})$ is a finite positive quantity, meaning that the belief value has yet converged. This has an effect on the false alarm rate.

The false alarm rate, (4.11), can be computed using (4.17) as

$$\begin{aligned}
&1 - \mathbb{E}_{\lambda_o}[\lambda_{\max}^{T_{\text{stop}}}] \\
&= 1 - \lambda_o \, \mathbb{E}_1[\lambda_{\max}^{T_{\text{stop}}}] - (1 - \lambda_o) \, \mathbb{E}_0[\lambda_{\max}^{T_{\text{stop}}}] \\
&= 1 - (\lambda_j(t) + \delta\lambda(t)) \, \mathbb{E}_1[\lambda_{\max}^{T_{\text{stop}}}] - (1 - \lambda_j(t) - \delta\lambda(t)) \, \mathbb{E}_0[\lambda_{\max}^{T_{\text{stop}}}] \\
&= 1 - \lambda_j(t) \, \mathbb{E}_1[\lambda_{\max}^{T_{\text{stop}}}] - (1 - \lambda_j(t)) \, \mathbb{E}_0[\lambda_{\max}^{T_{\text{stop}}}] \\
&\qquad - \delta\lambda(t) \left( \mathbb{E}_1[\lambda_{\max}^{T_{\text{stop}}}] - \mathbb{E}_0[\lambda_{\max}^{T_{\text{stop}}}] \right) \\
&= P_{FA,\lambda_j(t)} - \Delta P_{FA}
\end{aligned} \tag{4.18}$$

where $P_{FA,\lambda_j(t)}$ is the false alarm probability based on the true belief value of the $j^{th}$ channel and is therefore the true false alarm rate of the detector. $\Delta P_{FA}$ is the false alarm probability caused by the error $\delta\lambda(t)$. Note that $\Delta P_{FA}$ is a positive value and approaches 0 as $\delta\lambda(t) \to 0$. By applying the MMSSD threshold design and setting $\eta_d = 1 - \alpha$, the inequality below results:

$$P_{FA,\lambda_m(t)} \leq 1 - \alpha + \Delta P_{FA}. \tag{4.19}$$

As evident in (4.19), the design threshold $1 - \alpha$ is no longer a sufficient upper bound for the false alarm rate of the system. Therefore the detector designed using this methodology does not meet the false alarm rate constraint.

## 4.4 Appendix: Proof of Lemma 1

This section provides the proof for the properties of the value functions stated in Lemma 1. The proof generalizes the work in [29] to cases with arbitrary number of $M$ sensors, and $L$ channels. This section shows that the proof developed in [29] for the special case of $M = 1$ can be applied very similarly to the cases of arbitrary

$M \geq 1$. Many of results from [29], especially ones related to algebraic manipulation, are re-used in this proof.

Lemma 1.2 follows as a consequence of assuming that the ON-OFF process representing each of $L$ channels has identical channel usage and signal models, and that sufficiency of $\lambda_1, \lambda_2, ..., \lambda_L$ as the input values, which mean that "no other statistics which can be calculated from the samples of the observation provide more information any additional information as to the value of the parameter" [5]. Lemma 1.3 is true by definition of $V_{D_i}$ in (4.2).

To set up the proof for Lemma 1.1, a finite horizon problem is considered. In a finite horizon problem, a detector must stop and declare a channel to be idle after a finite time period, $K$. In this context, new value functions are defined to correspond to (4.1)-(4.2):

If $K = 1, 2, 3, ...$, the finite horizon value function is

$$\begin{aligned} V^K(\lambda_1, ..., \lambda_L) = \min\{&V^K_{\overline{C}_1}(\lambda_1, ..., \lambda_L), V^K_{\overline{C}_2}(\lambda_1, ..., \lambda_L), ..., \\ &V^K_{\overline{C}_{|\mathcal{C}|}}(\lambda_1, ..., \lambda_L), V_{D_1}(\lambda_1, ..., \lambda_L), V_{D_2}(\lambda_1, ..., \lambda_L), ..., \\ &V_{D_L}(\lambda_1, \lambda_2, \lambda_3)\}, \end{aligned} \tag{4.20}$$

and if $K = 0$, the finite horizon value function is then

$$V^0(\lambda_1, ..., \lambda_L) = \min\{V_{D_1}(\lambda_1, ..., \lambda_L), V_{D_2}(\lambda_1, ..., \lambda_L), ..., V_{D_L}(\lambda_1, \lambda_2, ..., \lambda_L)\}, \tag{4.21}$$

where $\{V_{D_l}\}$ are the conditional value functions for stopping and declaring a channel idle, for $1 \leq l \leq L$, which is defined according to (4.2). Since $\mathcal{C}$ is the set that contains all possible *continue* actions, the size of the set, $|\mathcal{C}|$, is then $L$ *chooses* $M$. $\{V^K_{\overline{C}_j}\}$, for $1 \leq j \leq |\mathcal{C}|$, are the conditional value functions for continuing the testing given that the detector must stop after $K$ time instants. Suppose a continue action $\overline{C}_1$ observes

channels 1, ,2, ..., M. For $\overline{C}_j$, the conditional value functions $V^K_{\overline{C}_1}$ are

$$V^K_{\overline{C}_1}(\lambda_1, \lambda_2..., \lambda_L) = 1+ \int\int_{x_1,x_2,...x_M} ... \int P(x_1, x_2, ..., x_M; \lambda_1, \lambda_2, ..., \lambda_M) V^{K-1}(\lambda_1^{'}, \lambda_2^{'}, ..., \lambda_L^{'}) dx_1 dx_2 ... dx_M. \tag{4.22}$$

where the integral in the second term is an expected value of the finite horizon value function defined in (4.20) taken over over the domain of $(x_1, x_2, ..., x_M)$, which corresponds to the observations belonging to the channels that are included in $\overline{C}_1$. The conditional value function for any action $\overline{C}_j$, for $j \neq 1$, is defined similarly to (4.22).

Note that the conditional value function $V^K_{\overline{C}_j}$ is defined in terms of the value function in (4.20) with $K = K-1$, because as the detection progresses, every decision to continue gets the detector one time instant closer to the end of the time horizon. In other words, at time $t+1$, the value function becomes $V^{K-1}(\cdot)$. Eventually, after a detector processes for $K$ time instants, the conditional value function $V^1_{\overline{C}_j}$ reaches a special case below (again, the action $\overline{C}_1$ is used as an example),

$$V^1_{\overline{C}_1}(\lambda_1, \lambda_2, ..., \lambda_L) = 1+ \int\int_{x_1,x_2,...x_M} ... \int P(x_1, x_2..., x_M; \lambda_1, \lambda_2, ..., \lambda_M) V^{0}(\lambda_1^{'}, \lambda_2^{'}, ..., \lambda_L^{'}) dx_1 dx_2 ... dx_M. \tag{4.23}$$

The finite horizon problem is related to the original problem by the following relationship between the respective value functions defined in (4.1):

$$V(\lambda_1, ..., \lambda_L) = \lim_{K \to \infty} V^K(\lambda_1, ..., \lambda_L) \tag{4.24}$$

In other words, if the proof applies to the finite horizon value functions for all values of $K$, it implicitly applies to the value function $V(\lambda_1, ..., \lambda_L)$. Therefore for the rest of the section, only the finite horizon problem based on $V^K(\lambda_1, ..., \lambda_L)$ is considered.

Inductive reasoning is employed to show that $V^K_{\overline{C}_j}$ satisfies that Lemma 1.1, i.e. $V^K_{\overline{C}_j}$ is concave and monotonically decreasing for all $K$. The property of the concavity is first shown, and followed by the proof of monotonicity.

For the remainder of this proof, a particular element belonging to the set of $\mathcal{C} - \overline{C}_1 = \{C_1, C_2, ..., C_M\} -$ is considered. A similar argument holds for all $\binom{L}{M}$ elements in the set $\mathcal{C}$ by the merit of the i.i.d. assumption (4.6). For this action, channels 1 to $M$ are sensed. Based on inductive reasoning, the case $K = 1$ is proven first. From (4.2), (4.21), and (4.22), the conditional value function for $K = 1$ is

$$\begin{aligned} V^1_{\overline{C}_1}(\lambda_1, ..., \lambda_L) &\equiv V^1_{(C_1, C_2, ..., C_M)}(\lambda_1, ..., \lambda_L) \\ &= 1 + \int ... \int_{x_1 ... x_M} P(x_1, ..., x_M; \lambda_1, ..., \lambda_M) V^0(\lambda_1^{'}, ..., \lambda_L^{'}) dx_1 ... dx_M \\ &= 1 + \int ... \int_{x_1 ... x_M} P(x_1, ..., x_M; \lambda_1, ..., \lambda_M) \min\{(1 - \lambda_1')\gamma, \\ &\qquad (1 - \lambda_2')\gamma, ..., (1 - \lambda_L')\gamma\} dx_1 ... dx_M \end{aligned} \tag{4.25}$$

where $\lambda_l'$ is the belief value for the $l^{\text{th}}$ channel at the next time instant $t + 1$ and updated via (4.4). As observations across the channels are assumed independent and identically distributed (i.i.d.) and satisfy the condition (4.6), the joint pdf for observations $P(x_1, ..., x_M; \lambda_1, ..., \lambda_M)$ is a product of the marginal pdfs for observations in each channel:

$$P(x_1, ..., x_M; \lambda_1, ..., \lambda_M) = \prod_{i=1}^{M} P(x_i; \lambda_i) \tag{4.26}$$

where the marginal pdf for an observation in a channel is defined as a mixture distribution as follows:

$$P(x_i; \lambda_i) = (\lambda_i \overline{p}_I + \overline{\lambda}_i p_B) f_1(x_i) + (\lambda_i p_I + \overline{\lambda}_i \overline{p}_B) f_0(x_i) \tag{4.27}$$

where $f_1(x_i)$ and $f_0(x_i)$ are the marginal pdfs for an observation under an idle or a busy state, respectively, and are defined in Section 3.2.2.4.

Now, multiply $P(x_1, ..., x_M; \lambda_1, ..., \lambda_M)$ into the $\min\{\cdot\}$ and substitute with (4.26) into (4.25), and consider only the integrand,

$$\min\left\{\prod_{i=1}^{M} P(x_i;\lambda_i)(1-\lambda_1')\gamma, \prod_{i=1}^{M} P(x_i;\lambda_i)(1-\lambda_2')\gamma, ..., \prod_{i=1}^{M} P(x_i;\lambda_i)(1-\lambda_L')\gamma\right\}. \tag{4.28}$$

At this point, let us focus on proving the concavity of $V_{\overline{C}_1}^1(\lambda_1, ..., \lambda_L)$ with respect to $\lambda_1$, given $\lambda_2, \lambda_3, ..., \lambda_L$, with out lost of generality. The main idea is that if all the arguments in $\min\{\cdot\}$ are linear in $\lambda_1$ given $\lambda_2, ..., \lambda_L$, the concavity of function $V_{\overline{C}_1}^1(\lambda_1, ..., \lambda_L)$ in (4.25) with respect to $\lambda_1$ is shown.

The argument with index $l$, $1 \leq l \leq L$, in the $\min\{\cdot\}$ (4.28), i.e., $\prod_{i=1}^{M} P(x_i;\lambda_i)(1-\lambda_l')\gamma$, pertains to the action to *stop and declare* channel $l$ as idle. It falls into either one of two types. The first type includes arguments where their corresponding indices $\{l\}$ are such that $l \in \{1 \leq i \leq M\}$. In other words, the channels that correspond to arguments that are to be observed according to the action $(C_1, C_2, ..., C_M)$. The second type of arguments belongs to indices $\{l\}$ corresponding to $l \notin \{1 \leq i \leq M\}$.

Consider an argument of the first type, such as $l = 1$,

$$\begin{aligned}
&\gamma \prod_{i=2}^{M} P(x_i;\lambda_i) P(x_1;\lambda_1)(1-\lambda_1') \\
&= \gamma \prod_{i=2}^{M} P(x_i;\lambda_i) P(x_1;\lambda_1)(1-\widehat{\mathcal{T}}(\lambda_1, x_1)) \\
&= \gamma \prod_{i=2}^{M} P(x_i;\lambda_i)(1-\widetilde{\mathcal{T}}(\lambda_1)) f_0(x_1)
\end{aligned} \tag{4.29}$$

The first equality is based on the definition of $\lambda_1'$ provided that Channel 1 is to be observed. The second equality is the result of the algebraic manipulation in [29]. It

is seen here that the expression in (4.29) is linear in $\lambda_1$, given the values of $\lambda_2, ..., \lambda_L$. Consider another argument of the first type, such as $l = 2$,

$$\begin{aligned} &\gamma \prod_{i=2}^{M} P(x_i; \lambda_i) P(x_1; \lambda_1)(1 - \lambda_2') \\ &= \gamma \prod_{i=2}^{M} P(x_i; \lambda_i) P(x_1; \lambda_1)(1 - \widehat{\mathcal{T}}(\lambda_2, x_2)). \end{aligned} \tag{4.30}$$

The argument in (4.30) is also linear in $\lambda_1$ because the product $(\gamma \prod_{i=2}^{M} P(x_i; \lambda_i(1 - \widehat{\mathcal{T}}(\lambda_2, x_2)))$ is considered constant and $P(x_1; \lambda_1)$ is linear in $\lambda_1$. The same procedure can be used to show that all arguments of the first type are linear in $\lambda_1$.

Now, consider a specific argument of the second type, where $l = M + 1$ (note: $l \notin \{1 \leq i \leq M\}$), where from (4.4),

$$\begin{aligned} &\gamma \prod_{i=2}^{M} P(x_i; \lambda_i) P(x_1; \lambda_1)(1 - \lambda_{M+1}') \\ &= \gamma \prod_{i=2}^{M} P(x_i; \lambda_i) P(x_1; \lambda_1)(1 - \widetilde{\mathcal{T}}(\lambda_{M+1})) \end{aligned} \tag{4.31}$$

Given the values of $\lambda_2, ..., \lambda_L$, it is seen that in (4.31), the expression is also linear in $\lambda_1$ because the products $\gamma \prod_{i=2}^{M} P(x_i; \lambda_i)(1 - \widetilde{\mathcal{T}}(\lambda_{M+1}))$ are merely considered constants.

It has been demonstrated that the integrand of (4.25) is the minima of multiple functions, which are linear in $\lambda_1$, given the values of $\lambda_2, ..., \lambda_L$. As it is known that a minimum function of a family of linear functions is a concave function and the integration is an infinite sum that preserves the concavity [29], $V_{\overline{C}_1}^{1}(\lambda_1, ..., \lambda_L)$ is then concave in $\lambda_1$. By symmetry, this applies to concavity of all with respect to all $\lambda_i$ given $\{\lambda_l | 1 \leq l \leq L, l \neq i\}$.

The concavity of $V_{\overline{C}_j}^{K}(\lambda_1, ..., \lambda_L)$ with respect to any $\lambda_i$ has been shown. The next step is to demonstrate that the concavity exists for cases $K = 2, 3, ....$ By

the assumption through inductive reasoning, $V^K(\lambda_1, ..., \lambda_L)$ and $V^K_{\overline{C}_j}(\lambda_1, ..., \lambda_L)$ are concave. Through this assumption, if $V^K(\lambda_1, ..., \lambda_L)$ and $V^{K+1}_{\overline{C}_j}(\lambda_1, ..., \lambda_L)$ are also concave, then $V^K_{\overline{C}_j}(\lambda_1, ..., \lambda_L)$ is concave for all values of $K$.

By the assuming that $V^1(\lambda_1, ..., \lambda_L)$ is a concave function, it can be expressed as a minima of an infinite number of linear functions in $\lambda_1, \lambda_2, ..., \lambda_L$. Let these linear functions be indexed by $y \in \mathbb{Z}$ and $\exists(b^y_0, b^y_1, b^y_2, ..., b^y_L) \in \mathbb{R}^L$,

$$V^K(\lambda_1, ..., \lambda_L) = \min_{y\in\mathbb{Z}} \left\{ b^y_0 + b^y_1\lambda_1 + b^y_2\lambda_2 + ... + b^y_L\lambda_L \right\}. \tag{4.32}$$

From this definition,

$$\begin{aligned}
V^{K+1}_{\overline{C}_1}(\lambda_1, ..., \lambda_L) &\equiv V^{K+1}_{\{C_1, C_2, ..., C_M\}}(\lambda_1, ..., \lambda_L) \\
&= 1 + \int_{x_1...x_M} ... \int P(x_1, ..., x_M; \lambda_1, ..., \lambda_M) V^K(\lambda'_1, ..., \lambda'_L) dx_1 ... dx_M \\
&= 1 + \int_{x_1...x_M} ... \int \prod_{i=1}^{M} P(x_i; \lambda_i) \min_{y\in\mathbb{Z}} \left\{ b^y_0 + b^y_1\lambda'_1 + b^y_2\lambda'_2 + ... + b^y_L\lambda'_L \right\} dx_i \\
&= 1 + \int_{x_1...x_M} ... \int \prod_{i=1}^{M} P(x_i; \lambda_i) \min_{y\in\mathbb{Z}} \Big\{ b^y_0 + b^y_1\widehat{\mathcal{T}}(\lambda_1, x_1) + b^y_2\widehat{\mathcal{T}}(\lambda_2, x_2) + ... \\
&\qquad + b^y_M\widehat{\mathcal{T}}(\lambda_M, x_M) + b^y_{M+1}\widetilde{\mathcal{T}}(\lambda_M) + ... + b^y_L\widetilde{\mathcal{T}}(\lambda_L) \Big\} dx_i
\end{aligned} \tag{4.33}$$

Placing $\prod_{i=1}^{M} P(x_i; \lambda_i)$ into $\min_{y\in\mathbb{Z}}\{\cdot\}$, the integrand in (4.33) becomes

$$\begin{aligned}
\min_{y\in\mathbb{Z}} \Bigg\{ & b^y_0 \prod_{i=1}^{M} P(x_i; \lambda_i) \\
& + b^y_1 \prod_{i=1}^{M} P(x_i; \lambda_i)\widehat{\mathcal{T}}(\lambda_1, x_1) + ... + b^y_M \prod_{i=1}^{M} P(x_i; \lambda_i)\widehat{\mathcal{T}}(\lambda_M, x_M) \\
& + b^y_{M+1} \prod_{i=1}^{M} P(x_i; \lambda_i)\widetilde{\mathcal{T}}(\lambda_{M+1}) + ... + b^y_L \prod_{i=1}^{M} P(x_i; \lambda_i)\widetilde{\mathcal{T}}(\lambda_L) \Bigg\}
\end{aligned} \tag{4.34}$$

Using the result from [29] such that

$$P(x_i; \lambda_i)\widehat{\mathcal{T}}(\lambda_i, x_i) = [p_B + (1 - p_B - p_I)\lambda_i] f_1(x_i), \tag{4.35}$$

the expression in (4.34) can be manipulated into

$$\begin{aligned}
\min_{y\in\mathbb{Z}} \Bigg\{ & b_0^y \prod_{i=1}^{M} P(x_i;\lambda_i) \\
& + b_1^y \prod_{i=2}^{M} P(x_i;\lambda_i)\left[p_B + (1-p_B-p_I)\lambda_1\right] f_1(x_1) \\
& + b_2^y \prod_{i=1,i\neq 2}^{M} P(x_i;\lambda_i)[p_B + (1-p_B-p_I)\lambda_2] f_1(x_2) \\
& + ... \\
& + b_M^y \prod_{i=1,i\neq M}^{M} P(x_i;\lambda_i)[p_B + (1-p_B-p_I)\lambda_M] f_1(x_M) \\
& + b_{M+1}^y \prod_{i=1}^{M} P(x_i;\lambda_i)\widetilde{\mathcal{T}}(\lambda_{M+1}) \\
& + ... \\
& + b_L^y \prod_{i=1}^{M} P(x_i;\lambda_i)\widetilde{\mathcal{T}}(\lambda_L) \Bigg\}
\end{aligned} \tag{4.36}$$

where it can be observed that the function inside the $\min_{y\in\mathbb{Z}}\{\cdot\}$ function in (4.33), for all values of $(b_0^y, b_1^y, b_2^y, ..., b_L^y)$, is a linear function in $\lambda_1$ with $\lambda_2, \lambda_3, ..., \lambda_L$ given. It has been shown that the integrand in the second term of (4.33) is a concave function because it is a minima of a family of functions that are all linear in $\lambda_1$. Hence, the overall function $V_{\overline{C}_1}^{K+1}(\lambda_1, ..., \lambda_L)$ is concave as a result. The concavity of $V_{\overline{C}_1}^{K+1}(\lambda_1, ..., \lambda_L)$ with respect to other $\lambda_l$ can be shown with exactly the same way.

Through inductive reasoning, the basis step, $V_{\overline{C}_j}^{1}(\lambda_1, ..., \lambda_L)$ is concave in any $\lambda_l$, and the inductive step, $V_{\overline{C}_j}^{K+1}(\lambda_1, ..., \lambda_L)$ is concave if $V_{\overline{C}_j}^{K}(\lambda_1, ..., \lambda_L)$ is concave. This completes the proof for the concavity of the $V_{\overline{C}_j}^{K}(\lambda_1, ..., \lambda_L)$ function for all values of $K$.

The next claim of Lemma 1.1 is that $V_{\overline{C}_j}^{K}(\lambda_1, ..., \lambda_L)$ is monotonically decreasing

with respective to any $\lambda_l$. To show that through inductive reasoning, monotonicity of $V^1_{\overline{C}_j}(\lambda_1, ..., \lambda_L)$ must be shown first.

Recalling from (4.25), the definition of $V^1_{\overline{C}_1}(\lambda_1, ..., \lambda_L)$ is

$$\begin{aligned} V^1_{\overline{C}_1}(\lambda_1, ..., \lambda_L) &\equiv V^1_{\{C_1, C_2, ..., C_M\}}(\lambda_1, ..., \lambda_L) \\ &= 1 + \int_{x_1 ... x_M} ... \int P(x_1, ..., x_M; \lambda_1, ..., \lambda_M) V^0(\lambda_1^{'}, ..., \lambda_L^{'}) dx_1 ... dx_M \\ &= 1 + \int_{x_1 ... x_M} ... \int \prod_{i=1}^{M} P(x_i; \lambda_i) V^0(\lambda_1', ..., \lambda_L') dx_i \end{aligned} \tag{4.37}$$

To examine monotonicity of (4.37), the partial derivative of $V^1_{\overline{C}_1}(\lambda_1, ..., \lambda_L)$ with respect to the function's inputs is considered. For the inputs $\lambda_1, \lambda_2, ..., \lambda_L$, there are $L$ partial derivatives in question. However, these partial derivatives fall into one of two groups. Given the action $\overline{C}_1 = \{C_1, C_2, ..., C_M\}$, i.e., channels with index in $[1, M]$ are sensed and those with index $[M+1, L]$ are not, the first group contains the partial derivatives with respect to a belief value that corresponds to a sensed channel, while the second the group contains the partial derivatives with respect to a belief value of an un-sensed channel. Within a group, the procedure to demonstrate the monotonicity of a partial derivative is the same as the rest. As such, without loss of generality, the partial derivative representing the first group as the partial derivative with respect to $\lambda_1$, and the one representing the second group as the partial derivative with respect to $\lambda_{M+1}$.

The partial derivative with respect to $\lambda_1$ is

$$\begin{aligned}\frac{\partial}{\partial\lambda_1}V^1_{\overline{C}_1}(\lambda_1,...,\lambda_L) &= \frac{\partial}{\partial\lambda_1}\int_{x_1...x_M}...\int\prod_{i=1}^{M}P(x_i;\lambda_i)V^0(\lambda_1',\lambda_2'...,\lambda_L')dx_i \\ &= \int_{x_1...x_M}...\int\frac{\partial}{\partial\lambda_1}\prod_{i=1}^{M}P(x_i;\lambda_i)V^0(\lambda_1',\lambda_2'...,\lambda_L')dx_i \\ &= \int_{x_1...x_M}...\int\left(\frac{\partial}{\partial\lambda_1}P(x_1;\lambda_1)\right)\prod_{i=2}^{M}P(x_i;\lambda_i)V^0(\lambda_1',\lambda_2'...,\lambda_L')dx_idx_1 \\ &\quad+\int_{x_1...x_M}...\int P(x_1;\lambda_1)\left(\frac{\partial}{\partial\lambda_1}\prod_{i=2}^{M}P(x_i;\lambda_i)V^0(\lambda_1',\lambda_2'...,\lambda_L')dx_idx_1\right)\end{aligned} \tag{4.38}$$

The second equality is the result of the application of Leibniz Integral Rule [6], and the third equality follows after the product rule has been applied to the derivative. In order to show that $V^1_{\overline{C}_1}(\lambda_1,...,\lambda_L)$ is monotonically decreasing with respect to $\lambda_1$, both terms in (4.38) must be non-positive.

The following shows that the integrand in the second term of (4.38) is non-positive:

$$\begin{aligned}&P(x_1;\lambda_1)\left(\frac{\partial}{\partial\lambda_1}\prod_{i=2}^{M}P(x_i;\lambda_i)V^0(\lambda_1',\lambda_2'...,\lambda_L')dx_idx_1\right) \\ &\qquad= P(x_1;\lambda_1)\prod_{i=2}^{M}P(x_i;\lambda_i)\left(\frac{\partial}{\partial\lambda_1'}V^0(\lambda_1',\lambda_2'...,\lambda_L')\right)\left(\frac{\partial\lambda_1'}{\partial\lambda_1}\right)dx_idx_1\end{aligned} \tag{4.39}$$

where the first equality is a result of the chain rule. In [29], or from (3.9), it can be shown that

$$\frac{\partial\lambda_1'}{\partial\lambda_1}=\frac{\partial\widehat{\mathcal{T}}(\lambda_1,x_1)}{\partial\lambda_1}\geq 0,\quad \text{if } \lambda_1'=\widehat{\mathcal{T}}(\lambda_1,x_1). \tag{4.40}$$

From the definition of (4.21), the value function $V^0(\lambda_1,...,\lambda_L)$ is a monotonically decreasing function; hence with respect to $\lambda_1$,

$$\frac{\partial}{\partial\lambda_1'}V^0(\lambda_1',\lambda_2'...,\lambda_L')\leq 0. \tag{4.41}$$

Consider that the remaining products in (4.39) are non-negative by definition and that there is only one negative product, the products that make up the integrand in the second term is in turn non-positive. As integrating over any non-positive function results in a non-positive value, the second term in (4.39) is non-positive.

Before the monotonicity of the first term in (4.39) is discussed, an inequality below needs to be established. It needs to be shown that following inequality is true, given the values of $\lambda_2, ..., \lambda_L$, and $x_2, ..., x_M$:

$$\inf_{x_1: f_1(x_1) \leq f_0(x_1)} V^0(\lambda'_1, ..., \lambda'_L) \geq \sup_{x_1: f_1(x_1) > f_0(x_1)} V^0(\lambda'_1, ..., \lambda'_L) \tag{4.42}$$

Or equivalently, where from (4.4),

$$\begin{aligned} &\inf_{x_1: f_1(x_1) \leq f_0(x_1)} V^0(\widehat{\mathcal{T}}(\lambda_1, x_1), \widehat{\mathcal{T}}(\lambda_2, x_2), ..., \widetilde{\mathcal{T}}(\lambda_L)) \\ &\quad \geq \sup_{x_1: f_1(x_1) > f_0(x_1)} V^0(\widehat{\mathcal{T}}(\lambda_1, x_1), \widehat{\mathcal{T}}(\lambda_2, x_2), ..., \widetilde{\mathcal{T}}(\lambda_L)) \end{aligned} \tag{4.43}$$

Using the fact that $V^0(\lambda_1, ..., \lambda_L)$ is monotonically decreasing and the functions

$$\left\{ \widehat{\mathcal{T}}(\lambda_2, x_2), ..., \widetilde{\mathcal{T}}(\lambda_L) \right\} \tag{4.44}$$

are held to constant for given values of $\lambda_2, ..., \lambda_L$, and $x_2, ..., x_M$, the inequality in (4.42) is transformed into the inequality below

$$\sup_{x_1: f_1(x_1) \leq f_0(x_1)} \widehat{\mathcal{T}}(\lambda_1, x_1) \leq \inf_{x_1: f_1(x_1) > f_0(x_1)} \widehat{\mathcal{T}}(\lambda_1, x_1). \tag{4.45}$$

Using the result from Lemma 3 of [29], the transformed inequality in (4.45) is proven to be true.

With the inequality in (4.42), one can proceed to show the monotonicity of the first term in (4.38):

$$\begin{aligned}
&\int_{x_1 \ldots x_M} \ldots \int \left( \frac{\partial}{\partial \lambda_1} P(x_1; \lambda_1) \right) \prod_{i=2}^{M} P(x_i; \lambda_i) V^0(\lambda_1', \lambda_2' \ldots, \lambda_L') dx_i dx_1 \\
&= \int_{\{x_1 \ldots x_M, x_m \neq x_1\}} \ldots \int \prod_{i=2}^{M} P(x_i; \lambda_i) \left[ \int_{x_1 \in \mathbb{R}} \left( \frac{\partial}{\partial \lambda_1} P(x_1; \lambda_1) \right) V^0(\lambda_1', \lambda_2' \ldots, \lambda_L') dx_1 \right] dx_i.
\end{aligned} \tag{4.46}$$

In [29], the following derivative is shown to have a more simple form:

$$\frac{\partial}{\partial \lambda_1} P(x_1; \lambda_1) = (1 - p_B - p_I)(f_1(x_1) - f_0(x_1)) \tag{4.47}$$

Substituting (4.47) into (4.46),

$$\begin{aligned}
&\int_{x_1 \ldots x_M} \ldots \int \left( \frac{\partial}{\partial \lambda_1} P(x_1; \lambda_1) \right) \prod_{i=2}^{M} P(x_i; \lambda_i) V^0(\lambda_1', \lambda_2' \ldots, \lambda_L') dx_i dx_1 \\
&= \int_{\{x_1 \ldots x_M, x_m \neq x_1\}} \ldots \int \prod_{i=2}^{M} P(x_i; \lambda_i) \left[ \int_{x_1 \in \mathbb{R}} (1 - p_B - p_I) \left( f_1(x_1) - f_0(x_1) \right) V^0(\lambda_1', \lambda_2' \ldots, \lambda_L') dx_1 \right] dx_i \\
&= \int_{\{x_1 \ldots x_M, x_m \neq x_1\}} \ldots \int \prod_{i=2}^{M} P(x_i; \lambda_i) (1 - p_B - p_I) \left[ \int_{x_1 \in \mathbb{R}} \left( f_1(x_1) - f_0(x_1) \right) V^0(\lambda_1', \lambda_2' \ldots, \lambda_L') dx_1 \right] dx_i.
\end{aligned} \tag{4.48}$$

Focusing on the integration within the square bracket in (4.48), the following shows

that the entire integration is non-positive:

$$
\begin{aligned}
&\int_{x_1\in\mathbb{R}} \left(f_1(x_1)-f_0(x_1)\right) V^0(\lambda_1',\lambda_2'...,\lambda_L')dx_1 \\
&= \int_{x_1:f_1(x_1)\le f_0(x_1)} \left(f_1(x_1)-f_0(x_1)\right) V^0(\lambda_1',\lambda_2'...,\lambda_L')dx_1 \\
&\quad + \int_{x_1:f_1(x_1)>f_0(x_1)} \left(f_1(x_1)-f_0(x_1)\right) V^0(\lambda_1',\lambda_2'...,\lambda_L')dx_1 \\
&\le \inf_{x_1:f_1(x_1)\le f_0(x_1)} V^0(\lambda_1',\lambda_2'...,\lambda_L') \int_{x_1:f_1(x_1)\le f_0(x_1)} \left(f_1(x_1)-f_0(x_1)\right) dx_1 \\
&\quad + \sup_{x_1:f_1(x_1)>f_0(x_1)} V^0(\lambda_1',\lambda_2'...,\lambda_L') \int_{x_1:f_1(x_1)>f_0(x_1)} \left(f_1(x_1)-f_0(x_1)\right) dx_1 \\
&\le \inf_{x_1:f_1(x_1)\le f_0(x_1)} V^0(\lambda_1',\lambda_2'...,\lambda_L') \int_{x_1:f_1(x_1)\le f_0(x_1)} \left(f_1(x_1)-f_0(x_1)\right) dx_1 \\
&\quad + \inf_{x_1:f_1(x_1)\le f_0(x_1)} V^0(\lambda_1',\lambda_2'...,\lambda_L') \int_{x_1:f_1(x_1)>f_0(x_1)} \left(f_1(x_1)-f_0(x_1)\right) dx_1 \\
&= \inf_{x_1:f_1(x_1)\le f_0(x_1)} V^0(\lambda_1',\lambda_2'...,\lambda_L') \int_{x_1\in\mathbb{R}} \left(f_1(x_1)-f_0(x_1)\right) dx_1 = 0. \qquad (4.49)
\end{aligned}
$$

The first inequality originates from upper-bounding the function $V^0(\lambda_1',\lambda_2'...,\lambda_L')$. That the upper bound to the first term is an infimum may be counter-intuitive at first. It is because the interval of $x_1$ that the first term integrates over results in a non-positive product in $(f_1(x_1)-f_0(x_1))$, consequently rendering the entire term non-positive. The second inequality results from the an application of (4.42). Finally, at the last equality, the infimum of the $V^0(\lambda_1',\lambda_2'...,\lambda_L')$ is factored out and by definitions of pdfs $f_1(x_1)$ and $f_0(x_1)$, the entire value equals zero. Therefore, it is shown that the integration within the square bracket in (4.48) is non-positive. Provided that $p_B+p_I\le 1$ in (4.48), the quantity (4.46) is also non-positive.

Going back to the original equation that defines $\frac{\partial}{\partial\lambda_1}V^1_{\overline{C}_1}(\lambda_1,...,\lambda_L)$, it is shown that both of the terms in the definition in (4.38) are non-positive. Hence, it is proven that the function $V^1_{\overline{C}_1}(\lambda_1,...,\lambda_L)$ is monotonically decreasing with respect to $\lambda_1$. As

the procedures to show $\frac{\partial}{\partial\lambda_1}V^1_{\overline{C}_1}(\lambda_1,...,\lambda_L)\leq 0$ are the same as $\frac{\partial}{\partial\lambda_l}V^1_{\overline{C}_1}(\lambda_1,...,\lambda_L)$, for $1\leq l\leq M$, these partial derivatives are also non-positive.

Next, the monotonicity of the second group of partial derivatives, i.e., the partial derivatives with respect to $\{\lambda_l|M+1\leq 1\leq L\}$, is examined. Consider the partial derivative with respect to $\lambda_{M+1}$, and the definitions

$$\frac{\partial}{\partial\lambda_{M+1}}V^1_{\overline{C}_1}(\lambda_1,...,\lambda_L)=\frac{\partial}{\partial\lambda_{M+1}}\int_{x_1...x_M}...\int\prod_{i=1}^{M}P(x_i;\lambda_i)V^0(\lambda'_1,...,\lambda'_{M+1},...,\lambda'_L)dx_i. \tag{4.50}$$

The above can be manipulated according to the following:

$$\begin{aligned}
&\frac{\partial}{\partial\lambda_{M+1}}\int_{x_1...x_M}...\int\prod_{i=1}^{M}P(x_i;\lambda_i)V^0(\lambda'_1,...,\lambda'_{M+1},...,\lambda'_L)dx_i\\
&=\int_{x_1...x_M}...\int\prod_{i=1}^{M}P(x_i;\lambda_i)\left[\frac{\partial}{\partial\lambda_{M+1}}V^0(\lambda'_1,...,\lambda'_{M+1},...,\lambda'_L)\right]dx_i\\
&=\int_{x_1...x_M}...\int\prod_{i=1}^{M}P(x_i;\lambda_i)\left[\frac{\partial}{\partial\lambda'_{M+1}}V^0(\lambda'_1,...,\lambda'_{M+1},...,\lambda'_L)\frac{\partial\lambda'_{M+1}}{\partial\lambda_{M+1}}\right]dx_i
\end{aligned} \tag{4.51}$$

where the first equality is obtained through Liebniz Integral Rule [6], and the second equality through the chain rule. From (3.10), it is shown that

$$\frac{\partial\lambda'_{M+1}}{\partial\lambda_{M+1}}=\frac{\partial\widetilde{\mathcal{T}}(\lambda_{M+1})}{\partial\lambda_{M+1}}\geq 0,\quad \text{if } \lambda'_{M+1}=\widetilde{\mathcal{T}}(\lambda_{M+1}). \tag{4.52}$$

From (4.41) and (4.52), it can be seen that the integrand in the expression in (4.51) has one product that is negative and hence is a non-positive function. As integrating a non-positive function results in a non-positive quantity, it is concluded that $\frac{\partial}{\partial\lambda_{M+1}}V^1_{\overline{C}_1}(\lambda_1,...,\lambda_{M+1},...,\lambda_L)$ is non-positive. Therefore, monotonicity of the function $V^1_{\overline{C}_1}(\lambda_1,...,\lambda_{M+1},...,\lambda_L)$ is shown.

At this point, the monotonicity of the function $V^K_{\overline{C}_1}(\lambda_1, ..., \lambda_L)$, where $K = 1$, has been shown to be non-increasing along all directions of $\lambda_l$. It turns out that showing the monotonicity for $K = 2, 3, ...$ through inductive reasoning, follow the same procedure to show that $V^{K+1}_{\overline{C}_1}(\lambda_1, ..., \lambda_L)$ is monotonically decreasing if $V^K_{\overline{C}_1}(\lambda_1, ..., \lambda_L)$ is assumed to be monotonic. So for all values of $K$, the function $V^K_{\overline{C}_1}(\lambda_1, ..., \lambda_L)$ is proven to be a monotonically decreasing function.

As mentioned earlier, concavity and the monotonicity is shown for the function $V^K_{\overline{C}_1}(\lambda_1, ..., \lambda_L)$ that is particular to the action $\overline{C}_1$. Without loss of generality, same procedures apply to any action $\overline{C}_j$. Based on this, the proof has shown that all the conditional value functions $\{V^K_{\overline{C}_j}(\lambda_1, ..., \lambda_L)\}$, for $1 \leq j \leq |\mathcal{C}|$, comply with Lemma 1.1.

# Chapter 5

# Simulation Results and Discussions

This chapter evaluates the performance of the multiband multi-sensor spectrum sensing detectors (MMSSD) using Monte Carlo simulations. Firstly, the performance impact of introducing additional sensors is examined through comparisons between MMSSDs and detectors with a single-sensor configuration. Secondly, a comparison study is conducted between MMSSD and its reduced-complexity version, RC-MMSSD, in order to determine the complexity vs. detection performance tradeoffs of RC-MMSSD. Later in this chapter, comparisons to quickest detection methods are performed to establish the performance of MMSSD relative to existing quickest detection techniques.

Besides comparing the performance among the detection methods, this chapter also examines how MMSSD performs if the underlying channel usage pattern does not conform to the statistical channel usage model assumed in Chapter 3. An alternative channel usage model derived experimentally from WLAN networks is used to perform this assessment.

The detector performance that is assessed is the expected detection delay and

corresponding false alarm rate. A detector is desired to be agile and reliable. High agility means that a detector possesses a low expected detection delay, while high reliability means that a detector possesses a low false alarm rate.

The 95-percent confidence interval is used to measure the accuracy of an empirically derived estimate, which in this case is an estimate of the system's expected detection delay and false alarm rate. The methodology below describes the procedure to determine the intervals for expected detection delay and false alarm rate.

Let $W$ denote the number of trials in a simulation. To compute the 95% confidence interval, the sample average and the sample variance need to be computed first. The sample average is the expected detection delay, which denoted by $T_{\text{delay}}$, and is computed as follows:

$$T_{\text{delay}} = \frac{1}{W} \sum_{i=1}^{W} \hat{T}_{\text{delay},i}, \tag{5.1}$$

where $\hat{T}_{\text{delay},i}$ is the detection delay for a single trial in the simulation, for $1 \leq i \leq W$. The sample variance, denoted by $\sigma^2_{\text{delay}}$ is computed as follows:

$$\sigma^2_{\text{delay}} = \frac{1}{W-1} \sum_{i=1}^{W} (\hat{T}_{\text{delay},i} - T_{\text{delay}})^2. \tag{5.2}$$

Using (5.1) and (5.2), the 95% confidence interval is computed via the following equation [23]:

$$\Delta T_{\text{delay}} = 1.96 \sqrt{\frac{\sigma^2_{\text{delay}}}{W}}. \tag{5.3}$$

The procedure to compute the 95% confidence interval for false alarm rate is similar to that of expected detection delay. Let the indicator function of a false alarm outcome of each realization be denoted as $\hat{P}_{\text{FA},i}$, for $1 \leq i \leq W$, where $\hat{P}_{\text{FA},i} \in \{0, 1\}$;

the value '1' represents an occurrence of a false alarm and the value '0' represents otherwise. Again, sample average and sample variance are needed to determine the interval. Sample average of the false alarm rate over the $W$ trials is as follows:

$$P_{\text{FA}} = \frac{1}{W}\sum_{i=1}^{W}\hat{P}_{\text{FA},i}, \tag{5.4}$$

and the sample variance for each of the false alarm rate, denoted by $\sigma^2_{\text{FA}}$, is

$$\sigma^2_{\text{FA}} = \frac{1}{W-1}\sum_{i=1}^{W}(\hat{P}_{\text{FA},i} - P_{\text{FA}})^2. \tag{5.5}$$

Based on these established parameters, the 95% confidence interval for the false alarm rate obtained via simulation, denoted as $\Delta P_{\text{FA}}$, is determined using the following equation [23],

$$\Delta P_{\text{FA}} = 1.96\sqrt{\frac{\sigma^2_{\text{FA}}}{U}}. \tag{5.6}$$

Two assumptions are made for the determination of the confidence interval: 1) $T_{\text{delay}}$ and $P_{\text{FA}}$ is an unbiased estimate of the true value of the false alarm rate, and 2) the errors are normally distributed around the mean of $T_{\text{delay}}$ and $P_{\text{FA}}$.

For the simulations, the number of trials $W$ is chosen to be $W = 10^5$ so that the 95% confidence intervals are $|\Delta T_{\text{delay}}| \leq 1$ and $|\Delta P_{\text{FA}}| \leq 0.001$.

## 5.1 Performance Impacts of Extra Sensors

Based on the signal model defined in Section 3.1.2, the marginal distributions of an observation for either a busy or an idle state are zero-mean normally distributed. In a busy state, the probability density function (pdf) of an observation, $f_0$, has a variance of $\sigma_0^2 = \sigma^2 + P$, which models the combined power from the transmission of the signal

occupying the channel plus the background white noise. In an idle state, the pdf $f_1$ has a variance of $\sigma_1^2 = \sigma^2$, indicating only the power of the background white noise is present. The signal-to-noise ratio (SNR) in decibels (dB) is defined as $10\log_{10}(P/\sigma^2)$. Within this section, the detectors are designed to meet the false alarm constraint of $\alpha = 0.1$, which is chosen to expedite the execution of the simulation. A lower false alarm constraint is used in later simulations and the results are consistent with these results. The number of trials used for the Monte Carlo simulations, i.e., $W$, is $10^5$.

When $M = 1$, MMSSD is in a single-sensor configuration, which is the detector developed in [29]. In order to compare expected detection delays, the detectors in question must be compared with similar false alarm rates. Fig. 5.1 shows the false alarm rates of MMSSD with different numbers of sensors as a function of $\lambda_o$, the fraction of channel idle time. First, it is clear that the threshold design rule $\eta_d = 1-\alpha$, as discussed in Section 4.2, satisfies the false alarm constraint of $\alpha = 0.1$. Secondly, Fig. 5.1 shows that no single detector is able to outperform others in terms of false alarm rate across all values of $\lambda_o$. Note that for the lower $\lambda_o$ values, the false alarms rates are very similar and quite invariant to $\lambda_o$.

Fig. 5.2 compares the expected detection delays of MMSSD for different values of $\lambda_o$. From Fig. 5.2, it is evident that the reduction in expected detection delay is more significant when the idle periods account for smaller percentages of time ($\lambda_o \to 0$). The reduction in expected detection delay obtained by adding extra sensors depends on how many sensors that are deployed. By adding an additional sensor from $M = 1$ to $M = 2$, the expected detection time experiences a large gain compared to adding a sensor from $M = 3$ to $M = 4$. In fact, an additional sensor for a detector with 3 sensors yields very little performance gain. Since $M = 4$ is a full-sensing detector,

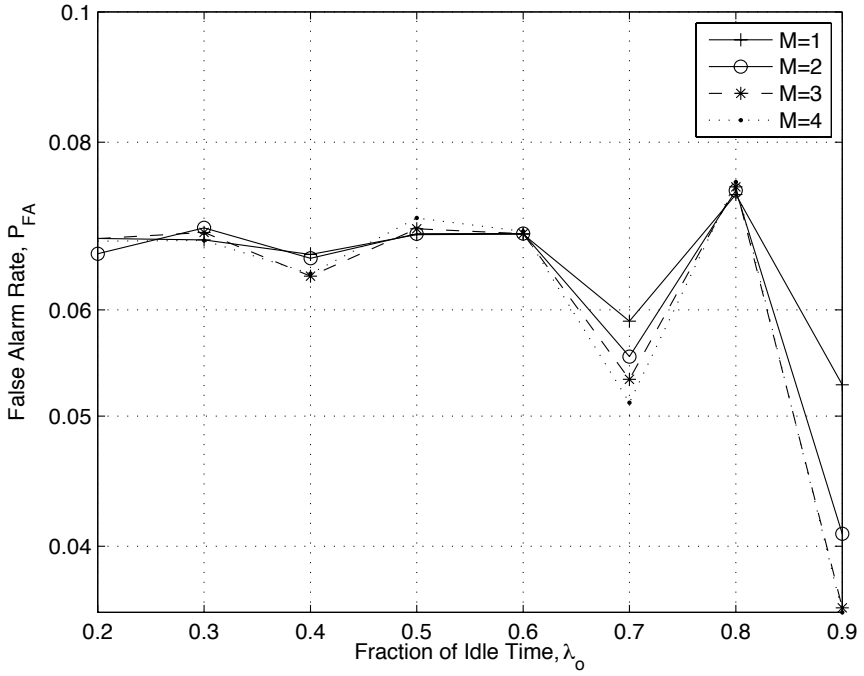


Figure 5.1: The false alarm rates of MMSSD with different numbers of sensors $M$. The 95% confidence interval is less than $\pm 0.01$ ($m_B = 300, \text{SNR}=0$ dB, $\eta_d = 0.9, L = 4, W = 10^5$).

i.e., a configuration with a sensor per channel, it is fair to claim that the performance of a full-sensing detector, in terms of expected detection delay, can be in large part achieved by deploying fewer than $L$ sensors.

Next, the performance of RC-MMSSD is compared to that of a single-sensor configuration. For this simulation, the number of available channels, $L$ is chosen to be large, e.g., $L = 100$, to ensure that $L >> M$ satisfy the conditions discussed in Section 4.3. The effect of violating these conditions is studied later. To establish a baseline false alarm rate, a threshold of $\eta_d = 1 - \alpha = 0.9$ is used. Fig. 5.3 shows the false alarm performances of RC-MMSSD with different numbers of sensors. It is seen that all detectors comply with the false alarm rate constraints, again verifying

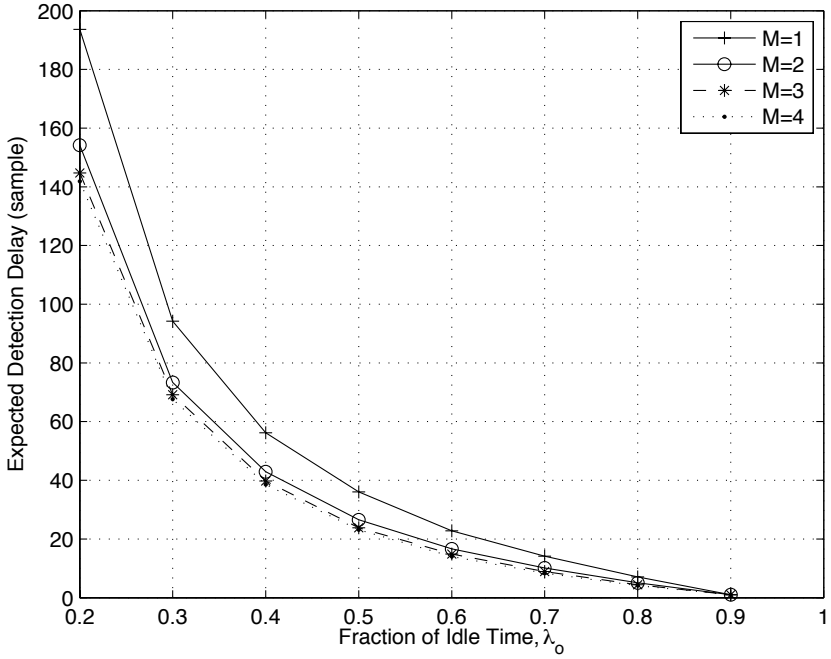


Figure 5.2: The expected detection delays of MMSSD with different numbers of sensors $M$. The 95% confidence interval does not exceed $\pm 1$ ($m_B = 300$, SNR=0 dB, $\eta_d = 0.9, L = 4, W = 10^5$).

the threshold design rule. In addition, the false alarm rates among detectors using different numbers of sensors remain similar, especially when $\lambda_o$ is small.

Fig. 5.4 shows a comparison of expected detection delay using RC-MMSSD. When $M = 1$, RC-MMSSD is in a single-sensor configuration, which is first developed and demonstrated in [29]. Similar to what the MMSSD comparison has shown, the largest reduction in expected detection delay comes from adding sensors when $M$ is small. As $M$ becomes larger, the improvement in adding extra sensors diminishes. This implies that by deploying a smaller number of sensors, a detector can achieve a performance in terms of expected detection delay that is close to that using a larger number of sensors.

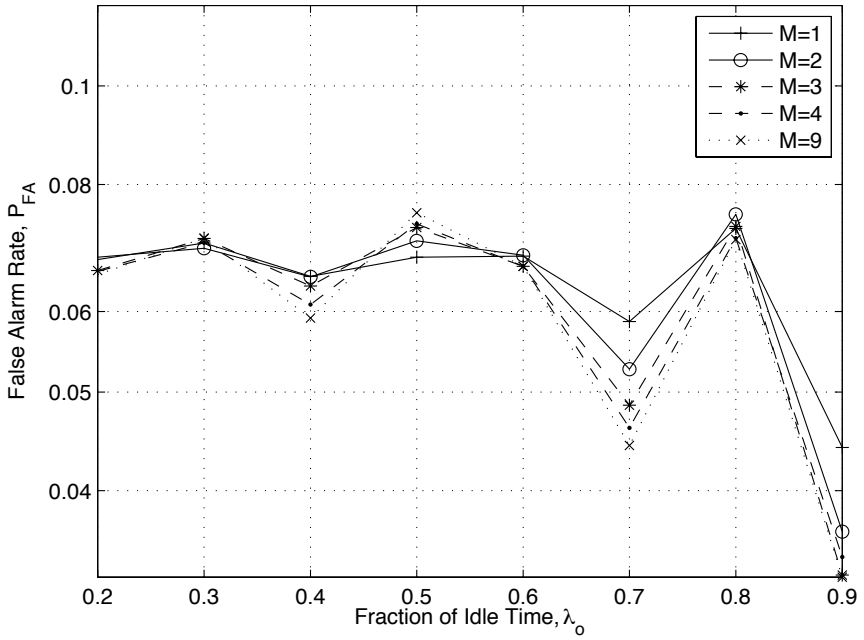


Figure 5.3: The false alarm rate of RC-MMSSD for different numbers of sensors, $M$. The 95% confidence interval is less than $\pm 0.01$ ($m_B = 300, \text{SNR}=0$ dB, $\eta_d = 0.9, L = 100, W = 10^5$).

In summary, the performances of MMSSD and RC-MMSSD both experience the greatest improvement in performance with the first few sensors added. Beyond a certain value of $M$, added sensors produce an insignificant performance gain. In additional, there is no evidence in the comparison of false alarm rates at different $M$ to suggest that a tradeoff exists between $M$ and the false alarm rate.

## 5.2 MMSSD versus RC-MMSSD

In the development of RC-MMSSD in Section 4.3, it is indicated that in the asymptotic condition $L - M \to \infty$, RC-MMSSD effectively behaves and performs like

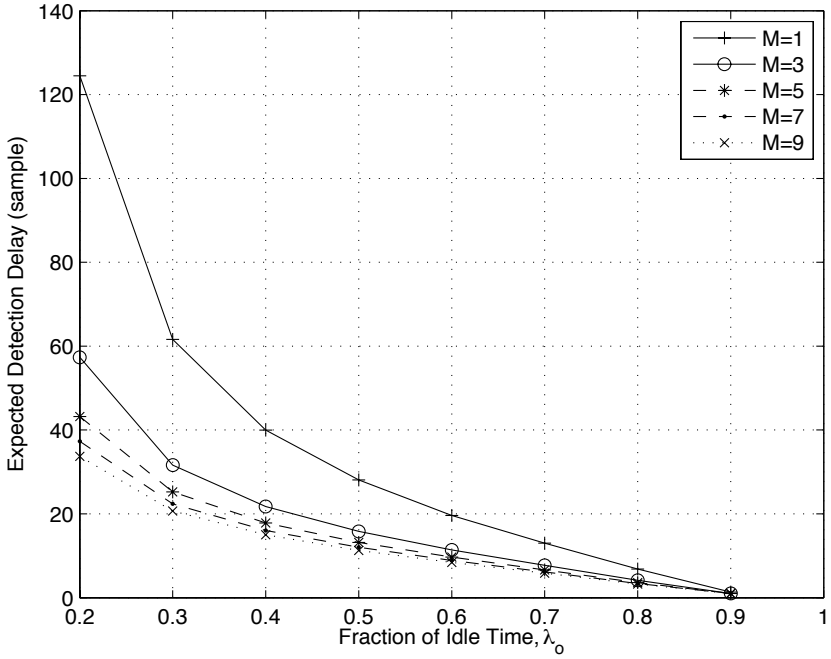


Figure 5.4: The expected detection delay of RC-MMSSD for different numbers of sensors $M$. The 95% confidence interval does not exceed $\pm 1$ ($m_B = 300$, SNR=0 dB, $\eta_d = 0.9, L = 100, W = 10^5$).

MMSSD. Here, a comparison between the performances of the two detectors is conducted through simulation. The expected detection delays and false alarm rates for each detector are shown in Figs. 5.5 and 5.6 for different values of $L$ and, for different SNR levels: 10dB and 0dB. With the value of $M$ fixed to 4, studying the system with varying values of $L$ offers insight into the relationship between system performance and size of the unobserved pool.

It is evident in Fig. 5.5 that when $L < 30$, there is a problem with designing RC-MMSSD with the threshold design rule $\eta_d = 1 - \alpha$, as the detector fails to meet the prescribed false alarm constraint $\alpha$. This observation is consistent with the analysis in Section 4.3 on the impact of having a small pool of unobserved channels on the

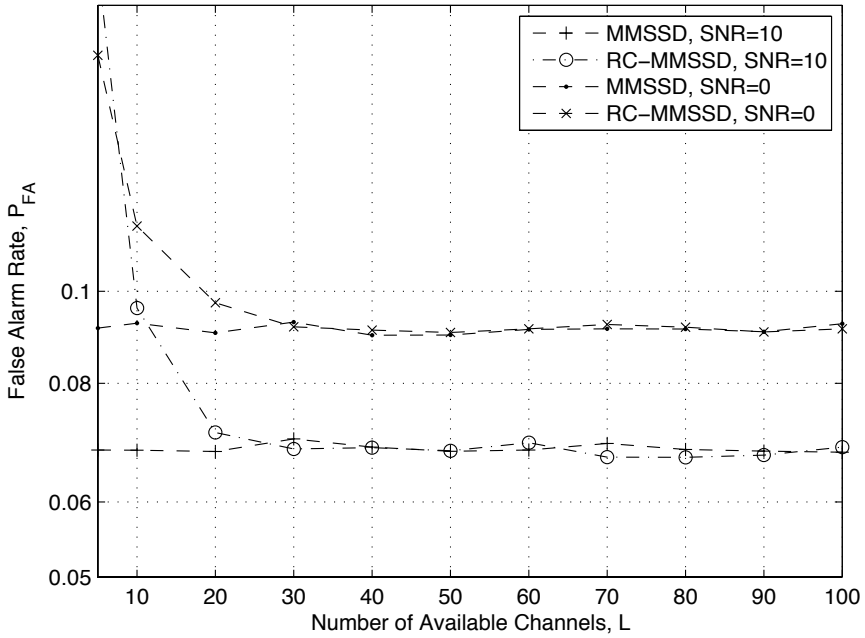


Figure 5.5: The false alarm rates of MMSSD and RC-MMSSD with respect to the number of available channels, for both SNR=0 dB and SNR=10 dB. Note the violation of the prescribed false alarm constraint $\alpha = 0.1$ when $L < 30$. The 95% confidence interval is less than $\pm 0.01$ ($\lambda_0 = 0.25, m_B = 300, \eta_d = 0.9, M = 4, W = 10^5$).

false alarm rate.

For $L > 30$, the false alarm rates of the two detectors are similar and Fig. 5.6 shows that the expected detection delays of MMSSD and RC-MMSSD are identical. This result indicates that when the number of available channels greatly outnumbers the number of sensors, MMSSD and RC-MMSSD have similar performances despite RC-MMSSD's reduced complexity, This result affirms the claims in Section 4.3 that MMSSD behaves no differently from RC-MMSSD as the pool of unobserved channels grows large, so that both detectors have very similar performances.

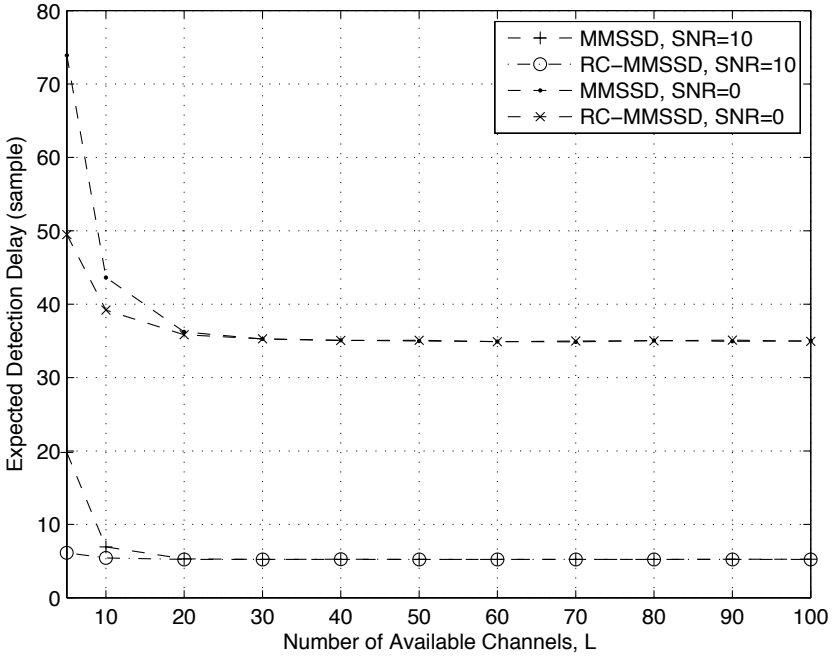


Figure 5.6: The expected detection delays of MMSSD and RC-MMSSD with respect to the number of available channels, for both SNR=0 dB and SNR=10 dB. The 95% confidence interval does not exceed $\pm 1$ ($\lambda_0 = 0.25, m_B = 300, \eta_d = 0.9, M = 4, W = 10^5$).

## 5.3 MMSSD versus Quickest Detection Methods

The comparisons that have been conducted so far investigate the effect of adding extra sensors to the detectors first developed in [29], which detect idle periods over multiple channels using only one sensor. MMSSD, RC-MMSSD, and the detectors developed in [29] are all based on partially observable Markov decision processes (POMDP). One area of performance evaluation that has not been explored in the open literature is how the performance of these POMDP-based detectors compare to quickest detection schemes. This section considers three different quickest detectors: Page's CUSUM (Section 2.3.1), Shiryaev's Bayesian detector (Section 2.3.2), and

minimum asymptotic risk (MAR) detector (Section 2.3.3).

Since quickest detection algorithms perform detection on a single channel at a time, a comparison to MMSSD in a multiband context requires some modification to these detectors. Full-sensing schemes based on these quickest detectors are developed here to enable detection using $M$ sensors over $L$ channels.

A full-sensing scheme based on quickest detection works as follows: a full-sensing system with $L$ sensors has each one independently performing quickest detection on its assigned channel in parallel. The detection continues until the time that the first sensor declares a channel to be idle, at which point the entire detection process also terminates. Since a quickest detector is unable to dynamically switch channels to sense, it always performs detection with the same number of sensors as the number of channels and hence is a full-sensing scheme.

Unlike the POMDP, there is an inherent incompatibility issue when applying quickest detection to the ON-OFF process model. Since by definition an ON-OFF process has multiple ON and OFF periods, there exist multiple transitions between idle and busy states over the time horizon of an ON-OFF process. The problem formulation for quickest detection methods assumes that there is a single change in signal energy and defines expected detection delay differently from the POMDP's definition. Second, due to multiple state transitions, once an ON-OFF process enters an idle state, it may again switch back to the busy state. This introduces a new type of false alarm situation because of the assumption of a single change on the part of quickest detection. Consider a system that employs a quickest detection method. In this system, the quickest detection methods may have an expected detection delay that exceeds the average length of the idle time. In this case, it is quite likely that

the detector may declare a busy-state-to-idle-state change after the channel switches back to a busy state from an idle state, which constitutes a false alarm. Under the quickest detection formulation of Eq. (2.14), the process cannot switch state more than once. Since this scenario is not accounted for, the result is an increase in false alarm.

As a consequence of not considering the above false alarm situation, the false alarm rate of these quickest detection methods in Chapter 2 reaches an error floor around the point where the expected detection delay exceeds the average idle period, independent of the value of the threshold. This effect is illustrated by examples through Page's CUSUM. In Fig. 5.7, the false alarm rate stops decreasing with respect to an increase in detection threshold after the ratio of expected detection delay to average idle duration starts to exceed unity. Hence, a CUSUM detector cannot be designed to meet false alarm requirements below this error floor. This is a limitation for all quickest detection methods, because channels may contain multiple state changes between busy and idle states.

Due to this limitation, in order to fairly compare the performance of MMSSD and RC-MMSSD to a quickest detection, such error floor problems needs to be avoided in the following simulation. Therefore, the SNR levels and average idle durations are chosen to achieve a sufficiently low ratio of expected detection delay to average idle period time for all the comparisons.

The method used to evaluate whether differences in performance are statistically significant is to compare expected detection delay of each detection method given the same level of false alarm rate. For a fair comparison, each detector is designed with the same actual false alarm rate of 0.01. The 95% confidence interval for each false

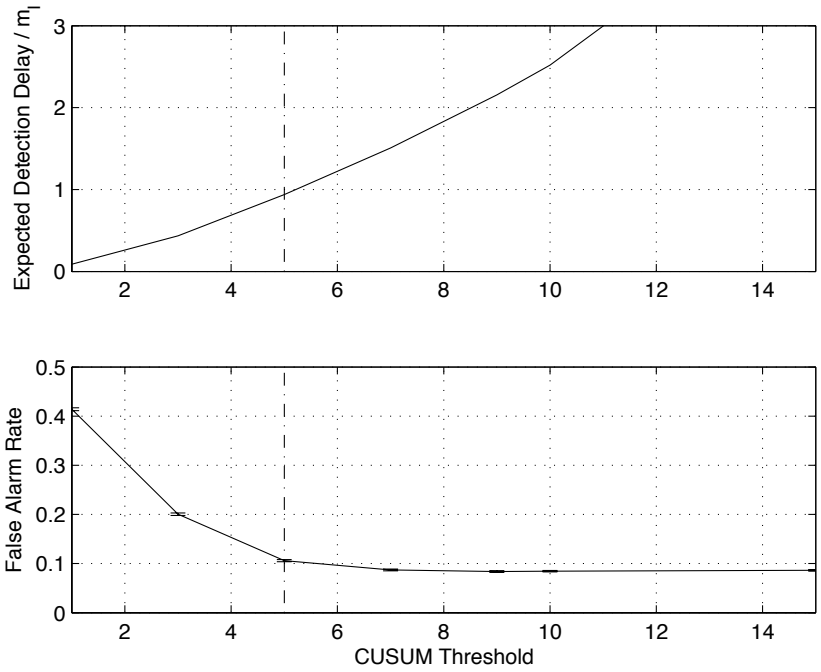


Figure 5.7: The false alarm rates reach an error floor in spite of increasing the detector threshold. The dashed line, i.e., where the ratio of expected detection delay to average idle time, $m_I$, in the top plot crosses 1, indicates where expected detection delay begins to exceed the average idle time, and where the false alarm rates begin to flatten in the bottom plot.

alarm rate is estimated via simulation. If there is no closed-form expression for the threshold design for a detector, a search is used for a threshold that yields the desired false alarm rate of $0.01 \pm 0.005$ with 95% confidence.

### 5.3.1 MMSSD versus Page's CUSUM

Figs. 5.8 and 5.9 show comparison between MMSSD (Section 4.2) and CUSUM (Section 2.3.1). The false alarm rates of MMSSD and CUSUM have been designed to achieve $\alpha = 0.01$ and Fig. 5.9 shows that the false alarm rates of CUSUM are set to be equal to or higher than those of MMSSD detectors by the 95% confidence interval

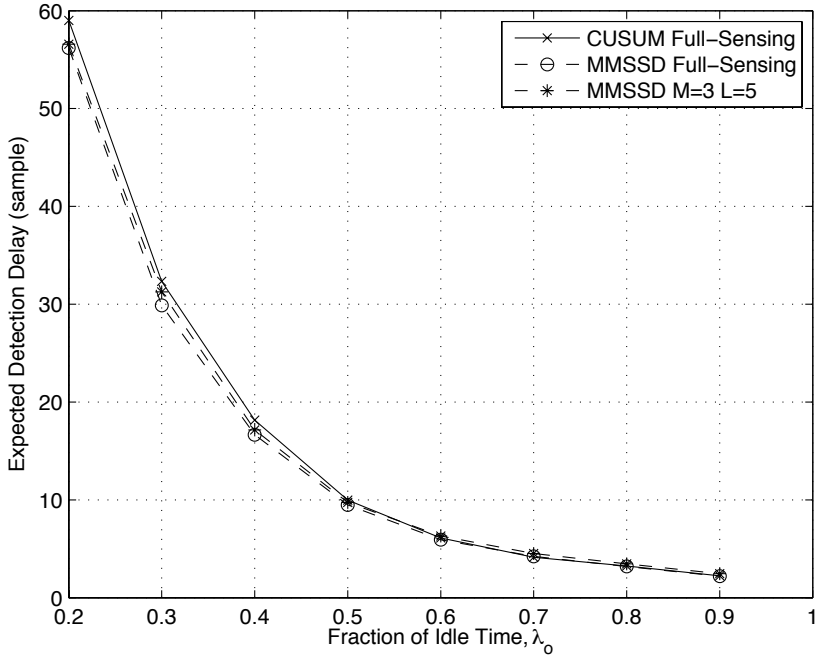


Figure 5.8: A comparison of the expected detection delays between full-sensing CUSUM detection and MMSSD detection that uses 3 and 5 sensors. (SNR=10dB, $m_B = 620, L = 5, W = 10^5$). The 95% confidence interval does not exceed $\pm 1$.

of 0.005. Fig. 5.8 shows a performance comparison among a full-sensing MMSSD, a full-sensing CUSUM, and a non-full-sensing MMSSD with three sensors. MMSSD's expected detection delay using 5 sensors is shown to perform similarly to CUSUM detection with 5 sensors. This suggests that MMSSD does not show a performance advantage over CUSUM in a full-sensing configuration.

The similarity in performance between MMSSD and CUSUM is unexpected as MMSSD has taken into account more information about the statistical behaviour of the channel traffic via a channel usage model. The reason for the similarity in performance lies in the values used for the average busy and average idle periods, $m_B$ and $m_I$, respectively. As $m_B$ and $m_I$ grow large, $p_B$ and $p_I$ both tend to 0 and

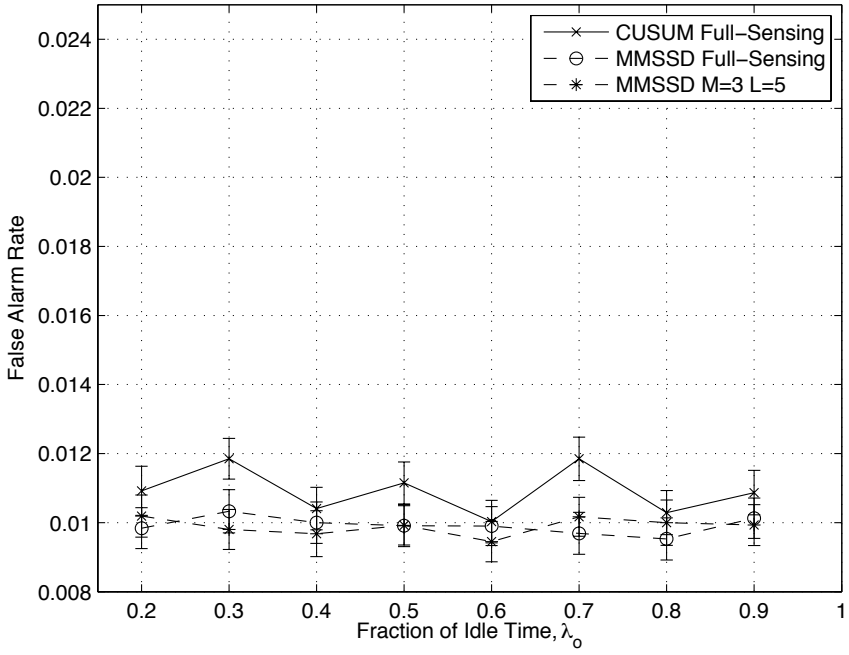


Figure 5.9: A comparison of the false alarm rate between a full-sensing CUSUM detection and MMSSD detection that uses 3 and 5 sensors. The error bars are the 95% confidence intervals for each points. (SNR=10dB, $m_B = 620, L = 5, W = 10^5$).

the geometric distributions that model the durations of busy and idle times become stretched out and flattened. To illustrate this trend, the probability mass function of the duration of an idle period is plotted for different values of $p_I$ in Fig. 5.10. This implies that as the value of $p_I$ (or $p_B$) used becomes smaller, idle period durations become closer to being equiprobable and such an a priori distribution begins to appear similar to a uniform distribution, which offers very limited information to the detector.

Even though the performance improvement of MMSSD given small values of $p_I$ and $p_B$ is limited, MMSSD's ability to dynamically determine which channels to sense helps the detector to obtain better utility of each sensor. It can be seen that

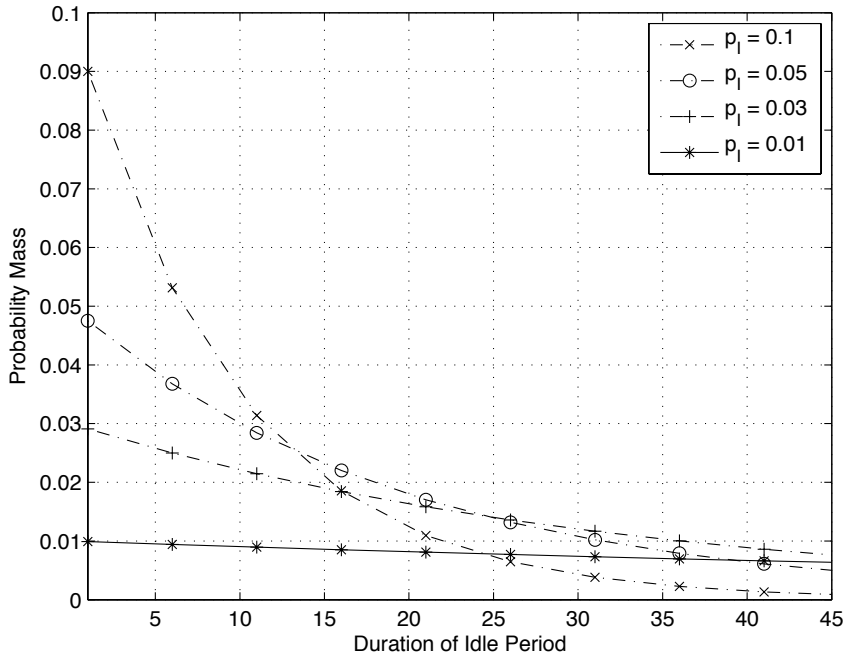


Figure 5.10: The probability mass function (PMF) of the duration of an idle period becomes flattened as the value of $p_I$ tends to zero.

that MMSSD with $M = 3$ sensors and $L = 5$ channels performs similarly to full-sensing CUSUM. MMSSD allows for the reduction of two sensors without paying a performance penalty. Although the reduction is small, this behaviour is consistent with the observations in Section 5.1. In the next study, the comparison between RC-MMSSD and CUSUM further demonstrates the benefits of the detector's ability to dynamically switch.

To investigate the effects of the channel usage model, performance is investigated with different channel usage parameters, where the value of $p_B$ is varied. However, the value $p_I$ must remain small due to the need to avoid the error floor that CUSUM encounters and maintain a fair comparison (See Fig. 5.7). Figs. 5.11 and 5.12 show the performances of the two detectors with respect to different SNR levels. Fig. 5.12

establishes a baseline false alarm rate at 0.01 in order to compare expected detection delays. In Fig. 5.11, the improvement in expected detection delay of MMSSD over CUSUM is significant at lower SNR values, while both detectors perform very similarly at higher SNR values. The result can be explained by examining the structure of the update function of the sufficient statistic in Eq. (3.9):

$$\widehat{\mathcal{T}}(\lambda, x) = \frac{(\lambda\overline{p}_I + \overline{\lambda}p_B)f_1(x)}{(\lambda\overline{p}_I + \overline{\lambda}p_B)f_1(x) + (\lambda p_I + \overline{\lambda}\,\overline{p}_B)f_0(x)}.$$

From the above equation, it can be seen that at higher values of SNR, the update function is dominated by the observations, while as the SNR lowers, the update function is more influenced by the a priori parameters of the channel usage models. What the simulation shows is consistent with that view: since CUSUM does not assume any a priori information about the channel and depends only on observations, as the SNR drops, its performance in expected detection delay deteriorates faster than that of MMSSD.

Although it can be seen that the a priori information in the channel usage model offers more performance improvement when $p_I$ is larger, or when $m_I$ is smaller, it is sometimes not practical to assume that a small $m_I$ if it is less than the expected detection delay. That limits the performance gain that results from knowledge of the channel model.

### 5.3.2 RC-MMSSD versus Page's CUSUM when $L >> M$

In the previous section, the comparison shows that full-sensing performance can be obtained with only a small reduction in number of sensors. In this section, the goal is to demonstrate that the case of $L >> M$ warrants the use of RC-MMSSD, i.e.,

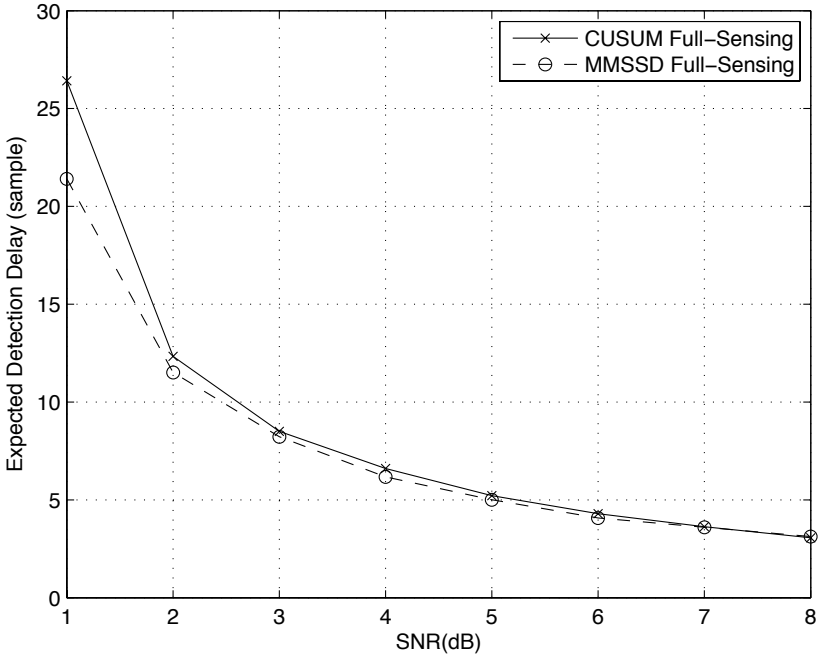


Figure 5.11: The expected detection delays of a full-sensing CUSUM detection and full-sensing MMSSD detection, and is plotted with respect to different SNR's. ($m_I = 300, m_B = 30, \lambda_0 = 0.9, L = 5$). The 95% confidence interval does not exceed $\pm 1$.

that full-sensing performance can be nearly achieved with a significant reduction in number of sensors.

Fig. 5.13 shows a performance comparison between RC-MMSSD and CUSUM. Similar to the comparison between MMSSD and CUSUM, in Fig. 5.14 RC-MMSSD detection is designed to have a similar false alarm rate to that of CUSUM. The expected detection delays for the CUSUM detector with $M = L = 3$ and $M = L = 30$ in Fig. 5.13 illustrate the potential performance gain as the number of channels, $L$, increases from 3 to 30. In order for CUSUM detection to realize such a gain, the number of sensors needs to be increased by tenfold. Without increasing the number of sensors, Fig. 5.13 shows that the expected detection delay of RC-MMSSD is

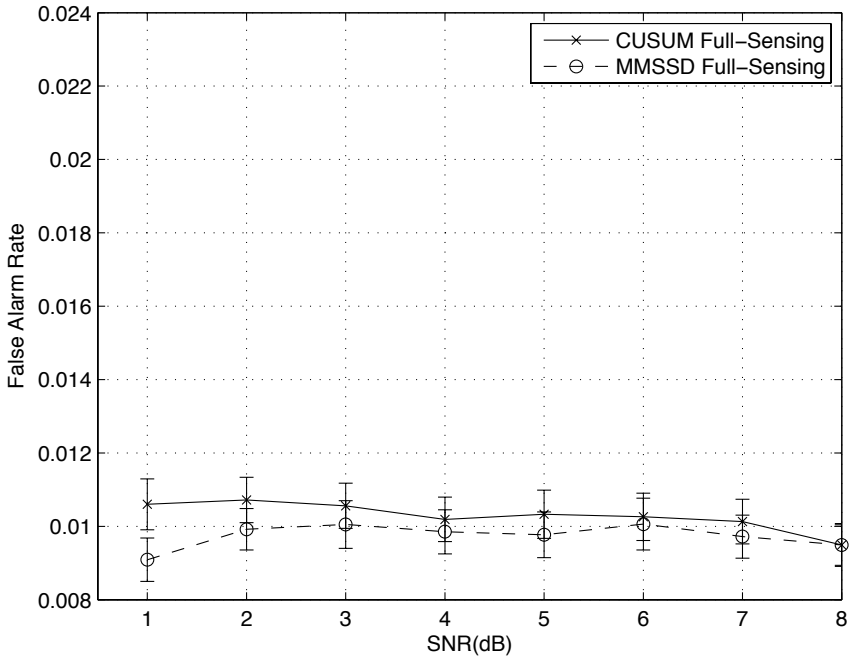


Figure 5.12: A comparison of the false alarm rate between a full-sensing CUSUM detection and full-sensing detection. The error bars are the 95% confidence intervals for each point. False alarm rates of the MMSSD's are designed to be slightly lower than those of CUSUM. ($m_I = 300, m_B = 30, \lambda_0 = 0.9, L = 5$).

significantly lower than that of CUSUM detection with $M = 3$. In addition, compared to CUSUM with $M = 30$ sensors, RC-MMSSD that reduces the number of sensors by 90%, is able to achieve very similar performance. Therefore, in scenarios where $L$ is large and $M$ is relatively small, the RC-MMSSD system equipped with a small number of sensors can achieve similar performance to that of CUSUM equipped with a larger number of sensors.

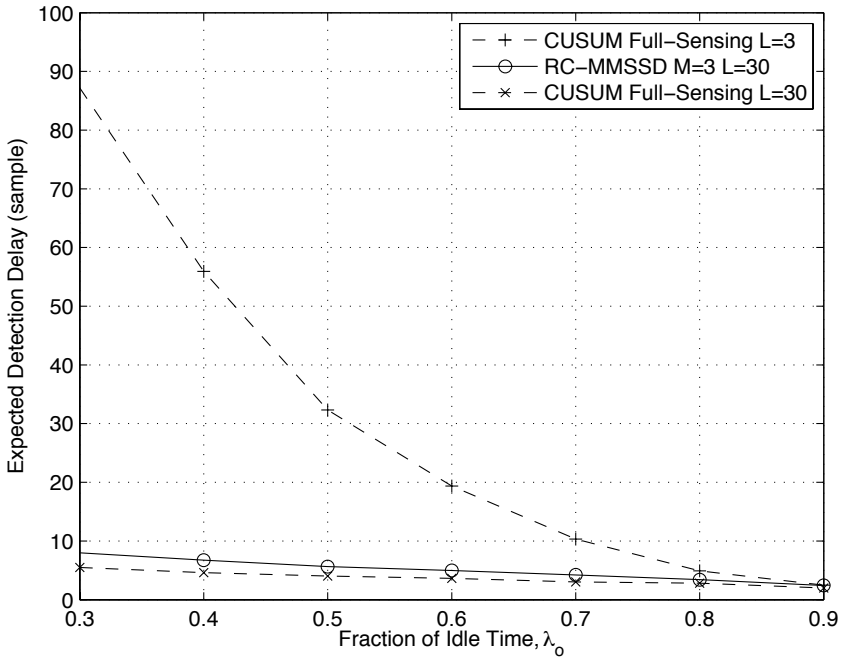


Figure 5.13: A comparison of the expected detection delay of an RC-MMSSD system that uses 3 sensors and CUSUM with 3 sensors and 30 sensors. (SNR=10dB, $m_B = 620, W = 10^5$). The 95% confidence interval does not exceed $\pm 1$.

### 5.3.3 MMSSD versus Shiryaev's Bayesian Detector

As mentioned in Chapter 2, the Shiryaev's Bayesian detector is a quickest detection method that is derived from a problem formulation based on a risk function that embodies a random change time. Like MMSSD, it assumes the duration of a busy period in the channel is geometrically distributed. At the same time, like CUSUM, it also assumes that once a change occurs from a busy to an idle state, a channel stays in the idle state indefinitely. In fact, these assumptions make the Shiryaev's Bayesian detector a special case of MMSSD where $p_I = 0$.

The simulation results that compare the performances of MMSSD and the Shiryaev's Bayesian detector are shown in Figs. 5.15 and 5.16. As in the previous comparisons

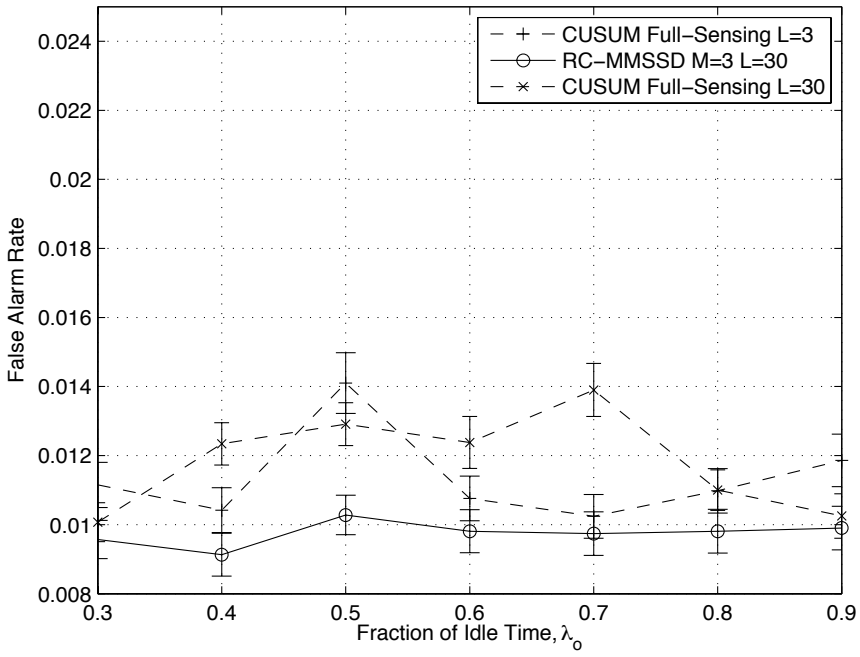


Figure 5.14: A comparison of the false alarm of RC-MMSSD system that uses 3 sensors to CUSUM with 3 sensors and 30 sensors. (SNR=10dB, $m_B = 620, W = 10^5$). From the figure, the false alarm rates are similar with a statistical confidence level of 95%.

to quickest detection algorithms, a baseline false alarm rate is first established in order to compare expected detection delay. The expected detection delay of full-sensing MMSSD matches that of the full-sensing Shiryev's Bayesian detector. This is expected since the values of $m_I$ are kept reasonably high so the quickest detector may avoid the error floor. It is also observed here that MMSSD with 3 sensors performs favourably compared to its full sensing counterpart, despite the reduction in the number of sensors.

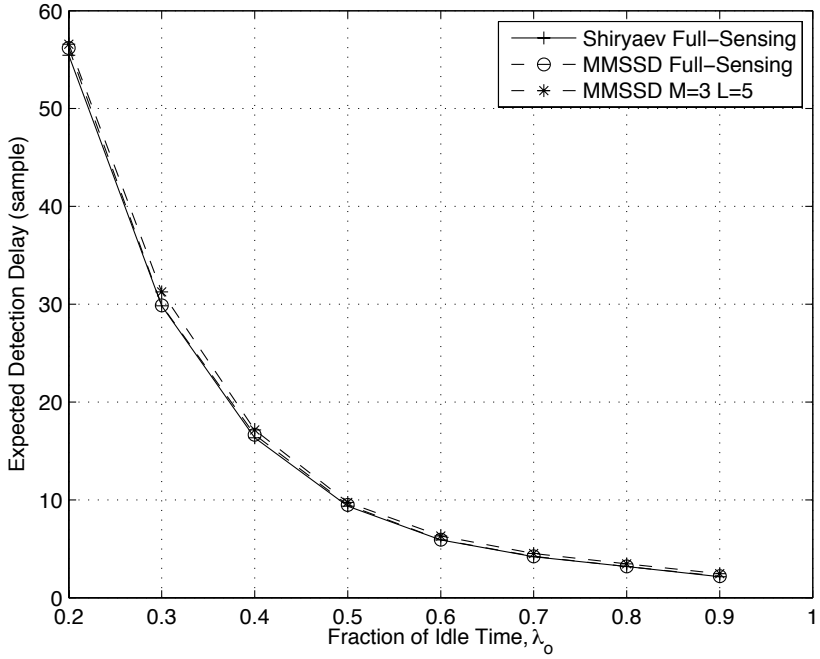


Figure 5.15: The expected detection delay of Shiryaev's Bayesian detection and MMSSD with M=3 and M=5. (SNR=10dB, $m_B = 620, L = 5, W = 10^5$). The 95% confidence interval does not exceed $\pm 1$ sample.

### 5.3.4 MMSSD versus Minimum Asymptotic Risk Detector

Minimum Asymptotic Risk detector (MAR) is detector derived from a problem formulation based on a minimizing a Bayes risk function, but assumes that the change time is an unknown, non-random, and fixed value [12]. With the false alarm rates of the two detectors lined up in Fig. 5.17, it is observed that MAR detector does not perform as well as MMSSD. Over a large part of fraction of idle time, $\lambda_o$, as seen in Fig. 5.18, MMSSD has a consistent gain over MAR detector in terms of expected detection delay. As mentioned in Section 2.3.3, the MAR detection is asymptotically optimal in the condition where $l(x_t) \to 1$, i.e., low SNR conditions. In a higher SNR condition, MAR may be performing in suboptimal conditions, which explains the

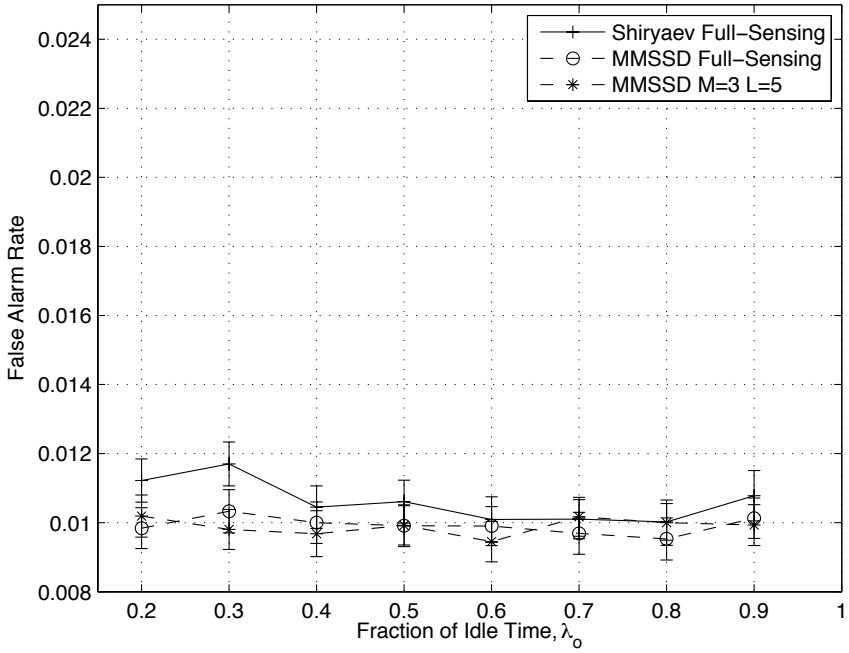


Figure 5.16: The false alarm rates of Shiryaev's Bayesian detection and MMSSD with M=3 and M=5 are designed to be 0.01±0.01 in order to establish a baseline for comparison. (SNR=10dB, $m_B = 620, L = 5, W = 10^5$).

longer expected detection times than that of MMSSD.

## 5.4 Performance of MMSSD in WLAN Traffic

In Chapter 3, the POMDP formulation requires a channel usage model that consists of geometrically distributed idle and busy times. This is a consequence of modeling the usage traffic using the exponential ON-OFF process. In this section, this assumption is tested on a traffic model derived from WLAN network characteristics with stationary UDP traffic.

An ON-OFF model is developed in [8] to characterize the channel usage of UDP in

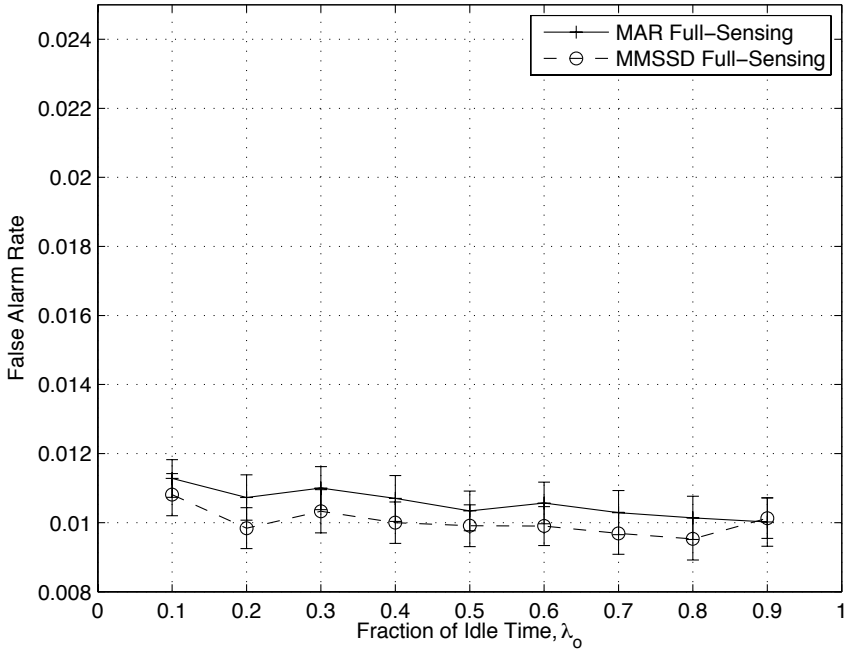


Figure 5.17: The false alarm rates of full-sensing MAR detection and MMSSD are designed to be $0.01 \pm 0.01$ in order to establish a baseline for comparison. (SNR=10dB, $m_B = 620, L = 5, W = 10^5$).

a WLAN network. Channel measurements of over-air UDP traffic generated by three 802.11 wireless terminals are performed. Using this empirical data, the measured traffic pattern is fit to mixture-based distributions according to the Kolmogorov-Smirnov criterion. The experimentally derived model has a certain structure: a WLAN channel can be in one of three states, namely, *busy, free*, and *contention* states. The busy states pertain to when the channel is used to transmit data. Since WLAN is a packetized network, the dwelling time in a busy state has a value of 0.0062 seconds [8] and is thus deterministic. If a terminal is unable to finish transmitting all its data within this time frame, it is required to relinquish the spectrum and contend for access again.

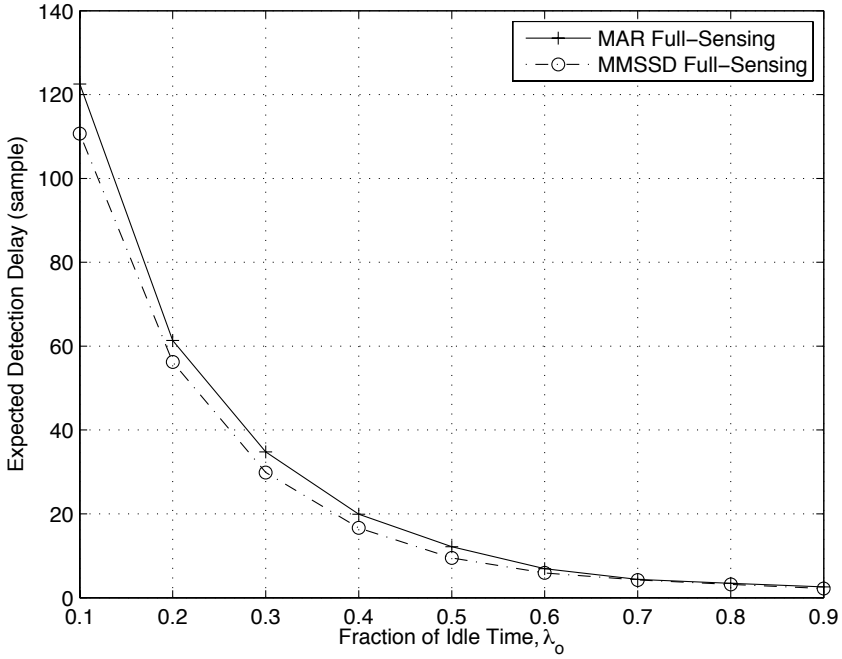


Figure 5.18: The expected detection delay of full-sensing MAR detection vs. full-sensing MMSSD. (SNR=10dB, $m_B = 620, L = 5, W = 10^5$). The 95% confidence interval does not exceed $\pm 1$.

The free state and the contention state are defined as follows: the former is when none of the terminals in the network is utilizing the channel, and the latter refers to when the terminals contend with one another to obtain access to the channel. In both states, the channel is unused, so the free state and the contention state are lumped into a single idle state in the traffic model. As shown in Fig. 5.19, the ON-OFF process that represents the WLAN traffic patterns has the ON state mapped to the busy state, and the OFF state to the lumped idle state that contains both free and contention states.

The cdf for the random dwelling time in the lumped idle state is characterized by

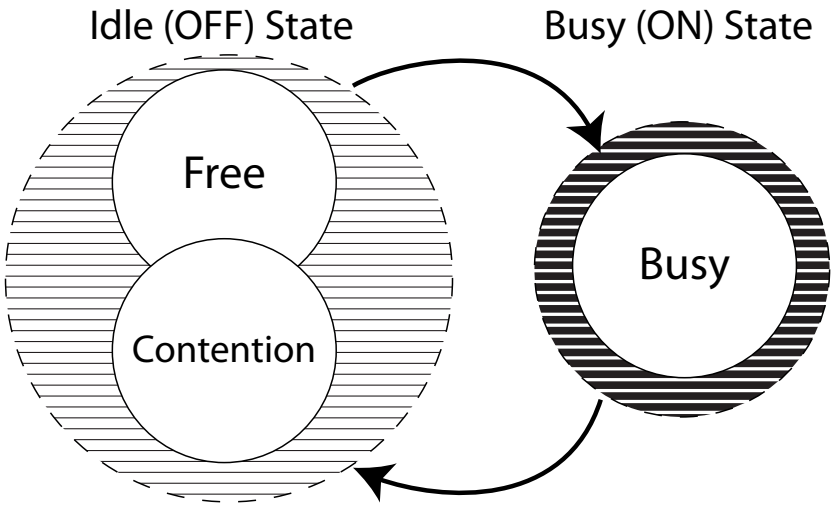


Figure 5.19: The states and the dynamics in the WLAN traffic models.

a mixture-based structure, as given by [8],

$$F(t; k, \sigma) = p_c F_c(t) + p_f F_f(t; k, \sigma), \tag{5.7}$$

where $p_c$ and $p_f \equiv (1 - p_c)$ are the fractions of times spent in either contention or free state, respectively; $F_c(t)$ is the cdf of the contention time that is assumed to be uniformly distributed on [0, 0.0007seconds]; and $F_f(t; k, \sigma)$ denotes the generalized Pareto cdf of the free channel time, parameterized by $k$ and $\sigma$:

$$F_f(t; k, \sigma) = 1 - (1 + k\frac{t}{\sigma})^{1/k}. \tag{5.8}$$

Table 5.1 provides the values of parameters used to simulate the WLAN traffic conditions. The values of the variables $k$ and $\sigma$ are provided in [8] and are directly adopted here. However, the value of $p_c$ is not given in [8]. The values of $p_c$ are

| | Transmission Packet Rate (packets/second) | | | | | |
|---|---|---|---|---|---|---|
| | 25 | 50 | 75 | 100 | 150 | 200 |
| $k$ | -0.3013 | -0.3604 | -0.4014 | -0.4893 | -0.3199 | 0.0164 |
| $\sigma$ | 0.0149 | 0.0162 | 0.0053 | 0.0053 | 0.0021 | 8.09E-4 |
| $p_c$ | 0.1 | 0.2 | 0.3 | 0.4 | 0.6 | 0.8 |
| $\lambda_o$ | 0.94 | 0.9393 | 0.8161 | 0.7859 | 0.5767 | 0.4167 |

Table 5.1: The values of parameters for the WLAN traffic model.

assumed in this study to increase linearly with the packet transmission rate on the basis that more transmissions result in more contention periods; the same assumption is adopted in [8]. Furthermore, in order to apply the MMSSD algorithm, the packet transmission rates need to be converted to fractions of idle time. The fraction of idle time of the WLAN model is computed at each transmission rate during simulation.

A traffic model with geometrically distributed idle and busy periods is used as a nominal, baseline model to identify performance deviation in the WLAN network. The simplest way to fit the exponential model to the WLAN traffic model is to match the first order statistics in both models. However, to ensure that the nominal traffic model is closely matched to the WLAN traffic models in a more systematic fashion, the measure of Kolmogorov-Smirnov (KS) distance is used to choose the values of the parameters in the nominal model; specifically, the values of $m_I$ and $\lambda_o$ that minimize the KS distance between the nominal distribution and the mixture distribution of the WLAN traffic model are chosen. The KS distance is computed using the *kstest()* function from Matlab. To illustrate the use of KS distance for distribution fitting, Fig. 5.20 shows a plot of the KS distance at different values of $m_I$ for a rate of 75 packets per second. It can be seen that at $m_I = 0.0022$, the KS distance is minimized. The same procedure is applied to choose the parameters for all the packet rates. Table

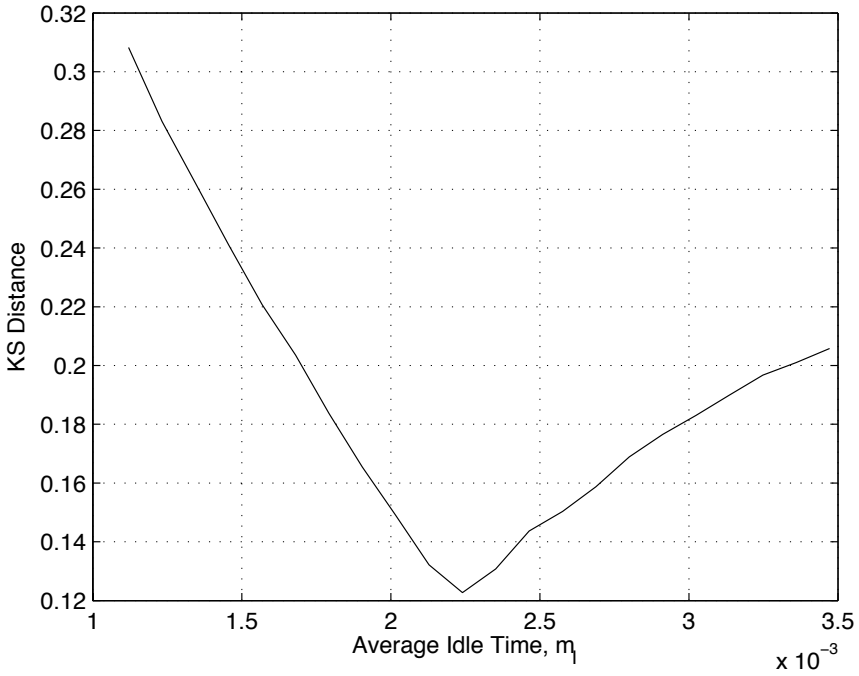


Figure 5.20: The KS distance between a WLAN model with the traffic of 75 packets per second and an exponential model parameterized by the variable $m_I$. When $m_I = 0.0022$, the KS distance is minimized.

5.2 shows these values.

In a WLAN network, the scenario that corresponds to high channel utilization contains terminals that attempt to transmit busty data. Since a terminal only has enough exclusive access to the channel to send one packet, if it needs to send multiple consecutive packets, it has to enter the contention state before it can send the next packet. Therefore, the more busty a transmission is, more frequently the contention period occurs; consequently, this causes the parameter $p_c$ to increase. For the low utilization scenario, the opposite is true.

Since the purpose of this study is to investigate how MMSSD performs with a more realistic channel usage model, MMSSD is first designed based on a nominal

| | Transmission Packet Rate (packets/second) | | | | | |
|---|---|---|---|---|---|---|
| | 25 | 50 | 75 | 100 | 150 | 200 |
| $m_I$ | 0.0103 | 0.0073 | 0.0022 | 0.0017 | 6.76E-4 | 4.25E-4 |
| $\lambda_o$ | 0.94 | 0.92 | 0.78 | 0.73 | 0.52 | 0.42 |
| min KS Distance | 0.0735 | 0.1462 | 0.1227 | 0.1474 | 0.0780 | 0.1085 |

Table 5.2: The values of the parameters in the exponential ON-OFF model, $m_I$ and $\lambda_o$, are chosen to minimize the KS distance between the nominal distribution and the mixture distribution of the WLAN traffic model.

channel usage model based on the best KS fit exponential ON-OFF traffic and then its performance is evaluated using the nominal traffic model. Since according to the 802.11 standard, the unlicensed 2.4GHz band contains three non-overlapping channels, the number of available channels, $L$, is assumed to be three in both models. Next, the traffic model is switched to the WLAN traffic model in the simulation, and the same MMSSD detector is tested. Fig. 5.21 shows that the expected detection delay of MMSSD is larger in a WLAN-based traffic model than that of the nominal exponential ON-OFF traffic model, and that the observed deviation is relatively small in regions of low spectrum utilization (i.e. large fraction of idle time) and grows to be more significant as the idle periods become more scarce (i.e. low fraction of idle time). In Fig. 5.22, it is observed that the false alarm rate generally rises in the WLAN-based traffic model compared to the nominal exponential ON-OFF traffic model. In regions of low spectrum utilization, false alarm performance does not deteriorate significantly; on the other hand, as spectrum utilization increases and idle periods become rare, the false alarm rate deviates further from the performance observed in the nominal exponential ON-OFF traffic model. In short, the assumption of geometrically-distributed idle and busy times has little impact on performance

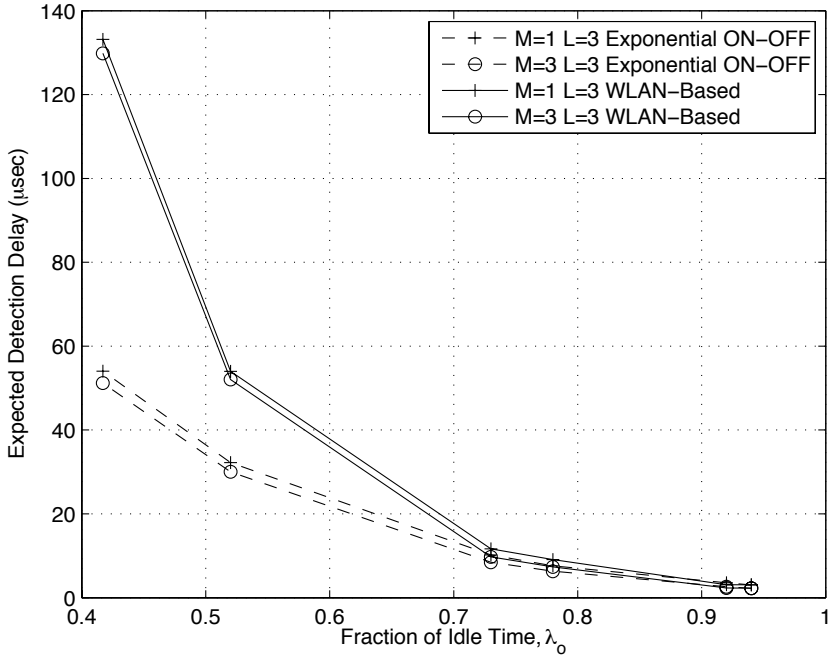


Figure 5.21: The expected detection delay of MMSSD in a WLAN-based traffic model is compared to the nominal traffic model (SNR=10dB, $m_B = 620, L = 3, W = 10^5$). The 95% confidence interval does not exceed $\pm 1$.

when the spectrum bands experience low utilization, but becomes inadequate as more bursty packet transmissions begin to take place.

Two points may help to explain the differences in the detector's performances between the WLAN-based traffic model and an exponential ON-OFF model: First, the number of states in a WLAN system is different from that of an exponential ON-OFF process. Beside the busy and idle states, there is the contention state, which governs terminals in a WLAN network. In the WLAN model, both the contention and the idle periods are considered to belong to the same state, and the duration of this state is randomly characterized using a mixture-based cdf as seen in Eq. (5.7). This model contains a mismatch with the exponential ON-OFF model because

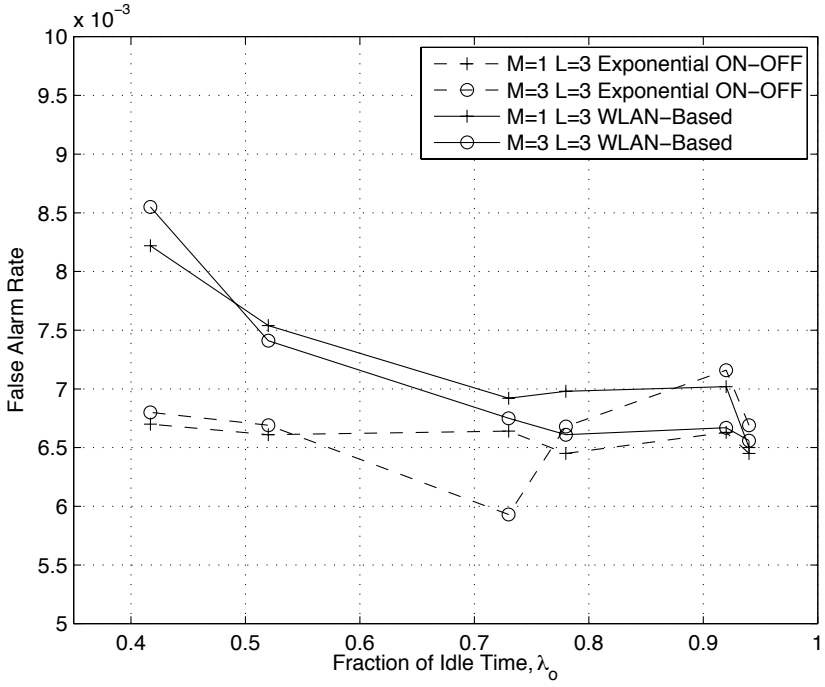


Figure 5.22: The false alarm rate of MMSSD in a WLAN-based traffic model is compared to the nominal traffic model. The 95 percent confidence intervals are less than $\pm$ 1e-3 and not plotted to maintain legibility. (SNR=10dB, $m_B = 620, L = 3, W = 10^5$).

the geometric distribution, which models the duration of either an ON or OFF state, generally does not fit well to a mixture-based distribution. Second, the busy period in the WLAN model is deterministic because of a fixed packet size. Fitting a geometric distribution to a non-random deterministic value creates another source of model mismatch between the WLAN-based model and the nominal exponential ON-OFF model. Since the MMSSD design is based on the exponential ON-OFF traffic model, it faces the performance limitation posed by the aforementioned model mismatches. As seen in Figs. 5.21 and 5.22, when there is less contention (when $\lambda_o$ is high) the performance mismatch seems to diminish. This observation motivates the question on

how well the match is between the Pareto and the exponential distribution. A study based on this question may be useful in the assessments the MMSSD performance in other networks and should be part of the future work on this topic.

# Chapter 6

# Summary and Conclusions

## 6.1 Summary

Spectrum sensing concerns the problem of discerning the state of availability for frequency bands, which is naturally cast as a detection problem. The thesis studies the spectrum sensing problem from a new perspective. Chapter 1 provides the motivation for spectrum sensing and describes the elements that make up the problem.

In Chapter 2, the background section surveys a number of detection methods that can be applied to the problem of spectrum sensing. The detection methods range from classical hypothesis testing [1, 2, 9, 17, 22], to the sequential probability ratio test (SPRT) [24], to various kinds of quickest detectors [10, 12, 18, 21, 25]. For each detection method, the problem formulations and the procedures are provided to offer insights into the system models, the assumptions needed, as well as to provide an overall framework.

In Chapter 3, a problem formulation for a unique spectrum sensing problem is constructed. This chapter illustrates the differences and similarities between the

proposed formulation and the existing ones. For example, while the existing detection-based frameworks deal with detecting idle periods either within a single channel or with a single sensor, this thesis considers a more general problem where the number of channels to sense and the number of sensors can both be arbitrary. Another difference mentioned in this chapter is that the approaches in the existing literature either assume that the state of a spectrum band does not change at all, as in the cases of classical hypothesis testing and SPRT [1, 2, 9, 17, 22, 24], or that the state changes only once, as in the case of quickest detection [10, 12, 18, 21, 25]. This chapter presents a channel usage model to represent the channels' changes in state as an on-off process in order to better model the channels' usage patterns. Furthermore, the durations of idle or busy periods are characterized as geometrically- distributed random variables. Some similarities to existing approaches are that the problem criterion considered in this thesis minimizes the expected detection delay as in the quickest detection methods, and that the geometrically distribution model for the durations in each state is adopted from a special case of Shiryaev's problem in [25]. Another similarity to Shiryaev's problem is the approach to measure system reliability via the false alarm rate.

The remainder of Chapter 3 formulates the problem of spectrum sensing into a new detection problem using partially observable Markov decision processes (POMDP). The problem is formulated by extending an existing problem formulation developed in [29] for one sensor to a new one involving multiple sensors.

In Chapters 4 and 5, new detectors are proposed based on the analysis of the POMDP framework, and their performances are evaluated via Monte Carlo simulation. A summary of the conclusions from these results in Chapters 4 and 5 are

highlighted in the following section.

## 6.2 Conclusions

The POMDP formulation and the optimal multiple process detection structure proposed in [29] is generalized to incorporate an arbitrary number of sensors that are co-located, provided that the observations from different channels are statistically independent. Based on this result, a new detector, named here as *multiband multi-sensor spectrum sensing detection* (MMSSD), is proposed as a low-complexity and suboptimal form of the optimal detector. The simulation results show that the detector derives most of its utility from the first few sensors and that the performance of a detector possessing a large bank of sensors can be achieved with a smaller number of sensors.

Recognizing that MMSSD has high computational cost when the number of channels becomes large, this thesis proposes a reduced-complexity version of MMSSD (RC-MMSSD). Unlike MMSSD, the complexity of RC-MMSSD in terms of storage requirements and computational complexity is independent of the number of available channels. Through simulations, it is demonstrated that RC-MMSSD also benefits from the addition of sensors in terms of shorter expected detection delays, and that the first few added sensors yield the most significant reduction in delay.

When comparing RC-MMSSD to MMSSD, the simulation results show that their performances, in terms of expected detection delay, are comparable. Although RC-MMSSD has lower complexity than MMSSD, there is no evidence that complexity is traded off for either system agility or reliability. However, a caveat with RC-MMSSD exists in that the number of channels must be much larger than the number of sensors.

If such a condition is not met, the designed threshold $\eta_d = 1 - \alpha$ for RC-MMSSD could not meet the false alarm requirement, $\alpha$. In this case, MMSSD must be used. In practice, this is an acceptable limitation because the scenario, where the number of available channels greatly exceeds the number of sensors for many spectrum sensing applications, is realistic. When designing a spectrum sensing system, where there is likely to be few sensors available, one can make a suitable choice between MMSSD and RC-MMSSD, depending on the number of available channels, to achieve both system agility and reliability.

The performances of MMSSD and RC-MMSSD are compared to other quickest detectors, which include Page's CUSUM (Section 2.3.1), Shiryaev's Bayesian Detector (Section 2.3.2), and MAR (Section 2.3.3). When these existing quickest detectors are applied to sensing a channel modelled as an on-off process, our results show that the false alarm rates encounter an error floor. Since the POMDP problem formulation factors in the on-off model, MMSSD and RC-MMSSD do not experience such an error floor. This enables the design of MMSSD and RC-MMSSD to satisfy a wider range of false alarm requirements.

The comparisons among MMSSD, RC-MMSSD, and the quickest detectors can only be conducted using simulation parameters that avoid the error floor. In addition, to compare the detectors in a multi-channel setting, the quickest detection method requires modification, since previously existing quickest detectors are designed to detect in a single channel. The modification produces a full-sensing quickest detector that can sense in multiple channels. Since there must be one quickest detector per channel, the number of sensors deployed for a quickest detection system is always

equal to the number of available channels. In these configurations, MMSSD performs comparably to the CUSUM and Shiryaev's Bayesian detectors. Initially, it was thought that the channel usage model could significantly affect performance due to the a priori information. However, in all the cases simulated, it is observed that the channel model offers little additional information to the detector when the average duration in either the busy or idle state grows large. The results suggest that the performance gain due to the channel usage model is limited when the error floor is not an issue for the quickest detectors.

It is also observed that the ability for MMSSD and RC-MMSSD to dynamically switch channels to sense provides for more efficient use of sensors than the quickest detectors. The MMSSD and RC-MMSSD consistently achieve similar performances to their full-sensing quickest detector counterparts with fewer sensors. When comparing RC-MMSSD with full-sensing CUSUM, the performance gain in terms of expected detection delay is most significant. For example, when there are 30 channels to sense, it is demonstrated through simulation that RC-MMSSD with 3 sensors achieves a very similar performance to CUSUM with 30 sensors. It is therefore evident that the utility per sensor of MMSSD and RC-MMSSD is much higher than that of the quickest detection methods.

A separate study examines the application of a nominal exponential on-off traffic model in the POMDP formulation to a WLAN-based traffic model that was experimentally verified [8]. The simulation results using MMSSD based on a nominal exponential on-off traffic model appear to be overly optimistic, as shown by the significant performance degradation observed for the WLAN-based traffic model.

## 6.3 Future Work

One of the goals of this thesis is to investigate how a priori information on channel usage impacts detection performance. When system reliability of the quickest detectors is not affected by the error floor, MMSSD has demonstrated limited performance improvement over the quickest detectors. This suggests that there is possibility for future research on incorporating improved models for channel usage into the detector optimization, e.g., to apply a better detection framework that incorporates a more realistic traffic models, or to research into scenarios when more than one sensor can sense the same channel, lifting the strong independence restriction. Specifically, it ought to be possible to develop a detector that directly exploits the more realistic WLAN traffic model.

Another area of future work is to further study the performances of MMSSD and RC-MMSSD using signals obtained from an actual wireless network. Studies using real world signals, which requires the access to a network, may be costly to set up. However, with a suitable industry partner, the ability to access the real world data may become feasible and would provide new ways to evaluate the practical performances of MMSSD and RC-MMSSD.

# Bibliography


[1] S. Chaudhari, J. Lunden, and V. Koivunen, "Collaborative autocorrelation-based spectrum Sensing of OFDM signals in cognitive radios," Conference on Information Sciences and Systems 2008, pp.191-196

[2] H.S. Chen, W. Gao, and D.G. Daut, "Spectrum Sensing Using Cyclostationary Properties and Application to IEEE 802.22 WRAN," IEEE GLOBECOM '07, pp.3133-3138.

[3] T.H. Cormen, *Introduction to Algorithm*, MIT Press, 2001.

[4] FCC, "Spectrum Policy Task Force," ET Docket, pp. 2-135, Nov, 2002.

[5] R. A. Fisher. On the Mathematical Foundations of Theoretical Statistics. *Philosophical Transactions of the Royal Society of London*, vol. 222, pp.309-368, 1922.

[6] G. Folland, *Real Analysis: Modern Techniques and Their Applications*, Wiley-Interscience, 1999.

[7] S. Geirhofer, L. Tong, and B. M. Sadler, "Cognitive radios for dynamic spectrum access - Dynamic spectrum access in the time domain: Modeling and exploiting white space," IEEE Commun. Mag., vol. 25, no. 5, pp. 6672, May 2007.

[8] S. Geirhofer, L. Tong, and B. M. Sadler, "Dynamic Spectrum Access in WLAN Channels: Empirical Model and Its Stochastic Analysis," Proc. 1st Int'l Wksp. Tech. and Policy for Accessing Spectrum, 2006.

[9] S.P. Herath, N. Rajatheva, C. Tellambura, "Unified Approach for Energy Detection of Unknown Deterministic Signal in Cognitive Radio Over Fading Channels," IEEE ICC 2009, pp.1-5

[10] L. Lai, Y. Fan, and H.V. Poor, "Quickest Detection in Cognitive Radio: A Sequential Change Detection Framework," IEEE GLOBECOM 2008, pp.1-5.

[11] H. Li, C. Li, and H. Dai, "Quickest Spectrum Sensing in Cognitive Radio," CISS 2008, pp.203-208.

[12] Y. Liu and S. D. Blostein, "Quickest Detection of an Abrupt Change in a Random Sequence with Finite Change-Time," IEEE Transactions on Information Theory, vol.40, no.6, pp.1985-1993, Nov. 1994.

[13] J.I. Marcum. *Table of Q Functions*. Rand Corporation, 1950.

[14] M. McHenry, E. Livsics, Thao Nguyen, and N. Majumdar, "XG Dynamic Spectrum Sharing Field Test Results," 2nd IEEE International Symposium on New Frontiers in Dynamic Spectrum Access Networks, DySPAN, pp. 676-684, Apr. 2007.

[15] M. A. McHenry, "BNSF Spectrum Occupancy Measurements Project Summary," Shared Spectrum Company Rep., Aug, 2005.

[16] J. Mitola III and G.Q. Maguire, "Cognitive radio: Making software radios more personal," IEEE Pers. Commun., vol. 6, no. 4, pp. 13-18, 1999.

[17] A.M. Mossaa and V. Jeoti, "Cognitive radio: Cyclostationarity-based classification approach for analog TV and wireless microphone signals," CITISIA 2009, pp.107-111.

[18] G. V. Moustakides, "Optimal Stopping Times for Detecting Changes in Distributions," the Annals of Statistics, vol.14, no.4, pp.1379-1387, 1986.

[19] J. Neyman and E. S. Pearson. On the problem of the most efficient tests of statistical hypotheses. *Philosophical Transactions of the Royal Society of London. Series A, Containing Papers of a Mathematical or Physical Character*, 231:pp. 289–337, 1933.

[20] V. Pla, J. Vidal, J. Martinez-Bauset, and L. Guijarro, "Modeling and Characterization of Spectrum White Spaces for underlay Cognitive Radio Networks," IEEE ICC 2010, pp.1-5.

[21] H.V. Poor and O. Hadjiliadis, *Quickest Detection*, Cambridge University Press, 2008.

[22] Z. Quan, S. Cui, H. Poor, and A. Sayed, "Collaborative Wideband Sensing for Cognitive Radios," IEEE Signal Processing Mgazine, vol. 25, no. 6, pp. 60-73, Nov 2008.

[23] D. G. Rees. *Essential Statistics, 4th Ed.* CRC Press LLC, 2000.

[24] S. Yeelin and Y.T. Su, "A sequential test based cooperative spectrum sensing scheme for cognitive radios," IEEE PIMRC 2008, pp.1-5

[25] A.N. Shiryaev. *Optimal Stopping Rules.* Springer, 1978.

[26] P.K. Tang, Y.H. Chew, and L.C. Ong, "On the Distribution of Opportunity Time for the Secondary Usage of Spectrum," IEEE Transactions on Vehicular Technology, vol.58, no.3, pp.1517-1527, Mar. 2009.

[27] A. Wald, "Sequential Tests of Statistical Hypotheses," the Annals of Mathematical Statistics, vol.16, no.2, pp. 117-186, 1945.

[28] S. Zarrin and T.J. Lim, "Cooperative Quickest Spectrum Sensing in Cognitive Radios with Unknown Parameters," IEEE GLOBECOM 2009, pp.1-6.

[29] Q. Zhao and J. Ye, "Quickest Detection in Multiple On-Off Processes," IEEE Transactions on Signal Processing, vol.58, no.12, pp.5994-6006, Dec. 2010